COLORADO
Department of Transportation

CDOT Applied Research and Innovation Branch

A Preliminary Evidence-Based Approach for Forecasting Cut Slope Deterioration

Keara Werley & Gabriel Walton

September 1st, 2024

Report No. 2024-11

The contents of this report reflect the views of the author(s), who is(are) responsible for the facts and accuracy of the data presented herein. The contents do not necessarily reflect the official views of the Colorado Department of Transportation or the Federal Highway Administration. This report does not constitute a standard, specification, or regulation.

Technical Report Documentation Page

1. Report No.	2. Government Accession No.	3. Recipient's Catalog No.
CDOT-2024-11		

4. Title and Subtitle	5. Report Date
A Preliminary Evidence-Based Approach for Forecasting Cut Slope Deterioration	6. Performing Organization Code

7. Author(s)	8. Performing Organization Report No.
Keara Werley, Dr. Gabriel Walton	

9. Performing Organization Name and Address	10. Work Unit No. (TRAIS)
Colorado School of Mines 1500 Illinois St, Golden, CO 80401	11. Contract or Grant No. 223.02

12. Sponsoring Agency Name and Address	13. Type of Report and Period Covered
Colorado Department of Transportation Applied Research and Innovation Branch 2829 W. Howard Place Denver, CO 80204	Final
	14. Sponsoring Agency Code

15. Supplementary Notes

Prepared in cooperation with the US Department of Transportation, Federal Highway Administration

16. Abstract

Constructed rock slopes may physically deteriorate over time, which can be represented with increasing rockfall frequency. Physical deterioration leads to performance deterioration, which corresponds to changes in slope risk through time. Thus, forecasting physical slope deterioration and therefore slope performance deterioration is critical to the long-term decision making of transportation agencies. However, deterioration modeling of cut slopes is not yet well-established. Therefore, this research proposes a new framework for physical deterioration modeling of cut slopes using conceptual models that predict how hazard components of a slope may change through time.

Conceptual models were developed for ditch effectiveness deterioration and rockfall frequency increases through time due to weathering since excavation of the cut slope, scaling, and rock bolting. The conceptual models may be directly incorporated into the pre-existing slope risk assessment framework developed for the Colorado Department of Transportation (CDOT) by BGC Engineering. Since rockfall frequency is a key input for the conceptual models, magnitude-cumulative frequency (MCF) distributions were created for seven Colorado cut slopes monitored with remote sensing. Since rockfall inventories may not be available for all slopes, a practical MCF curve estimation method developed by BGC Engineering was tested on these slopes. The estimation method generally produces MCF curves that are within one to two orders of magnitude of the remote sensing-based MCF curves.

Slope performance deterioration over time was evaluated using a dataset from the Washington Department of Transportation, which demonstrated that physical deterioration and slope performance deterioration do not consistently occur for slopes greater than 20 years old. Finally, physical slope deterioration was related to slope performance deterioration using the CDOT slope risk assessment framework. The proposed conceptual models generally predict lower performance deterioration compared to the current CDOT hazard deterioration models.

17. Keywords	18. Distribution Statement
Cut slopes, slope asset management, deterioration modeling, rockfall	This document is available on CDOT's website https://www.codot.gov/programs/research

19. Security Classif. (of this report)	20. Security Classif. (of this page)	21. No. of Pages	22. Price
Unclassified	Unclassified		

Acknowledgments

This research would not have been possible without the help of many. First, thank you to the Colorado Department of Transportation for funding this research, and to Thien Tran and Bob Group, who served as the Study Manager and Research Oversight Team Lead, respectively. Thank you to BGC Engineering, including Mark Vessely, Madeline Hille, and Zac Sala, for allowing the authors to collaborate on the work being done in the transportation industry. Mark Vessely is also recognized and appreciated for his contributions and valuable feedback in this research, along with Dr. Paul Santi and Dr. Mike Mooney at the Colorado School of Mines.

Thank you to the Washington Department of Transportation, and Marc Fish and Sam Johnston in particular, for providing a unique and valuable dataset used for analysis. Gratitude is also expressed to Cam Phillips, who documented and performed the analysis described in Section 4 to quantify rockfall frequency. Lastly, thank you to other previous graduate students in the Computational Geomechanics Lab at the Colorado School of Mines who processed lidar data for Colorado cut slopes that were used in this research.

Abstract

Constructed rock slopes may physically deteriorate over time, which can be represented with increasing rockfall frequency. Physical deterioration leads to performance deterioration, which corresponds to changes in slope risk through time. Thus, forecasting physical slope deterioration and therefore slope performance deterioration is critical to the long-term decision making of transportation agencies. However, deterioration modeling of cut slopes is not yet well-established. Therefore, this research proposes a new framework for physical deterioration modeling of cut slopes using conceptual models that predict how hazard components of a slope may change through time.

Conceptual models were developed for ditch effectiveness deterioration and rockfall frequency increases through time due to weathering since excavation of the cut slope, scaling, and rock bolting. The conceptual models may be directly incorporated into the pre-existing slope risk assessment framework developed for the Colorado Department of Transportation (CDOT) by BGC Engineering. Since rockfall frequency is a key input for the conceptual models, magnitude-cumulative frequency (MCF) distributions were created for seven Colorado cut slopes monitored with remote sensing. Since rockfall inventories may not be available for all slopes, a practical MCF curve estimation method developed by BGC Engineering was tested on these slopes. The estimation method generally produces MCF curves that are within one to two orders of magnitude of the remote sensing-based MCF curves.

Slope performance deterioration over time was evaluated using a dataset from the Washington Department of Transportation, which demonstrated that physical deterioration and slope performance deterioration do not consistently occur for slopes greater than 20 years old. Finally, physical slope deterioration was related to slope performance deterioration using the CDOT slope risk assessment framework. The proposed conceptual models generally predict lower performance deterioration compared to the current CDOT hazard deterioration models.

Table of Contents

List of Figures

List of Tables

List of Abbreviations

Annual Risk Exposure	ARE
Colorado Department of Transportation	CDOT
Colorado Rockfall Hazard Rating System	CRHRS
Department of Transportation	DOT
Federal Highway Administration	FHWA
Floyd Hill Rock Slope	FH
Geotechnical Asset Management	GAM
Idaho Springs Rock Slope	IS
Magnitude-Cumulative Frequency	MCF
Manitou Springs Rock Slope	MS
Montana Department of Transportation	MDT
National Highway System	NHS
Rockfall Hazard Rating System	RHRS
Structure from Motion	SfM
Transportation Asset Management	TAM
Terrestrial Lidar Scanning	TLS
Unstable Slope Management System	USMS
Vail Pass Rock Slope	VP
Washington Department of Transportation	WSDOT

1.0 Introduction

1.1 Background and Purpose

Assets along transportation corridors affect the proper functioning of the roadway and therefore must be maintained by the responsible transportation agency. In state departments of transportation in the U.S. and other transportation agencies around the world, assets are maintained systematically through specific frameworks known as asset management plans (e.g., FHWA, 2021). An asset's physical condition often changes through time; the condition may deteriorate due to weathering processes, usage, and subsequent degradation of material (Thompson, 2017; FHWA, 2022). In some cases, the condition will improve if the asset undergoes maintenance or stabilization measures (FHWA, 2022). Because the physical state of the asset may change through time, deterioration modeling is a component of asset management plans.

Deterioration modeling forecasts changes in the state of an asset's condition or risk through time. This allows for prioritizing assets for investment or proper maintenance in a timely manner. Routine maintenance and timely preservation of assets may prevent the transportation agency from having to pay a higher cost in the future (Dornan, 2002; Thompson, 2017).

Assets along a transportation corridor may include, for example, road pavement, bridges, tunnels, and geotechnical assets such as retaining walls, constructed embankments, and slopes (Thompson, 2017; Vessely et al., 2019; CDOT, 2022). Slopes may be natural or excavated to allow space for the roadway to be constructed or expanded. Additionally, slopes may be comprised of soil, rock, or a mixture of both. Rock slopes in particular pose a risk to roadway users due to rockfall, and cut slopes may experience changing rates of rockfall through time, unlike natural slopes (absent the influence of climate change) (Romana, 1993; Nicholson et al., 2000; Huisman et al., 2006; Chen et al., 2022).

The deterioration process of geotechnical assets such as rock slopes is not yet well understood, and the implementation of geotechnical asset management and therefore deterioration modeling is in early stages (Stanley and Pierson, 2013; Wolf et al., 2015; Salunke, 2023). Thus, the goal of this research is to propose a new approach for forecasting physical cut slope deterioration to aid in forecasting changes in slope performance. The proposed deterioration framework will consider risk variables related to rock slope hazard that are likely to change over time, namely ditch effectiveness and rockfall frequency.

Full technical details and supplemental material for each analysis presented in this report are included in Werley (2024).

1.1.1 Deterioration Modeling

As previously mentioned, deterioration modeling forecasts changes in asset condition or risk through time, ultimately aiming to reduce the asset's life cycle cost. Within transportation asset management (TAM) and geotechnical asset management (GAM), changes in asset condition or risk are typically forecasted within an engineering timeframe of approximately 10-100 years (e.g., Thompson, 2017; Boadi et al., 2022; Randall, 2022).

Many tools can be used in deterioration modeling, including Markov models, probability distributions, AI techniques such as case-based reasoning, and performance curves. However, in each of these methods, a lack of historical data can make it difficult to apply such models.

Markov models are a common method to model deterioration for traditional transportation assets and geotechnical assets, owing to their simplicity (Beckstrand et al., 2017; Thompson, 2017; Boadi et al., 2022). These models are well-established for bridges and pavement, but because geotechnical assets such as slopes deteriorate in a fundamentally different way than bridges and pavement, Markov models may not be the most effective approach. Though transition probabilities required for such models can be evidence-based, they are first established with expert judgement and are still uncertain for geotechnical assets. Furthermore, the interaction of stabilization measures with slopes is not yet well-integrated into deterioration modeling (Lane, 2006; P.D. Thompson, personal communication, November 16, 2022).

Though some deterioration modeling approaches can be used to model individual components of the asset, they are commonly used to forecast changes in the total condition or risk of the slope without considering individual components. In other models, an increasing rate of physical or performance deterioration rate may be applied to the condition/risk or individual components of the slope. In both of these cases, the amount of slope performance deterioration may be overestimated, thereby causing the transportation agency to dedicate an unnecessary amount of resources to some slopes. In reality, some components contributing to slope performance may remain constant over time and not experience physical deterioration.

1.1.2 Defining Deterioration in the Context of Rock Slopes

Definitions of deterioration differ across studies. Broadly, slope deterioration has referred to the progressive decline in condition and physical quality of a slope due to weathering, earth and water movement, and discontinuities in the rock mass, which often leads to a decline in slope performance (Cheung et al., 2005; Thompson, 2017; Briggs et al., 2019). Throughout this report, terms related to slope deterioration are defined according to the following:

- Rockfall activity: Rockfall activity is represented with a given slope's magnitude-cumulative frequency (MCF) distribution at any given point in time. Magnitude is represented with rockfall volume; cumulative frequency defines how often a rockfall of a given volume or larger occurs. In general usage, the occurrence of rockfall is commonly considered to be a form of "physical slope deterioration" (or processes associated with physical deterioration); however, in this research, rockfall activity is distinguished from physical deterioration and represents the underlying hazard at any given point in time.
- Physical property deterioration: The decrease over time of geotechnical properties that define the slope's mechanical behavior, such as intact rock strength. This may or may not lead to substantial increases in rockfall activity.
- Physical deterioration: A progressive decline in condition or physical quality of the slope that is associated with increases in hazard over time. Physical deterioration herein is represented as changes in rockfall activity, or changes in the MCF distribution, over time.
- Performance deterioration: A progressive decline in slope performance over time, indicated by impacts on the roadway, roadway users, and the transportation agency. Performance deterioration is herein represented with changes in the slope risk, which is

estimated based on the slope hazard and consequences on roadway users and the transportation agency.

1.2 Research Scope

The overall research objective is to develop a framework for predicting physical slope deterioration and therefore performance deterioration. To achieve this objective, the following tasks were defined:

Task 1: Conduct a literature review of practices in Transportation, Geotechnical, and Slope Asset Management.

Slopes are geotechnical assets, and geotechnical asset management plans have been heavily influenced by previously established practices associated with transportation asset management plans. Additionally, deterioration modeling is a required component of asset management plans, and therefore the literature review conducted informs previous methods of deterioration modeling, as well as areas for improvement. Since condition or risk assessments are inputs to deterioration modeling, previous methods of condition/risk assessments are also discussed. The findings of this objective are included in Section 2.

Task 2: Develop conceptual models to predict physical cut slope deterioration.

Rockfall hazard variables that will likely change over time were identified from the Colorado Department of Transportation (CDOT) slope risk assessment framework developed by BGC Engineering. Conceptual models were developed for these hazard variables since changes in hazard will cause changes in slope performance; specifically, changes in ditch effectiveness deterioration and rockfall frequency due to time since excavation of the cut slope, scaling, and rock bolting. The findings of this objective are discussed in Section 3.

Task 3: Analyze historical rates of rockfall for Colorado cut slopes.

Analyzing and quantifying rockfall activity for Colorado cut slopes allows for hazard assessment, MCF estimation of similar slopes, and an input for the rockfall frequency conceptual models. The rockfall rates will then be used to predict physical deterioration via the conceptual models.

Task 4: Evaluate a practical method to estimate rockfall frequency.

Rockfall frequency is a critical input to estimating Annual Risk Exposure (ARE) in the CDOT slope risk assessment framework. Rockfall frequency may be estimated from rockfall inventories built by remote sensing methods; however, creating a rockfall inventory for every cut slope is not feasible. Thus, the accuracy of a practical, rapid rockfall frequency estimation method developed by BGC Engineering was evaluated by comparing the results of the method to remote sensing-based magnitude-cumulative frequency (MCF) distributions. The findings of this objective are included in Section 5.

Task 5: Evaluate slope performance deterioration.

Slope performance deterioration over time was evaluated using a dataset from the Washington Department of Transportation's (WSDOT) Unstable Slope Management System (USMS). The analysis of this data was used to evaluate the plausibility of the conceptual model for rockfall frequency changing as a function of time since excavation of the cut slope. The findings of this objective are discussed in Section 6.

Task 6: Assess the relation between physical slope deterioration and slope performance deterioration.

To meet this objective, slope performance predicted by the proposed conceptual models was then compared to slope performance predicted by the current CDOT hazard deterioration models within the CDOT slope risk assessment framework developed by BGC Engineering. A sensitivity analysis was also performed within the time-since-excavation conceptual model to assess how sensitive slope performance deterioration is to physical deterioration. The findings are discussed in Section 7.

Lastly, recommendations on how to implement these findings are discussed in Section 8.

2.0 A Review of Practices in Transportation, Geotechnical, and Slope Asset Management

2.1 Introduction

Performance or physical deterioration modeling of slopes and other transportation assets in general, is a required component of an asset management plan. Therefore, to review previous and current methods of deterioration modeling of cut slopes, practices in transportation, geotechnical, and slope asset management are summarized in the following literature review.

Asset management is a "coordinated activity of an organization to realize value from assets" (ISO, 2014). Traditionally, transportation agencies in the U.S. have included bridges and pavements in Transportation Asset Management (TAM) plans. Over the past few years, Geotechnical Asset Management (GAM) plans are increasingly being developed for geotechnical assets, including but not limited to rock cuts, soil cuts, embankments, and retaining walls (Thompson, 2014). Thus, GAM plans are influenced by traditional practices in TAM, particularly as GAM plans are initially being established.

This section reviews the asset management framework used by the Federal Highway Administration (FHWA) and how this framework has been implemented into GAM. Specifically, the condition or risk assessment and deterioration modeling components are reviewed to better understand potential improvements in these areas. Condition/risk assessments are included because they serve as the asset's initial state that will be forecasted in deterioration modeling.

2.2 Transportation Asset Management

Federal legislation mandates that each state department of transportation (DOT) develop a risk-based TAM plan for the National Highway System (NHS) to maintain and improve asset conditions, thereby ensuring proper functioning of the transportation system (FHWA, 2021). To achieve this, state DOTs must maintain quality information of assets and develop a decision-based framework to select appropriate "maintenance, preservation, repair, rehabilitation, and replacement actions" throughout the assets' lifetime (FHWA, 2021). Actions should also strive to estimate and reduce the overall lifecycle cost.

At a minimum, TAM plans must include the following (Sanford-Bernhardt et al., 2003; FHWA, 2021):

- A summary listing all pavement and bridge assets on the NHS system (i.e., an inventory)
- Asset management objectives and measures
- Performance gap identification, condition assessment, and performance modeling
- Lifecycle cost and risk management analysis
- Financial plan
- Investment strategies
- Performance monitoring (feedback) of the TAM framework

Any asset management plan requires an inventory. Agencies must consider which assets to

include, which may be guided by law, as well as what information should be included and how the information will be stored (Wolf et al., 2015). Limitations in current TAM plans exist due to incomplete inventories or massive state-wide inventories (Wolf et al., 2015), which may make data management and standardization more difficult.

Asset management objectives and measures delineate the goals of the agency, which also may be dictated by laws and policies. These goals should realistically reflect what the program can accomplish and lay the foundation for the rest of the TAM plan (Wolf et al., 2015).

Condition assessments allow for identification of performance gaps and development of deterioration models to forecast changing conditions over time. To carry out condition assessments, consistent methods need to be outlined and taught to inspectors. Furthermore, each asset class requires measurable performance indicators and methods to derive condition ratings. Historical asset condition data is largely helpful for informing condition forecasting and model validation.

To assess lifecycle cost and planning, a quantitative analysis should be conducted considering asset conditions, asset deterioration, impact of unfavorable events, and maintenance and preservation over asset lifecycles (Thompson, 2017). Financial planning may be performed for the short-term and long-term. Plans are developed to repair, rehabilitate, or replace assets based on condition forecasting and cost modeling (Wolf et al., 2015).

Though TAM plans only require consideration of pavement and bridges in the U.S., most state DOTs incorporate additional assets such as highway signs, drainage culverts, high-mast light poles, and geotechnical assets, among others (Thompson, 2017). Furthermore, some states are expanding the scope from pavements and bridges in the NHS network to all roads on the state highway network (Thompson, 2017).

2.2.1 Methods of Condition Assessment

Condition assessments are conducted to evaluate the physical state of the asset. They inform modeling of the deterioration process and likelihood of engineering failure, which aids in making maintenance decisions (IPWEA, 2015). Monitoring may be performed visually or with nondestructive testing techniques, such as remote sensing (IPWEA, 2015; Omar, 2018; e.g., Chang et al., 2018).

If an agency owns a large quantity of assets, conducting physical condition assessments on each one may not be feasible. Thus, a sampling approach may be taken instead and extrapolated across datasets (IPWEA, 2015). Monitoring may be prioritized for assets that are either older, more critical, or more inclined to deteriorate faster due to environmental conditions. Frequency of assessment often depends on industry guidance, but advanced data collection and condition assessment practices may be based on risk (IPWEA, 2015).

A condition rating will typically be assigned from the assessment. Condition ratings of 1-5 are the most common, particularly for the purpose of deterioration modeling and in the initial stages of implementing asset management. As the asset management increases in maturity, the number of ratings may not increase, but condition assessments may use multi-criteria assessment. For

instance, subcomponents of the asset can be considered, as well as the extent of the defect and severity (IPWEA, 2015; Randall, 2022).

Ratings are determined from performance indicators, which are chosen based on the physical deterioration modes of the asset. For instance, scour is a common soil-structure interaction issue and is therefore assessed in bridges (Omar and Nehdri, 2018). Pavement performance indicators may include roughness, cracking extent, asphalt rutting, pothole area, and deflection (IPWEA, 2015; Blades, 2018).

Based on FHWA requirements for the National Bridge Inventory, condition ratings between 0-9 are given to each subcomponent of bridges, namely the deck, superstructure, substructure, and culvert (Boadi et al., 2022). These ratings can then be generalized into poor, good, or another intermediate rating. Pavement condition ratings may also be categorized into good, fair, or poor condition. Examples of standardized rating systems include the FHWA National Bridge Inspection Condition Rating, the Corps of Engineers' Repair, Evaluation, Maintenance and Rehabilitation Condition Index, and the Pavement Condition Index (Stanley and Pierson, 2013).

2.2.2 Methods of Deterioration Modeling

Deterioration modeling forecasts a condition rating or index and presents the following benefits (IPWEA, 2015):

- Mitigates risk
- Avoids unplanned outages of the asset and allows preemptive maintenance, which is often more cost effective than allowing the asset to fail
- Predicts future expenditures and investment
- Could extend asset service life
- Enables understanding of deterioration process
- Allows for assessment of probability of failure
- Allows for assessment of the remaining life of an asset

Four general categories of deterioration models exist (Morcous et al., 2002; IPWEA, 2015; Omar, 2018):

- Deterministic: The relationship between factors affecting deterioration and condition is modeled with mathematics or statistics; however, this model does not account for uncertainty or randomness.
- Stochastic: This model is similar to deterministic but accounts for random variables/uncertainty. For instance, a specified condition rating is not assumed at a particular asset age.
- Artificial Intelligence (AI): Data-informed computer-based techniques.
- Mechanistic: Describes a specific deterioration mechanism.

Deterministic models are created by plotting condition against time and using a regression to fit the data. They most often model deterioration without the influence of maintenance (IPWEA, 2015).

Stochastic models involve the use of probability distributions and Markov chains. Probability models describe "probabilities associated with all values of a random variable," which may be a condition rating of a bridge subcomponent, for example (Omar, 2018). Probability models are limited in that the distribution of the random variable needs to be known. This is commonly overcome with approaches such as a Monte Carlo simulation (IPWEA, 2015; Omar, 2018).

Model accuracy is informed by expert judgement or past data. However, past data can only be used when the asset and current environmental conditions are similar to the past, which is often not the case (e.g., due to climate change). As more data is collected, the model should be altered to more accurately reflect the deterioration that is occurring (IPWEA, 2015).

Markov chains are the most common tool for deterioration modeling due to their simplicity (Figure 2.1), which defines asset condition states and obtains the probabilities of an asset transition to one state or another during some time period, typically an inspection period (Morcous et al., 2002; e.g., Boadi et al., 2022). Advantages to Markov models include the following (Mirzaei et al., 2014; Boadi et al., 2022):

- They are the simplest model that still accounts for uncertainty.
- Transition times from one state to the next can be estimated from inspection database with a timeframe less than the asset lifespan.
- Transition times are calculated algebraically, and Markov models allow the investigation of other variables that influence deterioration. The data would be divided into different classes of that variable.

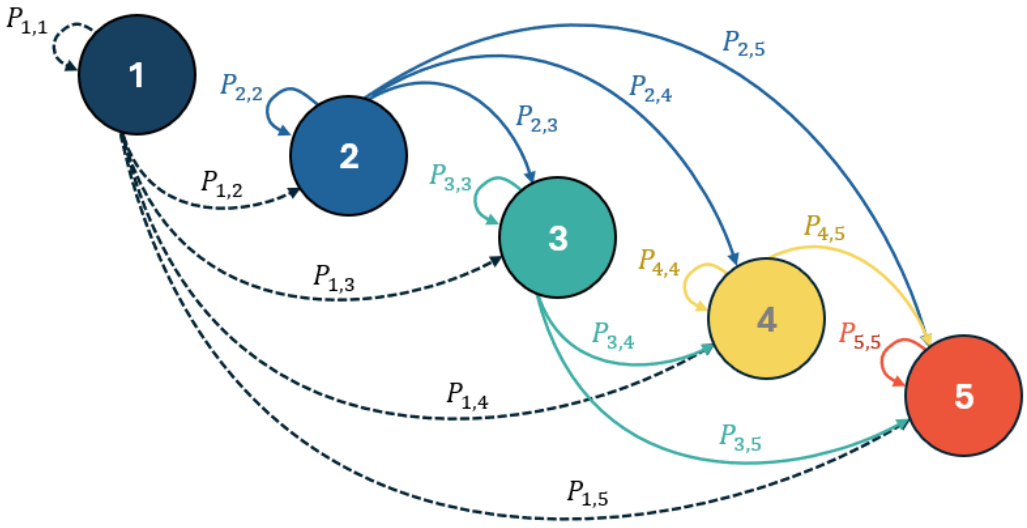

Figure 2.1. Visualization of Markov chain process, where P represents the probability of going from one state to the next or staying within the same state. For instance, P1,2 is the probability of going from State 1 to State 2, and P1,1 is the probability of remaining in State 1 (after McKibbins et al., 2019).

Limitations of Markov models include the following (Morcous et al., 2002, Thomas and Sobanjo, 2013, Han, 2021):

- Transition rates only depend on current condition, not asset history ("memorylessness").
- Transitions into lower, more deteriorated states may not reflect variables contributing to deterioration.
- Some models assume constant population, which may not be realistic.
- Some methods model discrete transition time intervals.
- Directly modeling repairs to the asset and therefore condition improvement is difficult to model.
- Models are difficult to update with new information (such as from a recent inspection).

To overcome Markov limitations, several methods of mixed-Markov or semi-Markov models exist, along with other methods such as AI (Mocous et al., 2002; Thomas and Sobanjo, 2013; Lin et al., 2019; Han, 2021). For instance, Markov chains may be used with Bayesian methods and Monte Carlo simulations. Despite these alternative methods, only Markov and Weibull models have been used and validated at the production-level for bridge systems (Boadi et al., 2022).

2.3 Geotechnical Asset Management

Geotechnical assets include natural slopes, cut slopes, embankments, retaining walls, or constructed subgrades that contribute to or impact the performance and operation of the transportation system (Thompson, 2017; Vessely et al., 2019). These assets can be further divided into sub-assets based on material or length, for example. The ultimate goal of GAM, like TAM, is to reduce lifecycle cost across the whole system (Sanford-Bernhardt et al., 2003). If GAM plans are written in a structure consistent with TAM plans, their usefulness and understanding increases and better contributes to state and federal performance measures (Sanford-Bernhardt et al., 2003; Thompson, 2017; Vessely et al., 2019).

Several frameworks exist internationally for designing and implementing GAMs, and many GAMs have been established (e.g., Waseem et al., 2022). Several states in the U.S. have written GAM plans since 2017 (e.g., Thompson, 2017; Oester et al., 2019; Macedo et al., 2023; Gautreau et al., 2023; Mines et al., 2023;). However, few discuss and account for the interaction between geotechnical assets and traditional assets such as pavements and bridges.

2.3.1 Methods of Condition Assessment

Geotechnical condition assessments serve the same purpose as traditional transportation condition assessments. Condition states are mainly defined on a qualitative basis by describing physical characteristics or active hazards of the asset, potentially leaving room to develop a more rigorous, quantitative metric to aid in defining condition states. For instance, a common method includes a ground inspection to assign a predefined condition based on specific characteristics, followed by a quantification of this assigned condition to use in deterioration modeling. Quantification may include weighted averages and indices with research behind the development, but they are rooted in qualitative observations that may vary with the inspector.

Parameters that comprise a visual assessment may vary for each type of geotechnical asset. For

instance, the Alaska DOT considers the following factors for the corresponding asset (Thompson, 2017):

- Rock slopes: Ditch effectiveness and rockfall activity
- Soil slopes: Roadway displacement, affected length of roadway, movement history
- Retaining walls: Vertical and horizontal wall alignment, impacts to roadway
- Material sites: Proximity, quality, and quantity of materials for each maintenance section

Depending on these parameters, assets may be placed into one of five categories that might be labeled as good, fair, or poor, and then quantified using a condition index if needed. A range of condition indices would already be assigned to a category based on the asset type (Thompson, 2017). Other methods may divide assets into sub-assets, and quantify a condition score based on location, length, and characteristics prevalent to failure (e.g., Randall, 2022).

Consistency in assigning condition states and recording historical condition states for deterioration model validation is particularly important. Inconsistent condition assessment may arise naturally as different geotechnical or geological engineers assess a site, and the impact of this inconsistency on deterioration modeling is largely unknown.

Remote sensing techniques have recently been proposed as alternatives or supplements to visual inspections (e.g., Wolf et al., 2015; Martinovic et al., 2016; Pritchard et al., 2018; Salunke et al., 2023; Wollenberg-Barron et al., 2023). Remote sensing methods would serve as performance monitors and ideally "streamline" the inspection process within GAM (Salunke et al., 2023; Wollenberg-Barron et al., 2023). This would limit bias and variability, as well as reduce cost in the long-term (Martinovic et al., 2016; Pritchard et al., 2018). However, limitations involve the need to manage larger datasets, interpret and analyze more complex data, and compare data of varying resolutions (Pritchard et al., 2018).

2.3.2 Methods of Deterioration Modeling

Examples of current work in geotechnical asset deterioration modeling make use of statistical methods (Power et al., 2016; Thompson, 2017; Randall, 2022; Briggs et al., 2022). Markov models specifically are implemented in GAM since they are widely used in TAM and are simple to use (Thompson, 2017; Randall, 2022). However, geotechnical assets may have more variables that affect deterioration than traditional transportation assets. To compare deterioration rates for different mitigation cases or geologic materials, subdivisions or cohorts are needed (e.g., Randall, 2022). Further subdivisions create smaller datasets, reducing reliability in models. Additionally, even within cohorts, stronger engineering judgment is needed to apply maintenance or preservation for a given asset. Furthermore, these cohorts may not necessarily isolate the impact of geology or mitigation on deterioration, which may make observing their impact on deterioration rates difficult.

Markov modeling presents some limitations in the context of GAM. For instance, assuming that future condition states depend only on the present condition state does not take into account the original date of construction or design of the asset. Newly constructed assets designed with better technology and expertise may perform better than older assets, thereby exhibiting slower deterioration rates. Another potential drawback in statistical modeling of deterioration of

geotechnical assets is the lack of asset condition history and small datasets, possibly resulting in reliance on expert speculations rather than firm data (Thompson, 2017).

Conceptual deterioration models include performance curves (Figure 2.2) (e.g., Thurlby, 2013; Briggs et al., 2019; Spink, 2019). Performance curves can be fit to a specific asset using a more quantitative hazard function with the aid of numerical modeling, laboratory tests, and information from inspections (e.g., Briggs et al., 2019). However, creating a performance curve for a specific asset or cohort of assets proves difficult, as a thorough understanding of the physical process of deterioration is also needed, along with the asset history (Briggs et al., 2019). Furthermore, though performance curves can aid in comparing performance expectations and lifecycles between assets, they do not represent random events adequately (Anderson and Rivers, 2013).

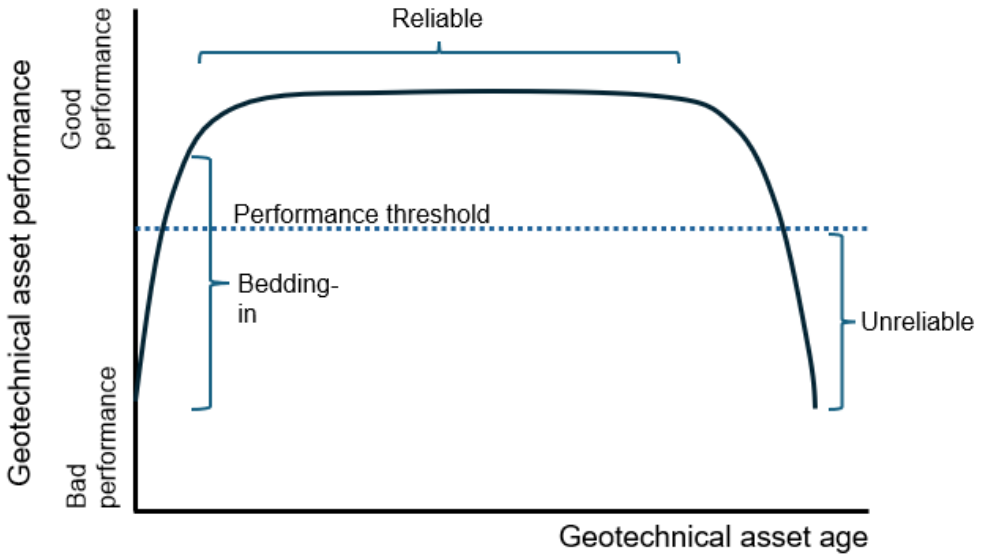

Figure 2.2. Generalized conceptual deterioration model showing lifecycle stages and corresponding asset performance. Performance curves may be adjusted to reflect a specific asset (after Spink, 2019).

2.3.3 Current Limitations in GAM

GAM remains in its early stages of development and implementation (Salunke, 2023). Certain challenges persist from modeling GAM after TAM:

- Collecting inventory data: Inventories can be large, incomplete, or contain impersistent records due to a lack of standardized condition assessments and improved data collection over time (Anderson and Rivers, 2013; Wolf et al., 2015).
- Conducting condition assessments: Standardized methods of condition assessment are lacking, especially on the national level; efficient and reliable methods of measuring and testing performance data are difficult to standardize (Anderson and Rivers, 2013).
- Forecasting conditions and deterioration modeling: Geotechnical asset lifecycle is poorly

understood (Stanley and Pierson, 2013; Wolf et al., 2015). Though Markov models are used due to their wide usage in TAM, transition rates are uncertain and derived from expert judgement. Performance curves do not model random events that substantially affect deterioration well.

Steps have been made to create standardized performance measurements and condition assessments for pavement, bridges, and geotechnical assets. These guides may be found in National Cooperative Highway Research Program (NCHRP) and FHWA manuals (Anderson and Rivers, 2013). Furthermore, individual state agencies may implement their own standardized methods.

2.4 Rock Slope Asset Management

Slope asset management plans are similarly modeled after TAM and GAM practices (e.g., Montana DOT (MDT) per Beckstrand et al., 2017; Wisconsin DOT per Anderson et al., 2022). Current inventories of rock slope data often exist from use of the Rockfall Hazard Rating System (RHRS) (Pierson, 1991) or similar systems, and recent work in slope asset management aims to incorporate this type of data into slope asset management plans as described below.

2.4.1 Methods of Condition Assessment

Since being developed in the 1980s, the RHRS has been used to assess rock slopes to identify rockfall risk and prioritize slopes. The RHRS varies and may be modified differently for each agency that uses it, but the general concept is that slopes are assessed based on rating several attributes that pertain to rockfall likelihood and consequence (Anderson et al., 2017b).

The historical use of RHRS means that many state DOTs have pre-existing inventories of slopes, overcoming a major obstacle of asset management. The use of RHRS can be considered as the precursor to slope asset management. RHRS may possibly be converted into condition states and inform relationships between asset condition, mitigation cost, and risk (Beckstrand and Mines, 2017). When estimating rock slope conditions from RHRS scores, researchers found that ditch effectiveness and rockfall activity were the most useful components of RHRS (Beckstrand and Mines, 2017).

RHRS primarily focuses on rockfall activity and provides an approximate risk proxy rather than a robust risk estimate. Therefore, slope condition assessments for asset management may need to be expanded upon. The MDT slope asset management plan employs the use of condition ratings of 1-5 that corresponds to either good, fair, or poor, as well as a condition index from 0-100 (Beckstrand et al., 2017). Other research focuses on correlating rock slope condition with mitigation cost and adverse event likelihood per unit area of a rock slope face (Beckstrand et al., 2015; Mines et al., 2018).

Slope mitigation measures or reinforcement systems (e.g., rock bolts, wire mesh, rockfall fences) are not well accounted for in deterioration modeling (Lane, 2006) or GAM practices. They may be treated and assessed as a separate asset altogether (Beckstrand et al., 2019; Arndt et al., 2016). Studies have investigated modes of deterioration and ways to incorporate mitigation measures into asset management plans (e.g., Lane, 2006; Fishman and Withiam, 2011). The

implementation of ground support asset management plans for underground construction and mining has also been proposed, which would seek to assess ground reinforcement lifetimes (Wellman et al., 2023). This could inform the lifecycle of some shared mitigation measures, such as rock bolts.

Though historically asset management plans have used condition indices to represent the physical state of the asset, which are then binned into condition states, some agencies such as CDOT now seek to measure the annual risk amount in dollars of a slope (e.g., AEM, 2020). Unlike condition states, risk measurements consider the hazards and consequences of an event and may be more useful to agencies. For instance, a condition state may communicate the physical state of a cut slope, but not the potential impact on a user's safety or financial loss to the agency. In addition to rockfall frequency and ditch effectiveness, risk assessments may incorporate costs related to a human life, detours from rockfall failures, vehicle operation, maintenance measures, and debris cleanup.

2.4.2 Methods of Deterioration Modeling

Markov modeling is also used in slope asset management to predict changes in condition states due to its simplicity (Beckstrand et al., 2017). One area of potential improvement in deterioration modeling is incorporating the effects of mitigation measures. Several state DOTs use a separate treatment model that predicts the costs and effects of mitigation for each condition state, but this mainly contributes to computation of lifecycle cost (Thompson, 2017). Furthermore, the lack of historical data on geotechnical assets limits the knowledge on exactly how mitigation impacts deterioration rates. The National Highways considers mitigation measures in deterioration modeling through different cohorts, such as slopes that have sheet pile walls, soil nails, or rock bolts and wire mesh (Randall, 2022).

Numerical simulations and Bayesian models are also used to understand rock and soil slope deterioration processes to create performance curves (e.g., Postill et al., 2021; Briggs et al., 2022; González et al., 2023), though they are more complex and often site-specific.

Other deterioration models may provide a constant rate of deterioration to individual components of the slope or risk score, such as rockfall frequency, ditch effectiveness, and cost inflation.

2.5 Conclusions

Traditional TAM has developed over decades, with states required to manage their pavement and bridges since the early 1990s. More recently, efforts have been ongoing to develop GAM frameworks, and states have started implementing them into existing TAM plans. Thus, GAM plans are modeled after TAM, with experts applying what they know from condition assessments and deterioration modeling in TAM to GAM. Many condition assessment methods are based on visual factors with ongoing research on potential remote sensing alternatives. These assessments typically classify geotechnical assets into one of five condition states that are then used in deterioration modeling. Since Markov models are widely used in TAM deterioration modeling for their simplicity, they are also applied often in GAM. However, knowledge is limited in geotechnical asset service life as well as deterioration rates. Therefore, transition times between condition states are first estimated with expert judgment. Overall, statistical data for model

validation as well as condition history is lacking in geotechnical asset inventories. Furthermore, agencies may still be discerning what type of performance indicators are measurable and most helpful in deterioration modeling for geotechnical assets.

In the context of slopes, existing inventories from an agency's RHRS may provide a practical starting point in slope asset management. Though a RHRS is not completely adequate for assigning condition states or assessing risk, experts have researched correlations between RHRS scores, condition states, and estimating mitigation or treatment costs. Furthermore, RHRS has allowed agencies to determine that ditch effectiveness and rockfall activity are thus far meaningful performance indicators for slopes. However, moving forward, utilizing a more direct and quantitative measure of risk may be preferable where possible.

For both slopes and geotechnical assets in general, mitigation components (e.g., slope support) and geologic material influences are not well reflected in deterioration modeling. Furthermore, standardized condition or risk assessments across different states would be helpful in developing validated deterioration modeling. Focus in these areas may aid in the improvement of a practical deterioration modeling framework for slope asset management.

3.0 Development of Conceptual Models to Predict Changes in Ditch Effectiveness and Rockfall Frequency through Time

3.1 Introduction

Common practice for physical or performance deterioration modeling of geotechnical assets includes using stochastic Markov models to forecast changes in condition states or risk values. While transition probabilities into different states may be evidence-based, Markov models only consider the present state of the asset rather than its past state to forecast changes in condition or risk (Thomas and Sobanjo, 2013). Furthermore, by applying deterioration to an entire condition state or risk value rather than individual components of the asset that deteriorate over time, the forecasted condition or risk may overestimate deterioration, as some aspects of the asset, in this case, slopes, may stay the same through time. Thus, some agencies, such as the Colorado Department of Transportation (CDOT), use deterioration models that apply deterioration to slope components used to calculate condition or risk, such as ditch effectiveness and rockfall frequency. This section presents conceptual models that predict how these slope components may change through time so that slope performance deterioration modeling may be more specific to a given slope and evidence based. Specifically, conceptual models are presented for ditch effectiveness deterioration and rockfall frequency changing as a function of time since excavation of the cut slope, scaling, and rock bolting.

To develop the conceptual models that aid in forecasting the slope's hazard and therefore the overall risk value, variables that are involved in calculating hazard and are related to the slope were first identified using the CDOT slope risk assessment (Sala and Vessely, 2022). Variables related to the consequences component of risk are generally economic or unrelated to the slope, and are therefore outside of the scope of this research.

3.2 Identification of Hazard Variables and their Tendency to Change through Time

Hazard variables relating to the slope were first identified from the CDOT slope risk assessment, as well as the likelihood that these variables may change over time (within ~100 years), thereby changing risk values (Table 3-1).

Table 3-1. Slope hazard variables used to calculate risk (Sala and Vessely, 2022).

Variable	Likely to change?
Shadow angle*	No
Ditch effectiveness	Yes
Rock mass type	No
Magnitude-frequency relationship of rockfall	Yes
Mitigation effectiveness	Yes

Ditch effectiveness is expected to change over time as the ditch fills up with rockfall debris, thereby reducing the capacity of the ditch. When the ditch is cleaned, ditch effectiveness may increase again.

Rockfall frequency is expected to change as a function of time since excavation of the cut slope, scaling, and rock bolting. In the case of excavated cut slopes, physical deterioration or increased rockfall may occur due to released confining pressures, fresh exposure to the external environment, and the cut slope approaching a new equilibrium (Nicholson et al., 2000; Huisman et al., 2011). Lithology affects the degree of weathering and disturbance a cut slope will experience from excavation largely due to rock strength; for instance, weaker sedimentary formations such as shales and mudstones may experience deeper and higher weathering effects, while sandstone and limestone formations may experience more moderate weathering effects (Huisman et al., 2011; Ersöz and Topal, 2018a).

Some methods for quantifying or assessing weathering effects on recently constructed slopes have been developed (Hack and Price, 1997; Nicholson, 2000; Ersöz and Topal, 2018b) and report that weathering most strongly influences intact rock strength, spacing of discontinuities, and shear strength along discontinuities by lowering these values. In the development of the Slope Mass Rating, Romana (1993) acknowledges that natural slopes are more stable due to long-term erosion rates that are approaching steady state.

In the case of scaling, or the intentional removal of loose rocks from slopes by hand tools or machinery (Beckstrand et al., 2020), rockfall frequency may temporarily reduce rockfall frequency. Since the effects of scaling are short term, it must be repeated at a specified interval of time (TRB, 2018; Beckstrand et al., 2020). some expert judgement estimates that scaling effectiveness may range from 2 to 10 years in the absence of other mitigation measures such as rock bolt installation (Andrew and Pierson, 2012, Pierson and Vierling, 2012, as cited in Beckstrand et al., 2020). Other sources estimate effectiveness lasting 8 to 15 years for slopes with freeze-thaw cycles and 12 to 15 years in dry climates (Brawner, 1994, as cited in Beckstrand et al., 2020). Minor scaling projects may be effective for 3 to 5 years (Wyllie and Mah, 2004, as cited in Beckstrand et al., 2020). To note, these periods are estimated and not based on robust data analysis, which explains the variation in ranges of effectiveness periods (Beckstrand et al., 2020).

Rock bolts are a form of stabilization that consist of tensioned or passive elements that aid in holding rock blocks in place. Construction for stabilization such as installation of rock bolts may cause disturbance and increased rockfall as the slope readjusts (Weidner and Walton, 2021) in the months following construction. In the long term, however, rock bolting is expected to decrease rockfall frequency of magnitudes dependent on the rock bolt spacing. Since rock bolts have a finite service life, rockfall frequency may increase as the effectiveness of bolting decreases.

Rock bolts may have life spans of tens of years. Longevity depends on the rock mass and reinforcement exposure to corrosiveness, and therefore the environment. Increased humidity, groundwater, fluctuating temperatures, and wetting-drying cycles increase corrosion rates (Kendorski, 2003; Lane and Fishman, 2005; Jiang et al., 2014). Longevity also depends on the type of anchor and degree of protection, for instance, the type of grout used and the free, unbonded length of the bolt (Lane and Fishman, 2005; Fishman and Withiam, 2011). Unprotected expansion-shell anchor rock bolts are estimated to have a service life of several decades, or around 50 years (Kendorski, 2003; Lane and Fishman, 2005). However, Split Set and Swellex bolts have previously been documented to last for less than ten years (Kendorski, 2003).

Stabilization considered in the "mitigation effectiveness" variable includes rockfall fences, concrete barriers, and draped mesh. Though the mitigation effectiveness of these measures likely decreases through time due to corrosion and repeated impact (Sasiharan et al., 2006; Luciani et al., 2018; Patnaik et al., 2019; Scavia et al., 2020), they are not directly related to the slope and are outside the scope of this research.

3.3 Conceptual Models

Considering the findings above, conceptual models were developed for ditch effectiveness deterioration and rockfall frequency changing as a function of time since excavation, scaling, and rock bolting. Each following subsection presents a conceptual model and the corresponding parameterization so that the model may be implemented for specific cut slopes.

3.3.1 Ditch Effectiveness Deterioration Conceptual Model

Figure 3.1 represents the ditch effectiveness deterioration conceptual model. This conceptual model is based on the assumption that initial ditch effectiveness, DE_0, is maintained until rockfall debris fills the ditch such that its angle is horizontal with a debris cross-sectional area of A_0. Ditch effectiveness is maintained until this point under the assumption that any influences of an elevated catchment surface are approximately offset by the reduced coefficient of restitution of a loose debris layer (in contrast to a compact ditch bottom). Thereafter, ditch effectiveness decreases linearly as a function of cross-sectional area of the talus pile (Figure 3.1A) and reaches a ditch effectiveness of 0 when the talus pile forms to its angle of repose at A_φ. Ditch effectiveness does not decrease linearly as a function of time (Figure 3.1B) since the amount of rockfall debris accumulating within the ditch is also a function of ditch effectiveness. As ditch effectiveness decreases, less rockfall stays in the ditch, thereby causing the talus pile to form at a slower rate and ditch effectiveness deterioration to occur at a slower rate. The accuracy of the model is evaluated with 2D numerical modeling of rockfall trajectories and talus pile growth simulation in Appendix A.

To apply the model and forecast changes in ditch effectiveness deterioration, the following steps are required:

1. Estimate the initial ditch effectiveness, DE_0.
2. Calculate the cross-sectional area of the talus pile needed to create a talus pile angle of zero.
3. Calculate the cross-sectional area of the talus pile when the talus pile is at its angle of repose, A_φ.
4. Derive an equation for ditch effectiveness deterioration as a function of cross-sectional area of the talus pile.
5. Express ditch effectiveness as a function of time. This involves estimating the volumetric flux of rockfall from the slope and the amount of time for the talus pile angle to become zero, t_0.

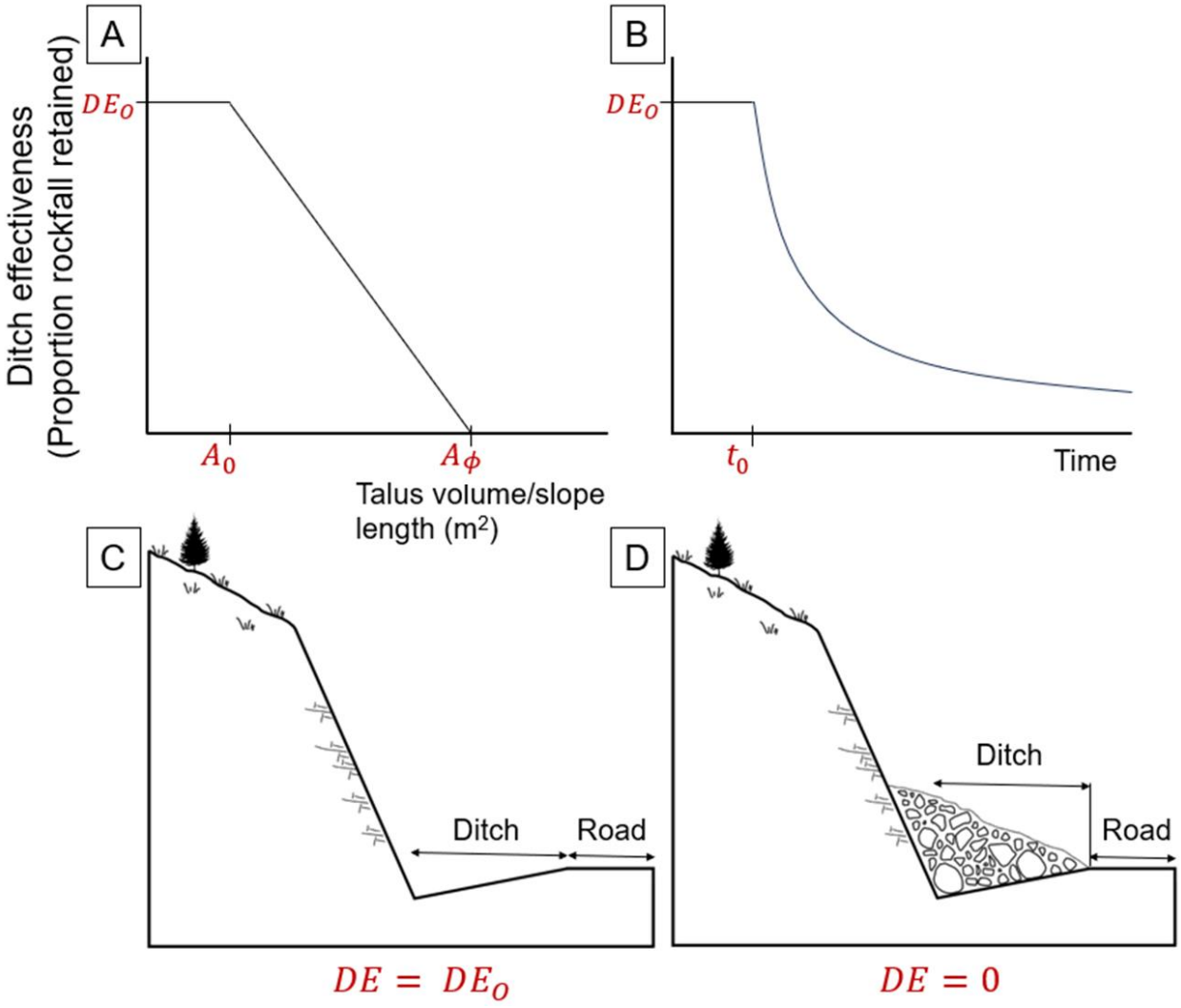

Figure 3.1. Conceptual model for ditch effectiveness deterioration. A: Ditch effectiveness deterioration as a function of the cross-sectional area of the talus pile. B: Ditch effectiveness deterioration as a function of time. C: The state representing initial ditch effectiveness, wherein the ditch is empty. D: The state representing a ditch effectiveness of zero, wherein the talus pile angle in the ditch has reached its angle of repose.

3.3.1.1 Represent Ditch Effectiveness as a Function of Cross-Sectional Area in the Talus Pile

Representing ditch effectiveness as a function of cross-sectional area of rockfall debris in the talus pile corresponds to Steps 1-4 above. The points (A_0, DE_0) and (A_0, 0) can be used to derive a linear equation for ditch effectiveness.

For Step 1, initial ditch effectiveness, DE_0, may be estimated from expert judgement or pre-existing literature and design guidelines, such as the design charts presented in Pierson et al. (2001) (e.g., Figure 3.2).

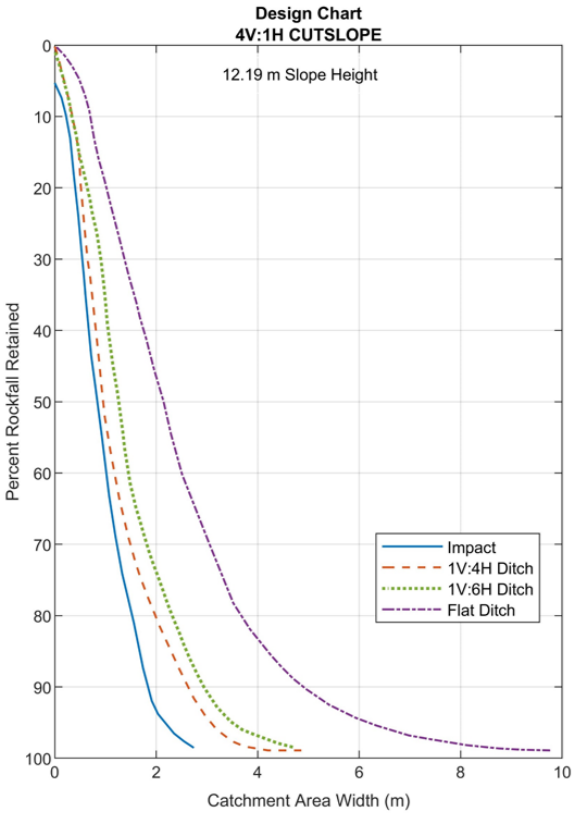

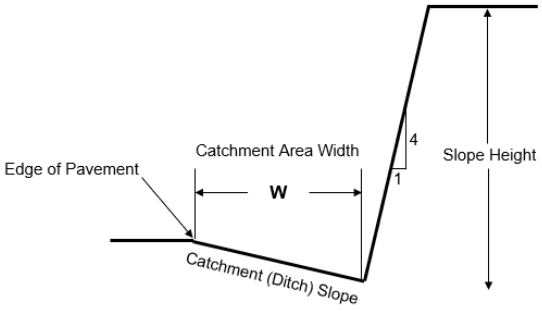

Quick Reference – 4V:1H, 12 m Cutslope Catchment Area Width - **W**				
Percent Rockfall Retained	Impact	Catchment Area Slope		
		1V:4H	1V:6H	Flat
	W (m)	W (m)	W (m)	W (m)
50%	0.8	0.9	1.3	2.1
75%	1.4	1.8	2.0	3.4
80%	1.5	2.1	2.3	3.7
85%	1.8	2.3	2.5	4.3
90%	1.8	2.7	2.9	4.9
95%	2.1	3.1	3.5	6.1
99%	2.9	4.8	4.9	9.8

Figure 3.2. Ditch design chart for a 12.2 m high 4V:1H cut slope, adapted from Pierson et al. (2001). Impact refers to the horizontal distance from the base of the cut slope to where the rock first hits the catchment area, not necessarily the final resting place.

In Figure 3.3, ditch geometry is defined by δ, α, l_b, and w, which represent the absolute value of the ditch slope angle, cut slope angle, backslope length, and ditch width, respectively. If the cut slope angle, ditch width, or ditch slope angle is unknown, they should be measured or estimated, for instance, with airborne lidar data, satellite imagery, or through an in-person field visit.

Equation 3.1 represents the cross-sectional area of an empty ditch (between the ditch base and the horizontal):

$$A_{empty} = -(0.5\, w \tan(\delta)\,[w + w \tan(\delta) \tan(\alpha_c)]) \quad (3.1)$$

where α_c is the complement of α.

Note that the convention $A_0=0$ is used for Step 2. With this convention, negative cross-sectional areas are used to represent empty space between the top of the talus pile and the horizontal, prior to the formation of a horizontal surface due to infilling. Correspondingly, negative talus pile angles represent states where the ditch has not yet filled to the point where it is flat.

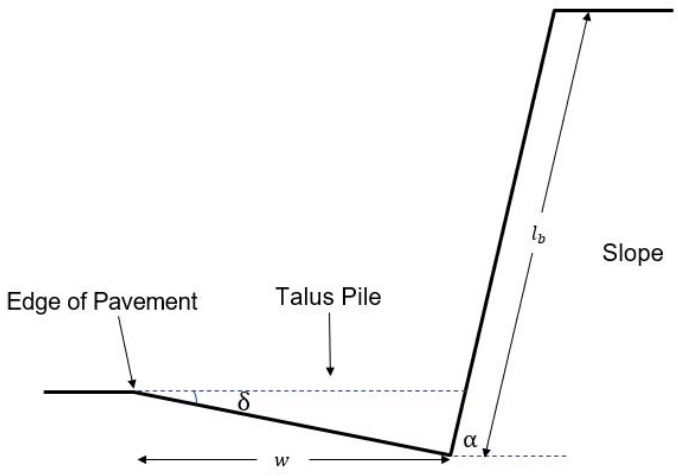

Figure 3.3. Approximation of talus pile geometry when talus pile angle is zero.

Note that all equations in this paper define angles in degrees; radians may be used if all instances of 90 degrees in equations henceforth are replaced with the equivalent value in radians, 1.57 ($\pi/2$).

To calculate A_φ in Step 3, Equation 3.2 is used and corresponds to Figure 3.4:

$$A_\varphi = 0.5 \sin(\varphi)[w + w \tan(\delta) \tan(\alpha_c)]^2[\cos(\varphi) + \sin(\varphi) \tan(\alpha_c+\varphi)] \quad (3.2)$$

Where φ is the angle of repose, which can be selected from typical values provided in the literature (e.g., φ= 34 to 37 degrees per Turner, 1996; Erlich et al., 2021). Per the convention that A_0= 0, Equation 3.2 provides the talus pile cross-sectional area above the horizontal; thus, the total cross-sectional area of all material in the talus pile is equal to the difference between A_φ and A_{empty}.

Now that the points (A_0, DE_0) and (A_φ, 0) are obtained, Step 4 can be accomplished to derive a linear rate of ditch effectiveness with respect to cross-sectional area:

$$r_A = - (DE_0 / A_\varphi) \quad (3.3)$$

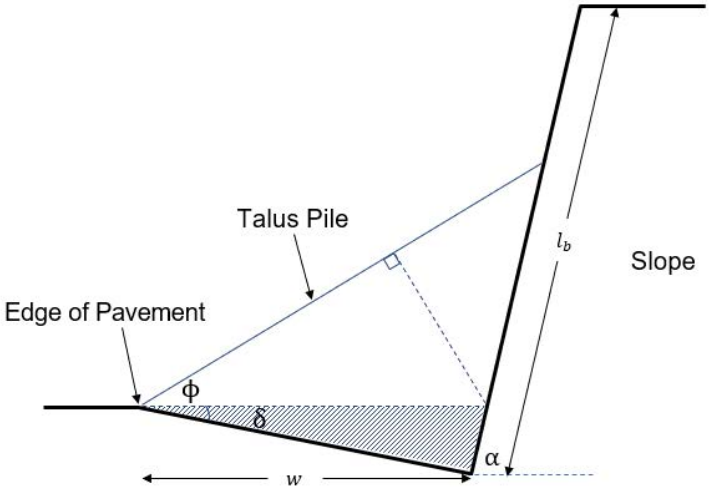

Figure 3.4. Approximation of talus pile geometry when talus pile is at its angle of repose. Equation 3.2 does not include the shaded area.

A linear equation for ditch effectiveness can now be defined:

$$DE(A) = DE_0 \qquad A \leq A_0 \qquad (3.4a)$$

$$DE(A) = DE_0 - (DE_0/A_\varphi) \qquad A > A_0 \qquad (3.4b)$$

3.3.1.2 Express Ditch Effectiveness as a Function of Time

Ditch effectiveness can be expressed as a function of time (Step 5), which allows ditch effectiveness deterioration forecasting. Ditch effectiveness is assumed to be zero once the talus pile angle has fully formed to its angle of repose; thus, the rate at which the talus pile grows depends on the rate of rockfall coming off the slope. However, the amount of rockfall that enters and stays in the ditch depends on the current ditch effectiveness at any given point in time. Therefore, the rate of ditch effectiveness deterioration is not linear with respect to time. Because ditch effectiveness decreases over time, the volume of rockfall retained by the ditch also decreases over time, and the ditch-filling and ditch effectiveness deterioration occur at an increasingly slower rate (Figure 3.1B). Equation 3.5 mathematically represents the dependence of the rate of ditch effectiveness deterioration on the current ditch effectiveness at any given point in time, t, greater than $t_{\theta=0}$:

$$dDE / dt = nDE \qquad (3.5)$$

where n represents a constant related to ditch geometry and the rate of rockfall. Equation 3.5 is a differential equation with the following solution for $t > t_0$:

$$DE(t) = DE_0 e^{n(t_r)} \qquad (3.6)$$

where t_r is the difference between t and t_0.

Note that time in Equation 3.6 is referenced to t_0, since ditch effectiveness begins decreasing at t_0, and DE_0 represents the initial condition at this point in time. To solve for n, consider the simplified case where $DE_0 = 1$, or 100%. The initial rate of ditch effectiveness deterioration as a function of time will be directly proportional to the rate of ditch effectiveness deterioration as a function of cross-sectional area, since 100% of rockfall is retained in the ditch. In particular, these values are related by the rate at which rockfall leaves the slope and adds to the cross-sectional area of the talus pile, r_{rf}. Thus, the initial rate of ditch effectiveness deterioration as a function of time is found by evaluating the derivative of DE(t) at time t_0 and relating this to r_A and r_{rf} (Equation 3.7):

$$n = r_{rf} r_A \tag{3.7}$$

However, in the case $DE_0 \neq 1$, not all rockfall volume enters the ditch. With this in mind, and to ensure Equations 3.5 and 3.6 are satisfied for all cases of DE_0, Equation 3.7 is generalized by multiplying the initial slope by DE_0 such that n can be more generally defined per Equation 3.8:

$$n = r_{rf} r_A DE_0 \tag{3.8}$$

Now t_0 and r_{rf} must be estimated to complete the equation of ditch effectiveness deterioration as a function of time. The time it takes for the talus pile angle to become zero, or the amount of time the initial ditch effectiveness remains can be found by relating the cross-sectional area of the talus pile at this point to r_{rf} (Equation 3.9):

$$t_0 = -(A_{empty}/r_{rf}) \tag{3.9}$$

To estimate r_{rf}, an MCF distribution is needed (Hungr et al., 1999; van Veen et al., 2017; Graber and Santi, 2022):

$$F(V) = aV^{-b} \tag{3.10}$$

where F(V) represents frequency of events with volume greater than or equal to V per unit time as a function of V, and a and b are intercept and scaling exponent constants, respectively. Equation 3.10 indicates that rockfall frequency is higher for smaller rockfall volumes than larger volumes.

The MCF distribution may be derived from rockfall inventories reporting the date of the rockfall and volume. Inventories may be built from remote sensing methods (e.g., DiFrancesco et al., 2020), manual rockfall identification and volume estimation (e.g., Imaizumi et al., 2020), dendrochronology (e.g., Stoffel et al., 2005), or previously documented rockfall reports (e.g., Bajni et al., 2021). In the absence of a rockfall inventory, MCF estimation methods may be used, such as the method described and evaluated in Section 5.

Once an MCF curve is obtained and normalized by slope surface area, it is integrated over a relevant volume range, $[V_l, V_u]$ (Hantz et al., 2003; Hantz et al., 2020). To obtain a rockfall rate in terms of cross-sectional area per time consistent with the conceptual model, the rate should be multiplied by the backslope, l_b. A bulking factor is additionally included to account for porosity in the talus pile:

$$r_{rf} = [ab/(d)]\left[V_l^d - V_u^d\right]l_b f_B \quad (3.11)$$

where d is equal to one minus b.

A starting value of 1.3 for f_B is recommended (Apted et al., 2006; Lato et al., 2015); however, reasonable bulking factors may range from 1.2-1.7 depending on slope material (FHWA, 2007).

Note that that for the specific case of b = 1, Equation 3.11 is undefined, and Equation 3.12 must be used instead (after Hantz et al., 2020):

$$r_{rf} = a \ln|V_l/V_u|l_b f_B \quad (3.12)$$

To use Equations 3.11 or 3.12, one needs to determine minimum and maximum volumes that are relevant to the ditch-filling process. Including smaller volumes provides a larger range of volumes considered, which may increase the rate of ditch effectiveness deterioration. Inclusion of large volumes relative to ditch size may cause the ditch effectiveness to instantly arrive at zero. Physically, the minimum volume may represent the smallest credible volume that will more likely land on the talus pile than land somewhere on the slope during its descent. The maximum volume represents the largest credible volume the ditch may retain; rockfall events larger than this volume require separate treatment from a risk assessment and asset management perspective. To establish a maximum volume, an approximate, experience-based relationship dependent on ditch width is proposed:

$$V_u = (f_w w)^{1.8} \quad (3.13)$$

where w represents ditch width in meters and f_w represents a scaling factor for ditch width. For cut slopes in Colorado, a scaling factor of 1.7-2.0 may be appropriate; in the absence of further information, 1.85 is recommended as a starting value. Realistically, V_u also depends on the slope height, slope angle, and launching features, as these factors determine the energy and final impact distance of rockfall. However, due to lack of empirical data and for simplicity, these factors are omitted.

The user is recommended to select a minimum volume, V_l, in the range of 0.0001-0.1 m^3.

3.3.2 Time-Since-Excavation Conceptual Model

The remaining conceptual models focus on how rockfall activity of a slope, represented by the MCF curve, changes through time. Figure 3.5 represents the time-since-excavation conceptual model in cumulative frequency-time space and cumulative frequency-volume space. Rockfall activity increases as soon as the cut is excavated at time t_1, which is represented by an upwards shift of the MCF curve, or an increase in the original intercept parameter a_0 by a factor of k_0. Rockfall activity continues increasing over time at a decreasing rate as the slope approaches a new equilibrium, until the slope is fully weathered at $t_f = t_1 + \Delta t$, and the final rockfall frequency is increased by a factor of $k_0 k_f$. In frequency-time space, the curvature of increasing rockfall frequency before the slope is fully weathered is represented by c.

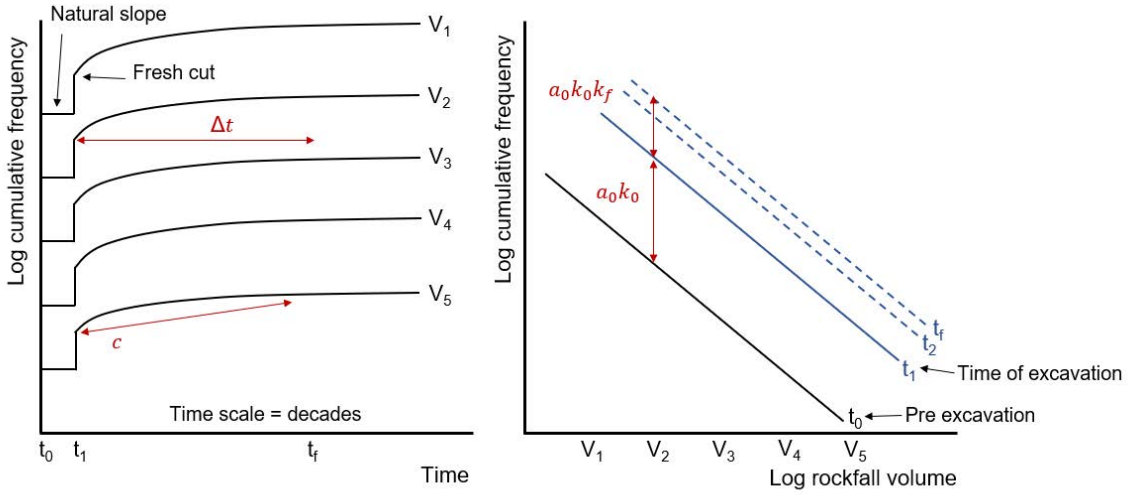

Figure 3.5. Change in rockfall frequency according to the time-since-excavation conceptual model.

The time-since-excavation conceptual model assumes pure translation of the MCF curve rather than a combination of rotation and translation. This implies that the relative distribution between small and large rockfalls does not change (Graber and Santi, 2022). Pure translation was chosen for this conceptual model for simplicity and since the intercept parameter a represents overall rockfall activity (Guerin et al., 2020), an increase or decrease in a is expected if the weathering profile changes. For instance, Weidner and Walton (2021) observed a translation in the MCF (controlled by the MCF intercept parameter a) that coincided with an increase in precipitation. Similarly, Malsam et al. (2021) and Hollander (2024) observed a shift in the MCF curve with different values of a for the same cut slope dependent on the time of year.

Rockfall frequency over time in the time-since-excavation conceptual model is represented by Equation 3.14, where the mathematical form of the middle two components of the piecewise function were modeled after equations developed by Walton and Diederichs (2015), originally in the context of rock dilatancy:

$$f(t,V) = a_0 V^{-b} \qquad t < t_1 \tag{3.14a}$$

$$f(t,V) = a_1(t) V^{-b} \qquad t_1 \leq t < t_1 + \Delta t\, e^{(f)/c} \tag{3.14b}$$

$$f(t,V) = a_2(t) V^{-b} \qquad t_1 + \Delta t\, e^{(f)/c} \leq t \leq t_1 + \Delta t \tag{3.14c}$$

$$f(t,V) = a_0 k_0 k_f V^{-b} \qquad t > t_1 + \Delta t \tag{3.14d}$$

where t is time, V is rockfall volume, a_0 is the initial MCF intercept parameter, t_1 is the time of excavation, k_0 is a factor that a_0 changes by as a result of excavation (generally, $k_0 \geq 1$), Δt is the amount of time it takes for the slope weathering state to reach an equilibrium, c defines the curvature of the rockfall frequency function through time, f is equal to c minus one, k_f is the factor that a_0k_0 changes by once the slope is fully weathered (generally, $k_f \geq 1$), and $a_1(t)$ and $a_1(t)$ are represented by the following (after Walton and Diederichs, 2015):

$$a_1(t) = a_0k_0 + [(a_0k_0k_f - a_0k_0)/\Delta t](t - t_1)(c/e^{(f)/c}) \quad (3.15)$$

$$a_2(t) = a_0k_0 + (a_0k_0k_f - a_0k_0)(c \ln((t - t_1)/\Delta t) + 1) \quad (3.16)$$

3.3.3 Scaling and Rock Bolting Conceptual Models

Figure 3.6 represents the scaling conceptual model in cumulative frequency-time space and cumulative frequency-volume space. Rockfall frequency immediately decreases at the time of scaling, t_1, and increases as scaling loses its effectiveness over time. At $t_1+\Delta t$, scaling is no longer effective, thereby causing rockfall frequency to return to its original state. The initial decrease in rockfall frequency is demonstrated in frequency-volume space by a downward shift of the MCF curve, Δf, which is reflected in a change in both a_0 and b_0 since the rockfall frequency does not change for volume V_{max} (i.e., the MCF curve undergoes translation and rotation). Minimum and maximum volumes affected by scaling are included since scaling likely only affects rockfall frequency for a certain range of volumes. Scaling may be more effective for smaller rockfall volumes; however, Weidner and Walton (2021) observed that mechanical scaling is potentially ineffective for smaller volumes less than 1 m^3. Any immediate increase in rockfall frequency after scaling is not included in the conceptual model for simplicity. The curvature of changing rockfall frequency through time is represented by c.

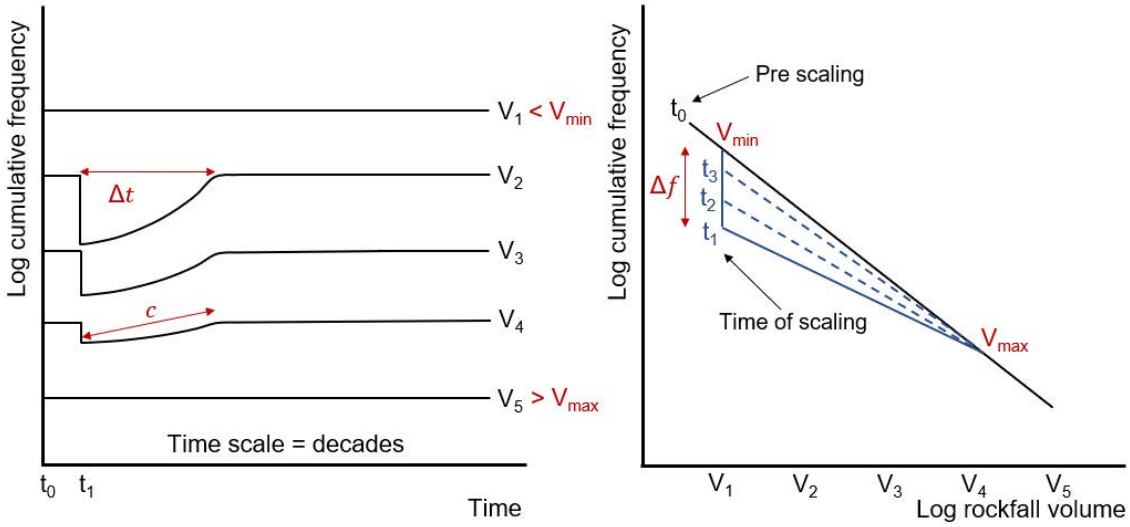

Figure 3.6. Change in rockfall frequency according to the scaling conceptual model.

Figure 3.7 represents the rock bolting conceptual model, which contains the same parameters as the scaling conceptual model. Bolting, however, is expected to be effective for a longer amount of time than scaling.

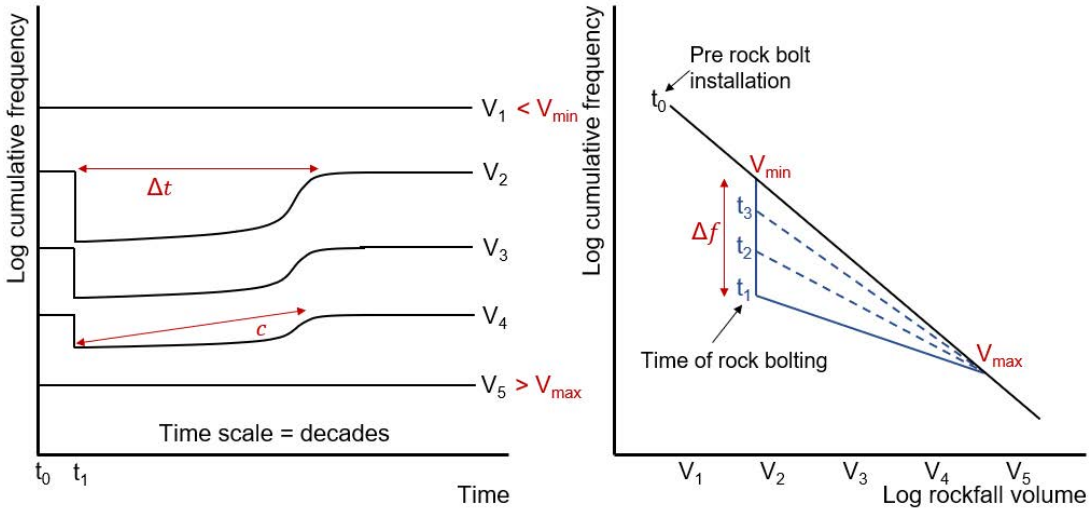

Figure 3.7. Change in rockfall frequency according to the rock bolting conceptual model.

The effect of scaling and bolting on rockfall frequency through time is represented with Equation 3.17 (after Walton and Diederichs, 2015):

$$f(t,V) = a_0 V^{-b_0} \qquad V < V_{min},\ V > V_{max} \tag{3.17a}$$

$$f(t,V) = a_0 V^{-b_0} \qquad t < t_1,\ t > t_1 + \Delta t,\ V_{min} \le V \le V_{max} \tag{3.17b}$$

$$f(t,V) = a_1(t) V^{-b(t)} \qquad t_1 \le t < t_1 + \Delta t\, e^{(f)/c},\ V_{min} \le V \le V_{max} \tag{3.17c}$$

$$f(t,V) = a_2(t) V^{-b(t)} \qquad t_1 + \Delta t\, e^{(f)/c} \le t \le t_1 + \Delta t,\ V_{min} \le V \le V_{max} \tag{3.17d}$$

where a_0 and b_0 are the initial MCF parameters before scaling, V_{min} and V_{max} are the minimum and maximum volumes that are affected by scaling or bolting respectively, V_{max} is a factor of that a_0 changes as a result of scaling or bolting (generally, $k \le 1$), c defines the curvature as rockfall frequency increases to its original activity, and $a_1(t)$ and $a_2(t)$ are represented by the following (after Walton and Diederichs, 2015):

$$a_1(t) = a_0 k + [(a_0 - a_0 k)/\Delta t](t - t_1)(c/e^{(f)/c}) \tag{3.18}$$

$$a_2(t) = a_0 k + (a_0 - a_0 k)(c \ln((t - t_1)/\Delta t) + 1) \tag{3.19}$$

Since b(t) is constrained at $V=V_{max}$, b(t)is represented with the following:

$$b(t) = -(\ln[a_0 V_{max}^{-b_0}/a(t)] / \ln(V_{max})) \tag{3.20}$$

3.4 Discussion

The conceptual models presented in this section were developed to predict changes in ditch effectiveness and rockfall frequency since these are hazard variables within the CDOT slope risk assessment framework that may change through time. However, ditch effectiveness and rockfall

frequency are common variables used to represent a slope's condition state or risk value (Beckstrand and Mines, 2017; Thompson, 2017); thus, the conceptual models may be adapted into other deterioration frameworks.

3.4.1 Ditch Effectiveness Deterioration Conceptual Model

One limitation of the ditch effectiveness deterioration conceptual model is that it treats ditch effectiveness as a direct proportion of rockfall retained. In this metric, the proportion or percentage of rockfall retained in the ditch is considered to be independent of rockfall volume. That is, the percentage of rockfall events of small volumes retained would be the same as the percentage of large rockfall volumes retained, until a rockfall event greater than V_u occurs, in which case the ditch effectiveness is considered to be zero. This may not be realistic for all cut slopes.

The ditch effectiveness deterioration conceptual model also assumes a constant rockfall volumetric flux, which is adjusted to account for a bulking factor. However, the rockfall rate may not remain constant over the time that the ditch effectiveness is forecasted to reach zero (as demonstrated in the rockfall frequency conceptual models), since this could take hundreds of years depending on the volumetric flux of rockfall. A maximum volume was also applied when deriving the rockfall rate, since any larger event would be assumed to reach the road and require separate treatment beyond ditch cleaning. Events larger than the maximum volume have the potential to substantially skew the estimated evolution of ditch effectiveness towards more rapid rates of decrease.

The conceptual model also assumes no maintenance or ditch-clearing; however, the model may be used to plan such activities. For instance, the model can be used to estimate the time at which the ditch will reach a target minimum ditch effectiveness when maintenance is desired. The approximated time can allow for proper planning of funds and maintenance at all stages of the slope life cycle from design to routine operations. Ditch-clearing would effectively cause a "reset" to the initial ditch effectiveness. Forecasting ditch effectiveness for these purposes may be most useful, rather than predicting when the ditch effectiveness will begin to approach zero. For instance, the design for a new slope can include guidance on estimated timing for ditch-cleaning as input into an agency's investment schedule for asset management plans. Estimating the timing for ditch-cleaning in design also can inform trade off analyses between different slope and mitigation configurations, such as narrower ditches and slope mesh compared with wider ditches and no mesh.

If the user of the conceptual model finds the model to be too conservative, such as in the case of shallow cut slopes as described in Appendix A, the conceptual model may be modified according to Figure 3.8. Possible modifications include initial ditch effectiveness being maintained to a volume greater than $-A_{empty}$ or ditch effectiveness reaching zero at some factor, f, of the original angle of repose selected as 35 degrees, or a combination of both modifications.

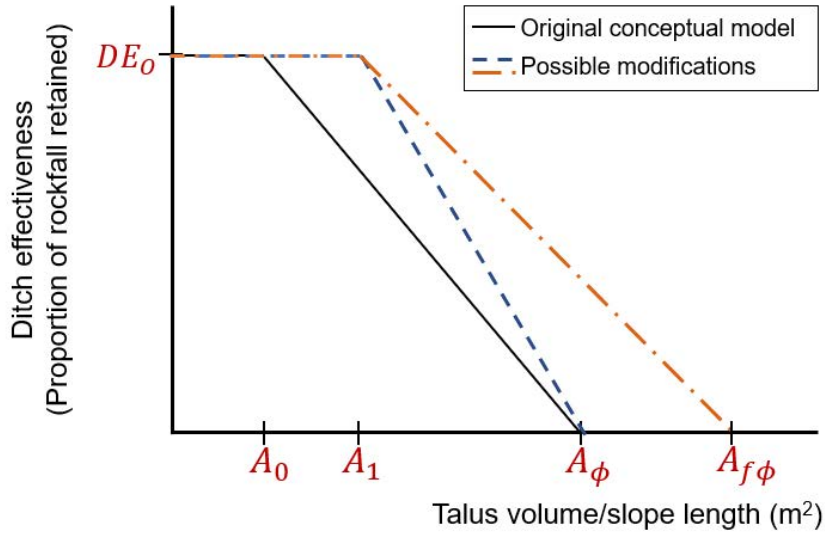

Figure 3.8. Possible modifications to the ditch effectiveness deterioration conceptual model.

3.4.2 Rockfall Frequency Conceptual Models

The rockfall frequency conceptual models are also intended to be idealized simplifications of reality. For instance, to allow for straightforward parameterization, the time-since-excavation conceptual model assumes pure translation and no rotation in the MCF curve to represent increased rockfall frequency. The scaling and rock bolting conceptual models show linear changes in the MCF curve, represented by a combination of translation for smaller affected rockfall volumes and rotation as rockfall volume increases. In reality, as rockfall frequency returns to its original frequency, the MCF may locally exhibit some curvature as opposed to the straight (and sometimes discontinuous) segments in the conceptual models.

The magnitude of change in rockfall frequency as a result of excavation, scaling, and rock bolting is uncertain. However, the effectiveness of scaling and rock bolting may be estimated if transportation agencies have some record of rockfall activity before and after mitigation, even if rockfall activity is not represented with MCF curves. Likewise, the effect of time since excavation can be estimated if transportation agencies have records of slope ratings or rockfall activity through time or before and after regrading a slope. Such records are provided by the Washington Department of Transportation and are used for analysis in Section 6.

The conceptual models predicting rockfall frequency also do not include short-term fluctuations of the MCF curve. Rockfall activity may change within the year due to seasonal variation (Luckman, 1976; Douglas, 1980; Macciotta et al., 2017; Imaizumi et al., 2020; Malsam et al., 2021; Hollander, 2024), with seasonal rockfall trends being site and location dependent. For instance, Malsam et al. (2021) observed less rockfall activity during winter for a cut slope in Colorado, while Dewez et al. (2013) observed increased rockfall activity during winter for a coastal cliff in northern France. Despite observing seasonal variation, Malsam et al. (2021) noted that rockfall activity remained consistent over a two-year monitoring period. Furthermore,

Phillips (2024) found that meteorological variables have limited impact on overall rockfall frequency but strongly influence what times of year rockfall tends to occur.

Rather than changing rates of physical deterioration, seasonal patterns may serve more as rockfall triggers that affect what times of year increased rockfall activity occurs. Climatic processes that are linked to seasonal variation and act as rockfall triggers include precipitation (i.e., intense rainfall), temperature variations (i.e., freeze-thaw cycles), and wet-dry cycles (Sass, 2005; Arosio et al., 2013; Delonca et al., 2014; Bajni et al., 2021; Mainieri et al., 2022). Thus, seasonal and other short-term fluctuations of the MCF curve are not included in the conceptual models because they do not necessarily reflect a change in the underlying hazard and therefore physical deterioration. Changes in the underlying climatic processes, however, may affect rates of physical deterioration.

The deterioration modeling within the CDOT slope risk assessment framework and the conceptual models are also simplified in that they do not consider climate change. In some regions, climate change is expected to increase slope risk (e.g., Randall, 2022). Specifically, climate change may alter weather patterns that trigger rockfall, thereby causing the rockfall frequency to change over time (Pratt et al., 2018; Graber and Santi, 2022). For instance, increased precipitation may increase rockfall. Freeze-thaw cycles may change, causing the timing of rockfall to change. Warmer temperatures may thaw slopes earlier and cause permafrost degradation in high mountain areas, which increases rockfall frequency (Allen and Huggel, 2013; Ravanel and Deline, 2014; Kellerer-pirklbauer et al., 2016; Graber and Santi, 2022).

Though not as well-studied, increased wildfire may also alter rockfall patterns. Possible mechanisms explaining a correlation between increased rockfall activity and wildfire in some regions includes the following (De Graff and Gallegos, 2012; Sarro et al., 2021):

- Loss of stabilizing effect from burned vegetation.
- Loss of vegetation that prevented rockfall runout.
- Thermal expansion and rock fragmentation in high temperatures.
- Degradation of mitigation measures.
- Inability for chemically altered soil to buttress the slope.

Though climate change is outside the scope of this research, climate change models may be added separately in addition to the conceptual models or a given transportation agency's deterioration framework.

3.5 Conclusions

Four conceptual models are presented in this section: Ditch effectiveness deterioration, and rockfall frequency changing due to time since excavation, rock bolting, and scaling. The ditch effectiveness deterioration conceptual model assumes a constant ditch effectiveness until the ditch fills with rockfall debris so that its angle is horizontal, followed by a linear decrease in ditch effectiveness as a function of material volume in the ditch. The time-since-excavation conceptual model assumes an initial increase in rockfall frequency at the time of excavation, followed by increasing rockfall activity at a decreasing rate until the slope is fully weathered. Lastly, the scaling and rock bolting conceptual models assume an initial decrease in rockfall

frequency at the time of mitigation, followed by an increase in rockfall activity to the slope's original rockfall frequency as the mitigation decreases in effectiveness over time.

The inputs of the conceptual models may be specific to the given slope's characteristics, such as age and geometry. Thus, unlike some prior deterioration modeling methods such as Markov models, the future condition or risk of the slope considers the slope's past rockfall activity and ditch effectiveness. Furthermore, changes in slope condition or risk only reflect changes in variables that are likely to change rather than stay the same throughout time. This would result in a more accurate representation of the slope and more effective management of resources within the transportation agency.

4.0 Historical Rates of Rockfall for Colorado Cut Slopes

4.1 Introduction

Quantifying rockfall frequency of Colorado rock slopes allows for both hazard assessment and initial inputs to estimate physical deterioration. As previously mentioned in Section 3.0, the MCF distribution for a given slope quantifies rockfall frequency for a given volume or larger, and can be derived from a rockfall inventory.

This section describes seven cut slopes in Colorado that were monitored with either photogrammetry or terrestrial lidar scanning (TLS) to create rockfall inventories with at least two years of data. These rockfall inventories were used to create a resulting MCF curve for each slope. The data was processed and updated by Cam Phillips, Jacob Hollander, Luke Weidner, and Adam Malsam. The data collection, processing, and results are summarized from Phillips (2024), where they are described in detail.

4.2 Studied Slopes

Rockfall frequency was quantified for rock slopes named Glenwood Springs (GW), Vail Pass (VP), Idaho Springs (IS), Floyd Hill (FH), Slope E (E), Slope HI (HI), and Manitou Springs (MS), largely after the location of the slope. The location of each slope is shown in Figure 4.1 (Phillips, 2024).

Slope characteristics, such as lithology, size, and aspect, may affect the level of rockfall activity at each slope. Slope characteristics are summarized in Table 4-1 after Phillips (2024).

Table 4-1. Slope characteristics for each studied Colorado cut slope after Phillips (2024).

Slope Characteristic	GW	VP	IS	FH	E	HI	MS
Lithology	Megacrystic granite (Kirkham et al., 2009)	Sandstone and mudstone (Kellogg et al., 2011)	Biotite gneiss (Sims, 1964)	Biotite gneiss (Sheridan and Marsh, 1976)	Granitic gneiss (Scott, 1972)	Granitic gneiss (Scott, 1972)	Arkosic sandstone and mudstone (Keller et al., 2003)
Base Width (m)	180	330	45	370	100	240	150
Height (m)	50	65	20	50	45	17	20
Area (m^2)	6,355	17,725	748	17,003	3,987	4,914	2,500
Slope Angle (degrees)	65	55	48	72	60	67	75
Aspect	SE	W	S	S-SE	S	S-SW	S
Elevation (ft)	5,860	10,020	7,950	7,950	6,140	6,020	6,600

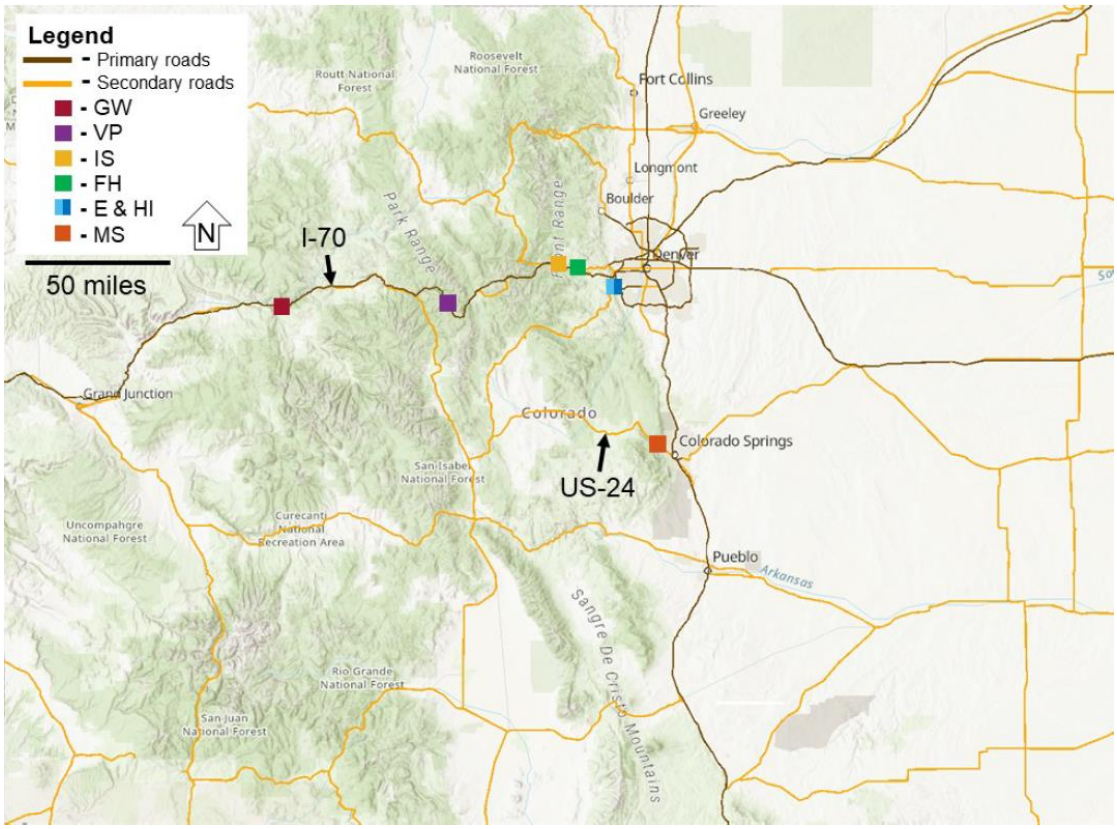

Figure 4.1. Location of each cut slope in Colorado monitored for rockfall in Phillips (2024). Slopes E and HI are separated by approximately 0.5 miles along CO-74.

4.3 Data Collection

To monitor rockfall and create rockfall inventories, repeated TLS and photogrammetry was used. A five-camera fixed-site photogrammetry was applied at IS (Hollander, 2024) and MS (Walton et al., 2023), while TLS with a FARO Focus Premium was used to obtain point clouds of the rest of the slopes. The temporal and spatial resolution of lidar data varied for each slope, depending on the distance from the Colorado School of Mines campus and the amount of overlap between each scan, respectively. For instance, sites that were further away from the Colorado School of Mines were scanned with less frequency. Additionally, sites that had more overlap between scans generally had point spacing of 2 cm or less. Data gaps are noted in Phillips (2024), and data collection is summarized for each slope in Table 4-2.

Table 4-2. Details of data collection and rockfall inventories for each studied cut slope (after Phillips, 2024).

Data Property	GW	VP	IS	FH	E	HI	MS
Location	Glen-wood Springs I-70	Vail Pass I-70	Idaho Springs I-70	Floyd Hill I-70	Morrison CO-74	Morrison CO-74	Manitou Springs US-24
Monitoring Method	TLS	TLS	Photo-gram-metry	TLS	TLS	TLS	Photo-gram-metry
Data Collection Interval	6 mo.	6 mo.	1 day	1 mo.	1 mo.	1 mo.	1 day
Dates Included in Analysis	10/19/17-10/07/22	12/03/21-10/15/23	03/13/18-09/15/23	02/11/16-05/01/22	02/22/21-10/26-23	02/22/21-10/26/23	01/24/20-09/16/23

4.4 Rockfall Inventory Development

To process the point clouds that were collected for each slope, the following general process was completed. A more detailed workflow is described in Phillips (2024), and photogrammetry setups and workflows are described in Hollander (2024) for IS and Walton et al. (2023) for MS.

1. Register new scans to a base or reference point cloud for the slope in CloudCompare (Girardeau-Montaut, 2024) using manual point matching followed by the Iterative Closest Point algorithm (Besl and McKay, 1992).

2. Remove clutter and noise not representing the rock slope, including the road, road infrastructure (e.g., signs and light poles), vegetation, snow, and ice.

3. Subsample the point cloud to a uniform point spacing.

4. Compute the forward and reverse Multiscale Model to Model Cloud Comparison (M3C2) change between two subsequent point clouds (Lague et al., 2013).

5. Merge the forward and reverse change and cluster negative changes that represent potential rockfalls. The cluster method used in this analysis was the Density Based Spatial Clustering of Applications with Noise (DBSCAN) (Ester et al., 1996).

6. Manually validate each cluster to identify true and false rockfalls.

7. Calculate the volume of each true rockfall cluster. The method used in this analysis was the iterative AlphaShape approach for surface reconstruction (Bonneau et al., 2019).

8. Note the date of each rockfall and the associated volume.

To derive the MCF distribution, the rockfall inventory for each slope is ranked from the largest rockfall to the smallest rockfall. Cumulative frequency is calculated by dividing the rank by the time constraint of the database (Graber and Santi, 2022). A least squares linear regression is then typically fitted over the ranked data to estimate the power law above a minimum threshold, x_{min}. x_{min} is applied since the data usually does not follow a power law below a minimum volume and can be found using statistical methods described in Clauset et al. (2009).

4.5 MCF Distributions

The resulting MCF curves are shown in Figures 4.2 and 4.3. Figure 4.3 is normalized by slope area for a more direct comparison between slopes (Janeras et al., 2023), since larger slopes may inherently produce more rockfall. VP produces the highest rate of rockfall, while IS produces the lowest rate of rockfall according to Figure 4.2 (Phillips, 2024). After normalization, it is evident that MS and VP produce the highest rockfall activity per square meter, while FH produces the lowest (Phillips, 2024).

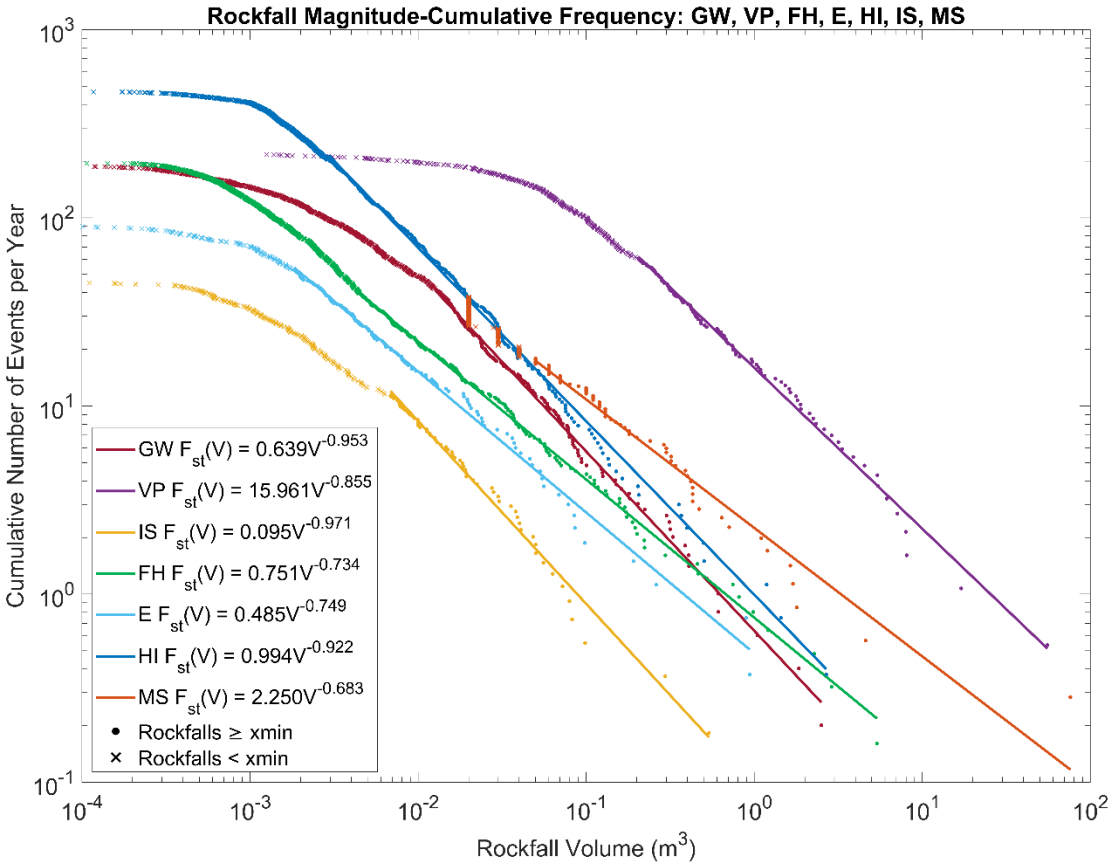

Figure 4.2. Rockfall MCF curves for the seven monitored cut slopes. Fitted power laws representing the MCF curves are shown in the legend (Phillips, 2024).

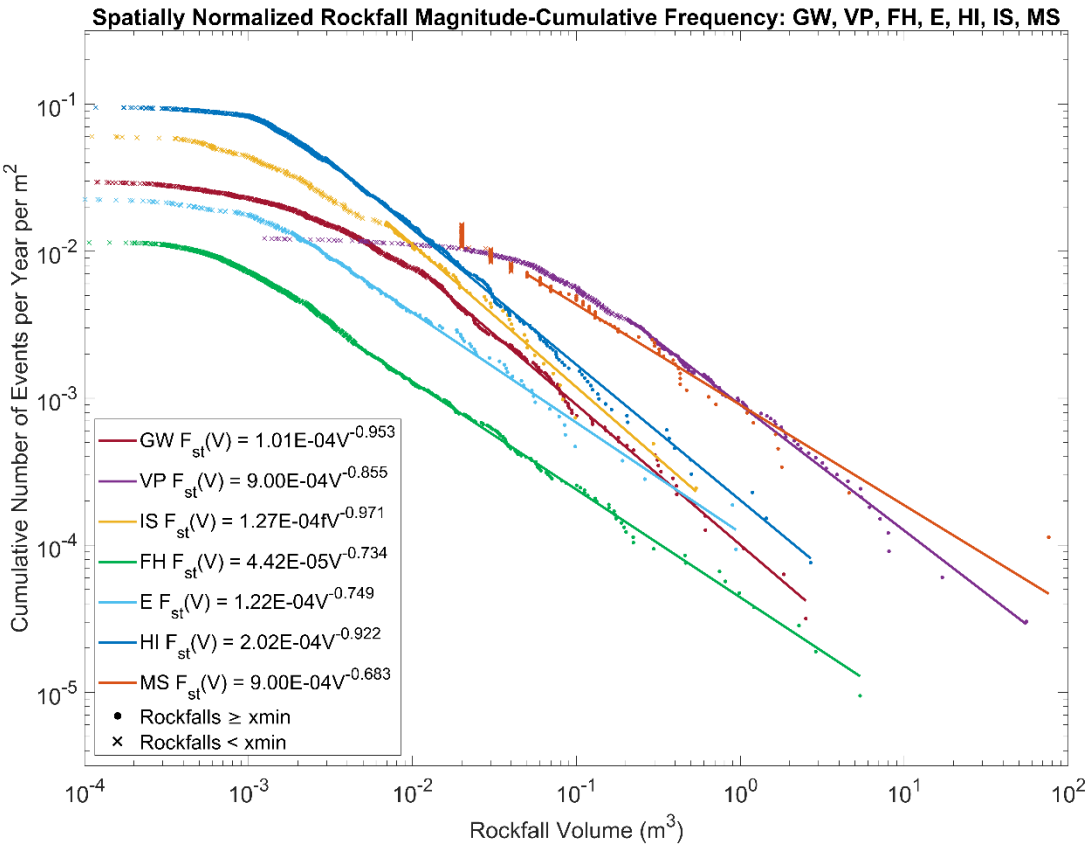

Figure 4.3. Rockfall MCF curves for the seven monitored cut slopes, normalized by slope surface area (Phillips, 2024). The intercept parameter a changes as a result of normalization.

4.6 Discussion

Phillips (2024) identified two major categorical causes for differing MCF curves of the studied Colorado slopes: conditioning and triggering factors due to climate and, more notably, lithology and geological structure.

Precipitation or total liquid input (the combination of liquid precipitation and snowmelt) is identified as the main triggering factor for rockfall in Colorado (Phillips, 2024). Precipitation was identified as the main triggering factor for slopes MS and IS rather than freeze-thaw cycles (Hollander, 2024; Malsam, 2022; Walton et al., 2023). Contrastingly, the higher elevation of VP results in longer freezing periods, more freeze-thaw cycles, and more snowmelt than MS. Despite climatic differences, VP and MS have similar rates of rockfall activity, which may occur either due to stronger lithological controls on rockfall or the combination of oversteepening and climate resulting in similar rockfall activity for each slope (Phillips, 2024). In other words, less oversteepening but harsher climate at VP results in similar rockfall activity as more oversteepening and a milder climate at MS.

The climate at the Front Range slopes (IS, FH, E, and HI) is generally the same, though exact

liquid input may vary for each of these slopes. GW experiences differences in weather conditions relative to the Front Range slopes since it is west of the continental divide and experiences more freeze-thaw cycles and higher differences in daily temperatures. Climatic differences may explain the timing of rockfalls during the year rather than long-term trends and major differences in rockfall activity (Phillips, 2024). Climatic metrics and their effect on the MCF curves are presented and discussed in further detail in Phillips (2024).

Lithology and geological structure may have a greater influence on differences in rockfall activity between slopes (Phillips, 2024). Phillips (2024) found that generally, blocky crystalline slopes (E, FH, and GW) had lower normalized "a" values and therefore lower rockfall activity than foliated, seamy, crystalline slopes (IS and HI). After identifying the number of discontinuity sets and performing kinematic analyses, Phillips (2024) additionally found that the total number of discontinuities, slope angle, oversteepening, and number of possible failure modes do not necessarily correlate with overall rockfall activity. Therefore, lithology may have a stronger control on rockfall activity. Identifying the geology (i.e., crystalline or sedimentary) and general rock mass structure (i.e., blocky, disintegrated, interbedded) may provide preliminary estimates on the normalized a and b MCF parameters, which are provided in Phillips (2024).

4.7 Conclusions

Rockfall activity is quantified for seven Colorado cut slopes with varying lithology and structure using MCF distributions. The slopes are repeatedly monitored at certain time intervals using TLS or photogrammetry. The resulting point clouds are used to identify rockfalls and calculate rockfall volumes, which allows for the creation of a rockfall inventory. The MCF distribution is the resulting power law fit of the ranked rockfall inventory.

MCF curves differ between slopes; however, VP and MS, which are both interbedded sedimentary slopes, have similar rates of rockfall. Phillips (2024) concluded that climatic differences between slopes control the timing of the rockfalls throughout the year but have limited influence on overall hazard level over longer timescales. Differences in rockfall activity may be more controlled by lithology and geologic structure (i.e., the general rock mass), which allows for preliminary estimates of MCF parameters for Colorado slopes.

The MCF curves in Figures 4.2-4.3 can be used to estimate rockfall activity for other Colorado cut slopes with similar lithological and rockmass characteristics, which provides a hazard assessment and an initial input for rockfall frequency in the proposed conceptual models. Physical deterioration may then be predicted using the conceptual models.

5.0 Evaluating a Practical Method for Rockfall Magnitude-Cumulative Frequency Estimation

5.1 Introduction

Monitoring rockfall along transportation corridors is imperative for understanding rockfall frequency and estimating risk associated with cut slopes (Hungr et al., 1999). A risk value communicates both the hazard of the slope and the potential consequences to roadway users. Rockfall hazard is represented by rockfall magnitude-cumulative frequency (MCF) distributions, which describes how often a certain rockfall volume or larger will occur. Thus, the MCF curve can be used as a key input for estimating cut slope risk.

As previously mentioned, the MCF distribution is typically derived from a rockfall inventory. Remote sensing methods have the potential to provide a higher temporal and spatial resolution record of rockfall occurrence (Graber and Santi, 2022) and more accurate volume estimations than other methods. However, they often require several years of monitoring to capture infrequent, large events and accurately represent rockfall hazard. Furthermore, transportation agencies in mountainous regions may have hundreds to thousands of slope assets; thus, maintaining rockfall inventories and remote sensing-based monitoring is infeasible for every slope. Terrestrial lidar scanning (TLS) monitoring, for instance, requires repeated scans at a specific time interval. Remote sensing-based monitoring may also require a significant amount of data processing to develop a rockfall inventory from raw data. Consequently, a practical method of estimating the MCF curve for a given slope, absent a detailed rockfall inventory, is valuable for preliminary risk assessments.

In this study, a rapid, practical method of estimating the MCF curve is tested on six cut slopes in Colorado that have at least two years of remote sensing data. The estimated MCF curves are then compared against the remote sensing-based MCF curves to evaluate the accuracy of the estimation method. Though the remote sensing-based MCF curves are considered to represent the “true” MCF distributions in the context of this study, they have some uncertainty dependent on data resolution and steps in the data processing (e.g., Williams et al., 2019; DiFrancesco et al., 2021; Walton and Weidner, 2022).

Large portions of this section are reproduced from the following conference paper with permission of the American Rock Mechanics Association: Werley, K., Sala, Z, Hille, M., Vessely, M., and Walton, G. Evaluating a Practical Method for Rockfall Magnitude-Cumulative Frequency Estimation. Proceedings of the 58th Rock Mechanics Symposium, paper no. ARMA-24-0147.

5.2 Methods

The MCF estimation method (Figure 5.1) was developed by BGC Engineering (Sala and Vessely, 2022) to aid in rock slope risk estimation for CDOT, based on previous work by Lato et al. (2016). The method averages the inspector inputs of rockfall frequency proportions with literature values for the chosen rock mass type to produce an MCF curve. To apply the method, the inspector may perform a desktop inspection of the given slope, using Google Earth or other GIS data, or by assessing the slope in the field.

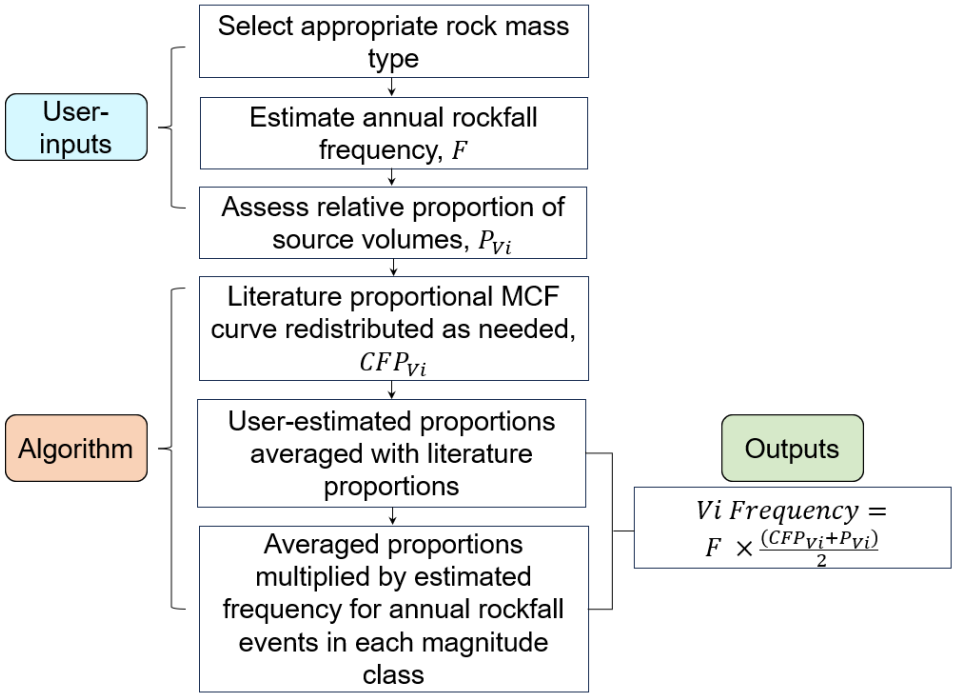

Figure 5.1. MCF curve estimation method used by CDOT. Literature curves are redistributed if the user believes the slope is not capable of producing block sizes of a certain volume class (i.e., proportion of zero for a volume class).

Possible rock mass types include “massive”, “typical”, “fractured”, and “block-in-matrix.” The user estimates proportions of source volumes for five different volume classes according to Table 5-1.

Table 5-1. Rockfall source volume classes.

Category	V_1	V_2	V_3	V_4	V_5
Volume range (m^3)	< 1	1-10	10-100	100-1000	> 1000
Representative volume (geometric mean) (m^3)	0.3	3	32	316	3162

The MCF estimation method was applied via field inspection at six different cut slopes in Colorado (Tables 4-1, 4-2, and Figure 5.2). Each site has a rockfall inventory derived from TLS or photogrammetry monitoring and therefore a remote sensing-based MCF curve to compare the

estimation method against. To compare the variability between users, three inspectors with experience in engineering geology applied the MCF curve estimation to each site, except for Manitou Springs, where only two inspectors were available. To establish consistent practices in applying the method, the inspectors collaborated when first applying the method to slopes E and HI.

After user inputs were entered into the algorithm, three sets of MCF curves were obtained for each slope: MCF curves based solely on the user-estimated annual frequency and proportions, the literature MCF curves using redistributed proportions, and the final averaged MCF curves considering redistributed literature and user- estimated proportions. These MCF curves were then compared against each other and the remote sensing-based MCF curves.

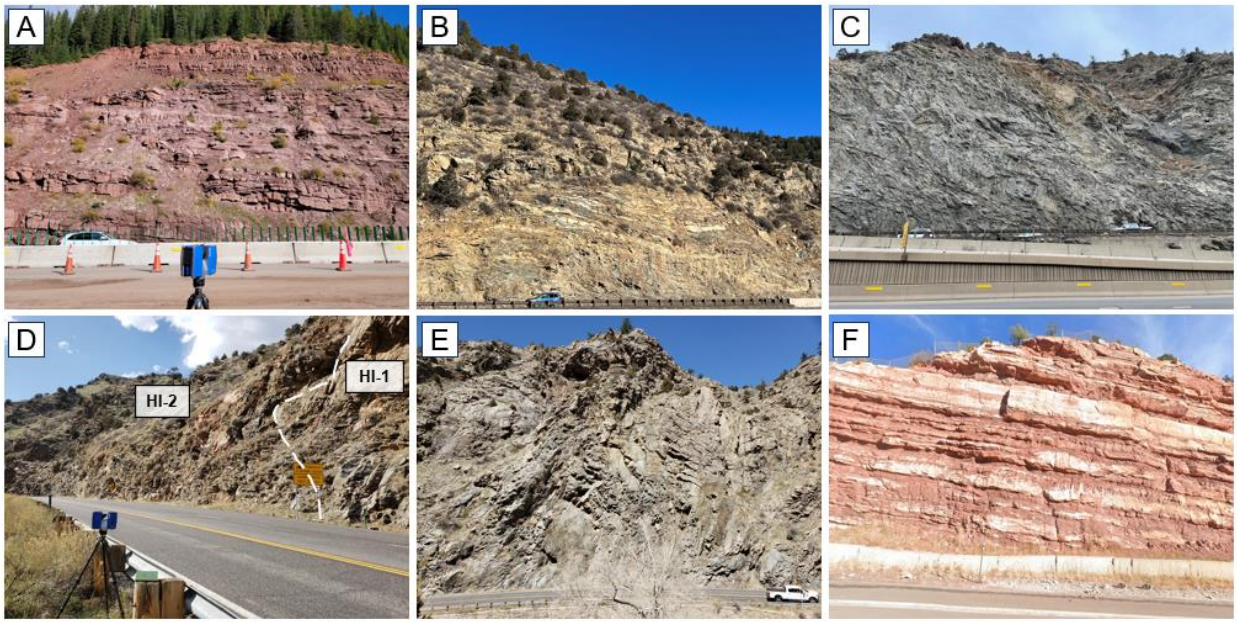

Figure 5.2. Cut slopes used for testing the MCF curve estimation method. A: Vail Pass (Courtesy of Cam Phillips). B: Idaho Springs (Courtesy of Jacob Hollander). C: Floyd Hill (Courtesy of Ellie Longar). D: Slope HI (Courtesy of Luke Weidner). E: Slope E (Courtesy of Luke Weidner). F: Manitou Springs (Google Earth imagery, 2023).

5.3 Results

The resulting MCF curves for each inspector and slope are shown in Figure 5.3. The selected rock mass type determines the literature MCF values and therefore influences the averaged MCF curve at each site; thus, rock mass types are shown in Table 5-2. The majority of cut slopes are considered "typical," and a discrepancy between inspectors occurred at the Floyd Hill site. At slope HI, the inspectors decided that the proportions of different rockfall source volume classes varied across the slope enough to justify splitting the slope into two different inspections. HI-1 refers to the east portion of the slope (approximately 30% of the entire slope length) while HI-2 refers to the west portion (approximately 70% of the slope length).

The Root Mean Squared Error (RMSE) of the log-transformed cumulative frequency values was

calculated based on comparison of the averaged MCF curves and the remote sensing-based MCF curves (Table 5-2), as the remote sensing-based MCF curves are considered the best approximation of the true MCF curve for each slope. The method performed moderately well with an average RMSE of 0.96 across all slopes and inspectors. Because the RMSE is log-transformed, this equates to an average error that is just under one order of magnitude. The estimation method performed most poorly for Idaho Springs. Furthermore, the method overestimated rockfall frequency for all sites except Vail Pass.

Table 5-2. Assigned rock mass type and RSME for log-transformed frequencies for averaged MCF curves. For rock mass type, numbers 1-3 correspond to the individual inspector.

Site	Rock mass type	RMSE (Inspector 1, 2, 3)
Vail Pass	Typical (1,2,3)	0.54, 0.27, 0.28
Idaho Springs	Typical (1,2,3)	1.88, 1.76, 1.81, 1.82
Floyd Hill	Massive (1,3), Fractured (2)	0.69, 0.78, 0.56
E	Typical (1,2,3)	1.25, 1.25, 1.25
HI-1	Typical (1,2,3)	1.01, 1.01, 1.21
HI-2	Typical (1,2,3)	1.00, 0.98, 1.01
Manitou Springs	Typical (1,2,3)	NA, 0.47, 0.28

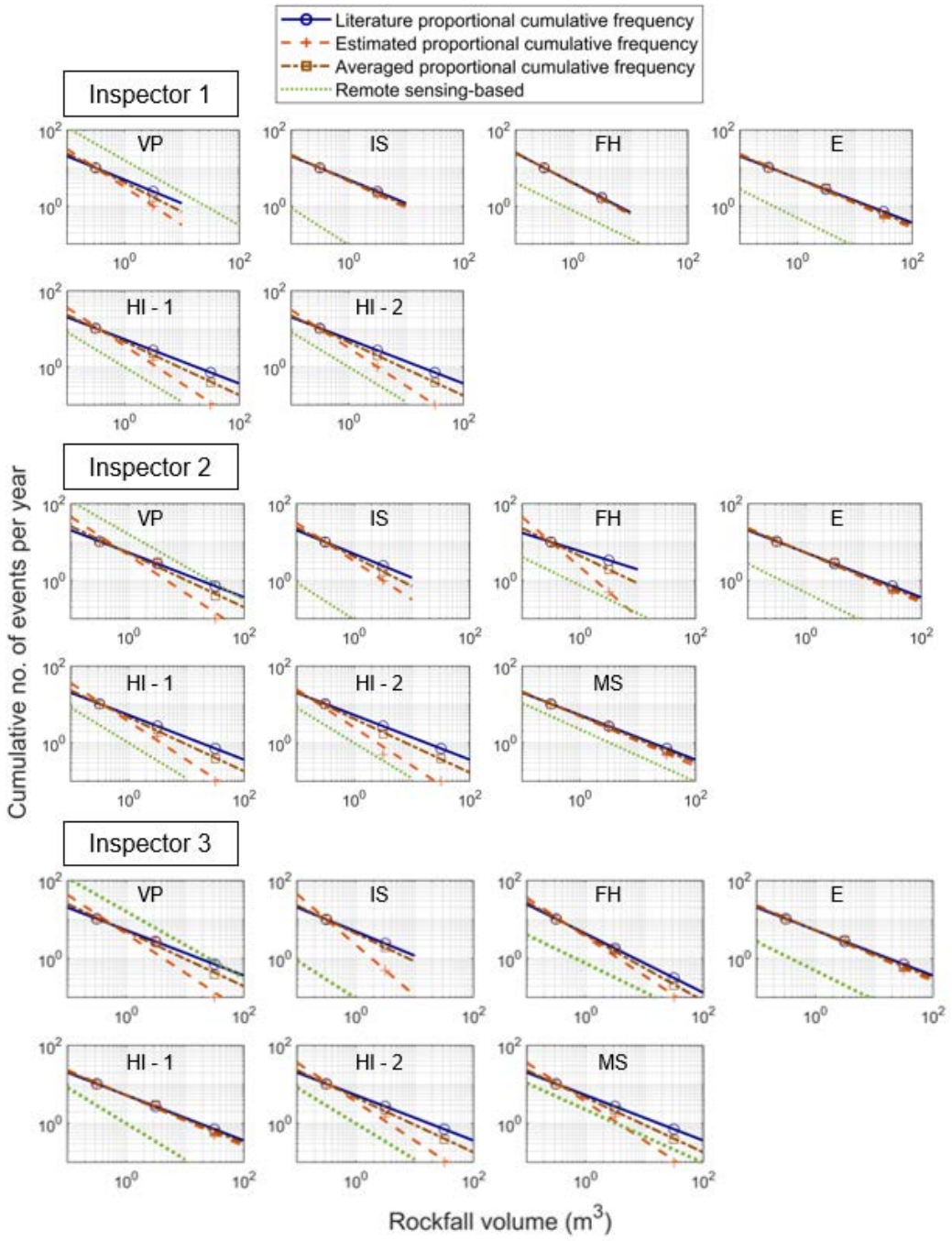

Figure 5.3. Redistributed literature, estimated, and averaged MCF curves for each cut slope for Inspectors 1-3. Remote sensing-based MCF curves shown for comparison. The domain of the remote sensing-based curves reflects the observed range of volumes in the rockfall inventory for the slope. The domain of the literature, estimated, and averaged MCF curves from the estimation method reflects the rockfall magnitude classes deemed kinematically possible by the inspector.

Figure 5.4 depicts the variability of MCF curves across all slopes. The remote sensing-based MCF curves show greater variability in rockfall frequency between slopes than the MCF curves produced from the estimation method, indicating that the estimation method outputs limited variability in MCF curves regardless of user input. The variability in MCF curves across slopes is further reduced when the estimated proportions are averaged with the literature proportions (compare Figure 5.4A to Figure 5.4B).

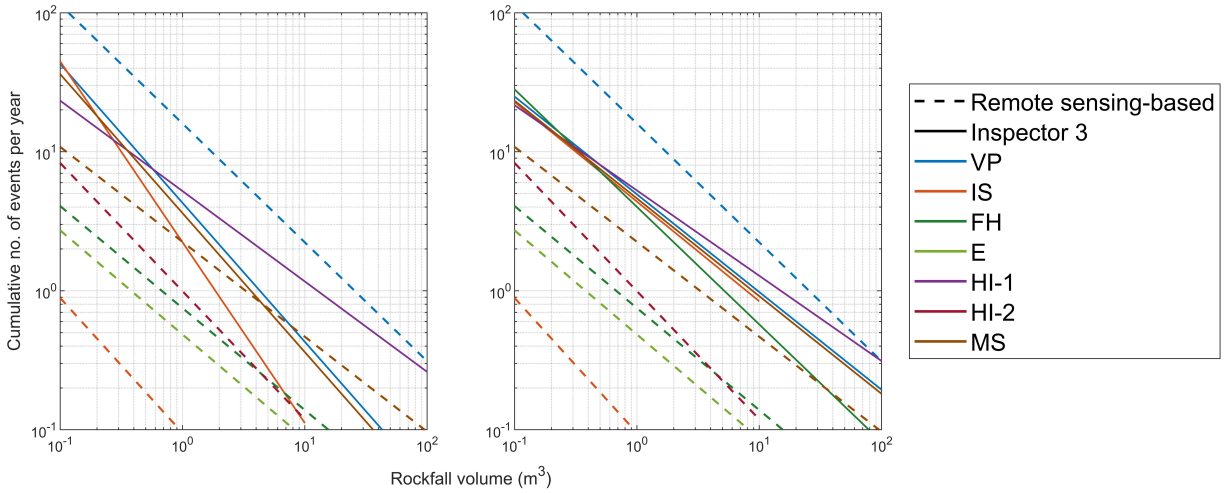

Figure 5.4. Variability in MCF curves across all slopes. A: MCF curves from estimated source volume proportions with remote sensing-based MCF curves for comparison. FH, E, and HI-2 overlap exactly with some curves and are not visible. B: Averaged MCF curves with remote sensing-based MCF curves for comparison.

5.4 Discussion

The MCF curve estimation performs moderately well when compared to the remote sensing-based MCF curves, with RSME values in log space ranging from 0.36-1.82 (Figure A.3). However, for most sites, the method overestimates rockfall frequency. Idaho Springs has the greatest overestimation of rockfall frequency and is also the smallest of the study sites in terms of slope area. Conversely, Vail Pass has the greatest underestimation of rockfall frequency and is the largest slope in terms of slope area. Thus, some of the discrepancy between MCF curves occurs from a lack of scaling the results according to slope area. This may occur due to the tendency of inspectors to focus on an area of the slope that they can most easily conceptualize. Furthermore, the estimation method provides limited options for annual rockfall frequency (Table A.2). A large slope such as Vail Pass may have such large total rockfall frequency that it is difficult to properly conceptualize and exceeds the maximum annual frequency option of 10 for the smallest volume category.

Some discrepancy between averaged and remote sensing-based MCF curves additionally may be due to the use of literature curves that do not represent Colorado cut slopes very well, as the averaged MCF curves were more weighted towards the redistributed literature proportions on the logarithmic scale. Figure A.3 indicates that when the estimated proportions are averaged with the

redistributed literature proportions, the average favors whichever curve is higher, which tends to be the literature proportions. This occurs since the arithmetic mean is calculated on a logarithmic scale rather than the geometric mean.

Figure 5.4 indicates little variability in estimated MCF curves across slopes. This may have occurred due to identifying all slopes but one as a "typical" rock mass. The "typical" rock mass type may be described in a general manner to the point where it applies to too many slopes which, in reality, have different rockfall frequencies. Additionally, the term "typical" may indicate a middle ground choice for inspectors. The tendency for inspectors to default to "typical" may be reduced by development of more detailed guidance in the rock mass descriptions. Lastly, Figure 5.4A indicates that user-estimated proportions result in MCF curves that do not capture the rockfall variability between slopes, regardless of the selected rock mass type. Users may tend to estimate similar source volume proportions across different slopes.

The MCF curve estimation method allows for rockfall risk assessment in the absence of rockfall inventories and remote sensing-based monitoring. Thus, it can be used to estimate rockfall frequency and risk for an entire slope inventory in the context of slope asset management. Risk assessments allow for informed decision-making and proper allocation of resources for mitigation and maintenance measures by the transportation agency. The discrepancy between the estimated MCF curves and the remote sensing-based curves, as well as the variability of the estimated curves between sites, is significant if the final risk value is not assigned or binned to the appropriate category of risk level. For instance, if the MCF curve estimation doesn't capture the variability of rockfall frequency between sites and assigns all slopes as moderate risk level rather than different risk levels, resources may not be appropriately allocated within the agency and the correct maintenance measures may not be employed. Similarly, if the MCF estimation overestimates rockfall frequency by an order of magnitude or more as it does in this study, slopes may incorrectly be placed in a higher risk category with higher priority, leading to more funds allocated to them than necessary. However, if the MCF curve estimation results in a proper binning of the risk level despite any discrepancy with the remote sensing-based curve, the estimation method performs satisfactorily.

5.5 Conclusions

The MCF curve estimation method performs moderately well based on the remote sensing-based curves, with average RSME values in log space ranging from approximately 0.36-1.82. However, none of the estimated curves matched the remote sensing-based curves completely, and the method overestimated rockfall frequency for all sites but Vail Pass. Some inaccuracy may be due to a scaling effect, as inspectors may not conceptualize rockfall frequency for a very small or very large slope area. One solution to counteract this may be to apply the method along a certain length of the slope and the entire height, then to scale the results by the entire length.

Other sources of inaccuracy in the estimation method may include inspector tendency to estimate similar source volume proportions at different slopes, literature values that don't represent Colorado cut slopes well, or an inspector bias towards choosing a "typical" rock mass. Ongoing research includes informing or replacing literature curves with remote sensing MCF curves, such as the ones used in this study, to provide inputs that are more region or geology specific.

The performance of the MCF curve estimation method is critical for accurate rockfall risk assessment, particularly in the absence of rockfall inventories and the need to assess large slope inventories. The estimation method must be accurate to the point where slopes are assigned the appropriate risk level, despite any discrepancies with the remote sensing-based MCF curves. Risk assessments ultimately allow informed decision making and resource allocation by transportation agencies.

6.0 Evaluating Physical and Slope Performance Deterioration of Cut Slopes Through Time

6.1 Introduction

Rockfall activity of a cut slope may change over time as the slope ages. This directly impacts physical deterioration and performance deterioration of the slope. If a slope experiences increasing rockfall activity through time, the risk of the slope increases and the transportation agency must manage the slope appropriately, taking risk mitigation measures as appropriate. In some cases, slope stabilization or hazard mitigation will be implemented, such as scaling or rock bolting.

Though literature suggests that rockfall activity and geotechnical strength parameters change due to excavation (Huisman et al., 2006; Tating et al., 2013; Ersöz and Topal, 2018a; Chen et al., 2022), the specific change in the magnitude-cumulative frequency (MCF) curve representing rockfall is more uncertain. The conceptual models presented in Section 3 predict changes in the MCF curve and therefore physical deterioration of the slope over time. The time-since-excavation conceptual model predicts increasing levels of rockfall at decreasing rates as a function of time since excavation of the cut slope, and thus decreasing physical deterioration with time. If scaling or rock bolting is implemented rockfall frequency is expected to initially decrease and increase as the effectiveness of scaling declines or the rock bolts have reached the end of their service life.

In this section, changes in rockfall activity and slope performance were evaluated through time using data from the Washington Department of Transportation (WSDOT) Unstable Slope Management System (USMS). The effects of mitigation were also considered. The results of these analyses were compared to the conceptual models for time-since-excavation, the influence of scaling, and the influence of bolting.

6.2 Methods

6.2.1 Description of Data and Characterization of Slopes

The WSDOT USMS provides a systematic way of maintaining a slope inventory and prioritizing slopes for mitigation and maintenance (Ho and Norton, 1991). A numerical rating is assigned to the slope after an inspection by geotechnical personnel, which represents slope performance. The inspection is typically carried out in the field but can be performed remotely. The slope rating is determined from the sum of several factors related to hazard and consequence of slope failure, such as the typical volume of rockfall found in the catchment or estimated movement rate of soil (movement magnitude), failure frequency, roadway impedance, and maintenance costs. Each rating subcomponent is given a score of 3, 9, 27, or 81 points. Slope performance declines with an increasing slope rating. The slope rating form was updated in 2019, which added movement magnitude as another rating category. Movement magnitude quantifies either the soil movement rate or the volume of rock blocks in the catchment.

Rating subcomponents related to rockfall hazard include failure frequency and problem type. Failure frequency represents how often significant rockfall (generally 5 yd3 or larger) occurs that

reaches the highway. The WSDOT geotechnical office commonly receives this information from maintenance crews that clear rockfall debris from the highway; therefore, there is some variation on what maintenance considers a failure (S. Johnston, personal communication, April 23, 2024). The problem type subcomponent first identifies if the problem is a soil or rockfall event. If the event is related to rockfall, the score assesses how well the catchment performs in containing the rockfall event, which is related to the dimensions of the ditch.

A list of all known 720 rock slopes in the WSDOT USMS was provided for this analysis, including the location, all past ratings with associated dates of inspection, the slope status, year of mitigation work if applicable, and estimated age of the slope as of 2019. Slopes are not distinguished between natural or cut, and the number of ratings varies for each slope. Known cut slopes that were cut back or resloped were assigned an age based on the date of resloping. For instance, a cut slope that was resloped in 2015 would have an age of four years.

Detailed data was received for 72 slopes out of the inventory of 720. The exact data varied for each slope but included the slope rating form for all inspections so the score of each rating subcomponent could be digitized. Other documentation for each slope may have included the following:

- Photos of the slope on different dates.
- Conceptual mitigation designs (designs of recommended mitigation measures); conceptual designs often included descriptions of the rock mass and geology.
- Construction/mitigation records, including photos, email correspondences, daily site visit reports during construction, and geotechnical reports.
- Records of notable rockfall events, including photos, site visit reports, email correspondences, and notes in the summary USMS page for the given slope.
- GIS files and numerical modeling files for rockfall analyses.
- Digitized or scans of field notes from any site visits.
- Maintenance records for cleaning the highway of rockfall debris.

Notable characteristics for each of the 72 slopes were summarized using the above information and are included in Appendix D of Werley (2024). For instance, slopes were distinguished between natural and cut using photos. All slopes were considered cut except Slope 1979.

Mitigation measures and dates of mitigation installation were recorded. The most common types of mitigation included scaling, rock bolts, dowels, and/or anchors. Other mitigation measures included wire mesh, resloping, shotcrete, rockfall fences, gabion walls, jersey barriers, horizontal drains, and ecology blocks. For the purposes of this study, resloping or cutting back is considered intense scaling or additional blasting that changes the grade of the slope and/or pushes the slope back further from the highway. Scaling, on the other hand, includes removal of certain blocks or overhangs that are potentially unstable using hand bars or excavators. Scaling is distinguished from resloping within the data provided. The exact date of mitigation was noted when possible, though some mitigation dates may be inaccurate by a few weeks.

6.2.2 General Trends of Slope Performance through Time

To discern any trends of slope performance through time, the slope ratings from the entire

database of 720 slopes were examined. First, the average change in slope rating per year was plotted against the mean slope age for each slope. Mean slope age was found by calculating the age of the slope at the time of each inspection since the age of the slope as of 2019 and the date of inspection are known. The average change in slope rating per year was found by fitting a linear regression to the ages and associated slope ratings for each slope.

Secondly, the most recent slope rating for each slope was plotted against the age of the slope at the time of the most recent inspection. For both plots, only inspections conducted between 2000 and 2019 were used. As previously mentioned, only geotechnical personnel conducted inspections starting in 2000. Furthermore, the slope rating form was updated in 2019 with the addition of the movement magnitude category; however, since the individual rating subcomponents are not included for all 720 slopes, the movement magnitude score is unknown and cannot be subtracted out of each slope rating. Slopes that have been resloped were not included so as not to result in negative ages.

Finally, to examine how rating subcomponents most related to hazard change over time, these two plots were recreated for an unmitigated subset of the 72 slopes. The average changes in slope rating, failure frequency, and the problem type score per year were plotted against the mean slope age. The most recent slope rating, failure frequency, and problem type score were also plotted against the age of the slope at the time of the most recent inspection. Slopes included in this analysis did not have any mitigation work performed. Ratings before 2000 were not included. To account for the updated rating form, the movement magnitude score was subtracted out of the overall rating for ratings after 2019.

6.2.3 Influence of Scaling, Bolting, and Resloping on Slope Performance through Time

To consider the effects of scaling, bolting, and resloping, subsets of the 72 slopes with detailed data were used. All ratings after 01-January-2000 were considered, and the movement magnitude score was subtracted out of each slope rating so that ratings before and after 2019 were comparable.

For the scaling analysis, slopes that had only experienced scaling and no rock bolting or resloping were included. To observe the general influence of scaling on slope performance through time, average change in overall slope rating, failure frequency, and problem type score was plotted against the mean slope age.

To evaluate the change in slope performance due to scaling, ratings were compared before and after scaling. For each slope that was scaled and had at least one inspection before and after scaling, the average slope rating, average failure frequency, and average problem type score were calculated for all inspections before scaling and then all inspections that took place after scaling. The difference between the before and after averages was then calculated for the overall ratings and subcomponent scores. Additionally, ratings, failure frequency, and problem type scores were plotted for slopes individually in relation to time since scaling rather than averaging scores.

This analysis was repeated for slopes with rock bolting and slopes that were resloped or cut back. Slopes that had bolts, dowels, and/or anchors installed, regardless of any additional mitigation, were included in the bolting analysis. Henceforth, the term “rock bolt” will be used as a general

term to refer to bolts, dowels, and/or anchors. Similarly, any slopes that were resloped or cut back, regardless of any mitigation measures installed before or after resloping, were included in the resloping analysis.

6.3 Results

6.3.1 General Trends of Slope Performance through Time

Figure 6.1 displays the average change in slope rating vs. mean slope age and the most recent rating vs. age considering all 720 slopes in the USMS inventory. Because only ratings from 2000-2018 were used and resloped slopes were removed, 577 slopes were included in the analysis. The average change in slope rating per year is additionally constrained to show changes with a magnitude less than 150 to avoid outliers skewing the visualization.

Figure 6.1A depicts no definitive trend; however, many slopes show average changes in slope rating per year that are zero or close to zero. As mean age increases to 50-100 years, some slopes reflect an improvement in slope rating over time, indicated by a negative change in rating.

Figure 6.1B indicates no strong correlations that can be identified visually. Older slopes (greater than 60 years) appear to have a similar range in slope rating as relatively younger slopes (less than 60 years).

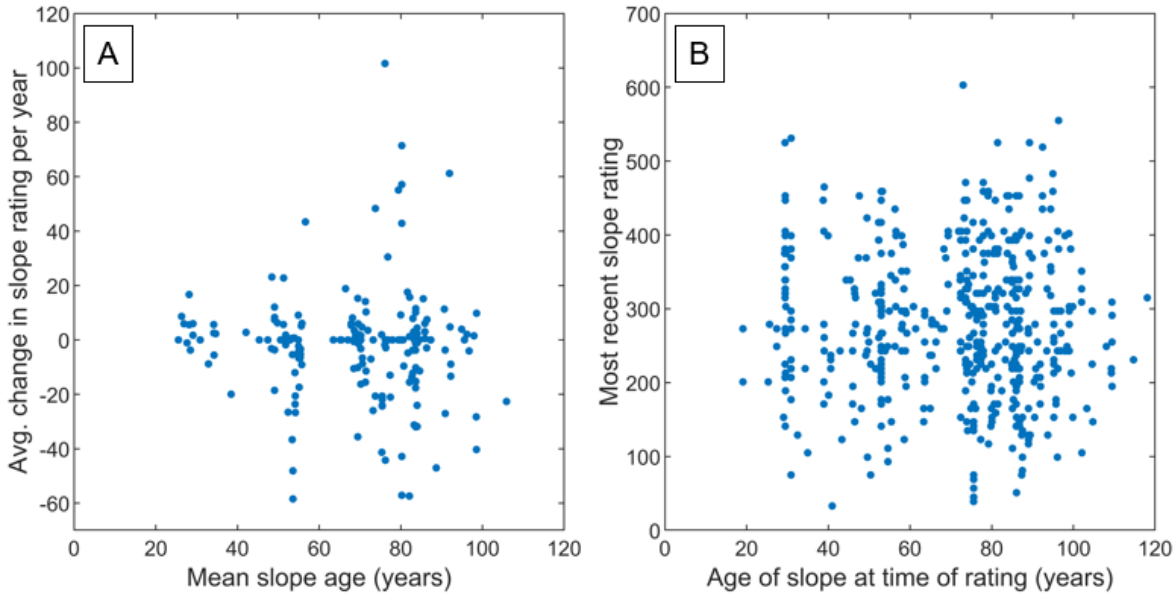

Figure 6.1. Slope performance through time using a subset of the 720 slopes in the USMS dataset.

Figure 6.2 presents the same results but for the unmitigated subset of the 72 slopes, which includes 29 slopes. In addition to the overall slope rating, the failure frequency and problem type score are shown to indicate how the hazard components of the rating may change over time. Figure 6.3A-C show the average rating change per year vs. the mean slope age, while Figure

6.3D-F show the most recent rating vs. the age of the slope at the time of the most recent inspection.

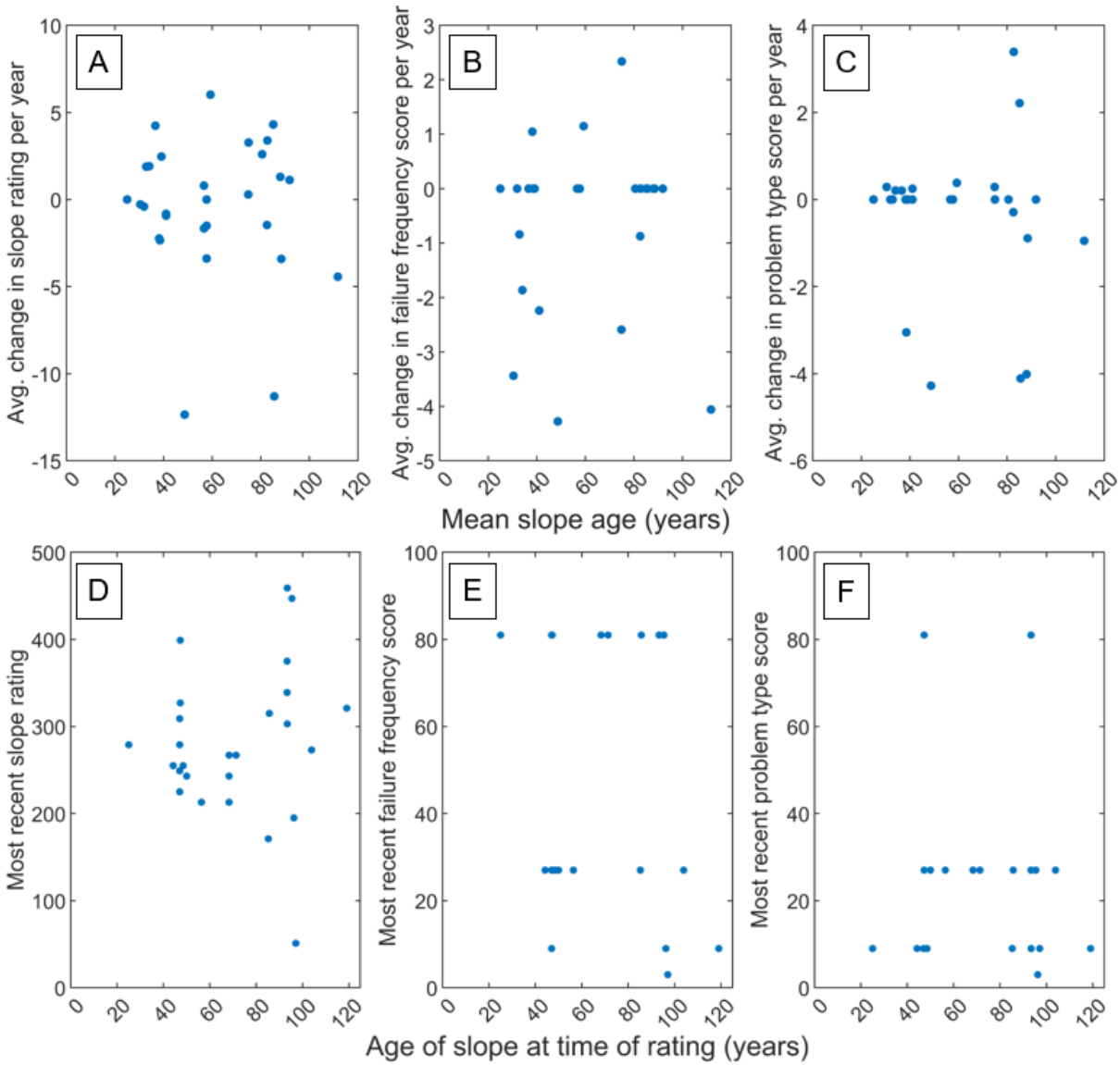

Figure 6.2. Change in overall slope ratings and rating hazard components over time since excavation.

Similar to Figure 6.1, there are no distinct trends in Figure 6.2. Most unmitigated slopes have an average change in slope rating per year within a magnitude of five points, regardless of age. Most slopes also indicate no change in the failure frequency and problem type score regardless of age, meaning that the frequency of rockfall events reaching the roadway and the performance of the catchment does not change. More slopes improve in rating, failure frequency, and problem type score than worsen, regardless of age. Furthermore, the average changes in failure frequency and problem type score per year are relatively small, all being within a magnitude of five.

Figure 6.2D shows that older slopes generally appear to have slightly higher total ratings.

However, considering the lack of trend in Figure 6.2A, these older slopes may have had higher slope ratings and worse performance throughout their entire lifespan, meaning slope rating does not necessarily increase with slope age. Hazard components of the overall rating do not show any clear trend with slope age.

6.3.2 Influence of Scaling, Bolting, and Resloping on Slope Performance through Time

Seventeen out of 72 slopes experienced varying extents of scaling and no rock bolting or resloping. Slope details are summarized in Werley (2024). When plotting the average change in slope rating and hazard components per year against mean slope age (Figure 6.3), the ratings appear to improve with age. Furthermore, the amount of improvement in rating and hazard scores increases with older slopes. With that being said, for most of the slopes, the failure frequency and problem type scores do not change (Figure 6.3B and C), and any improvement in hazard scores is relatively small (within a magnitude of seven).

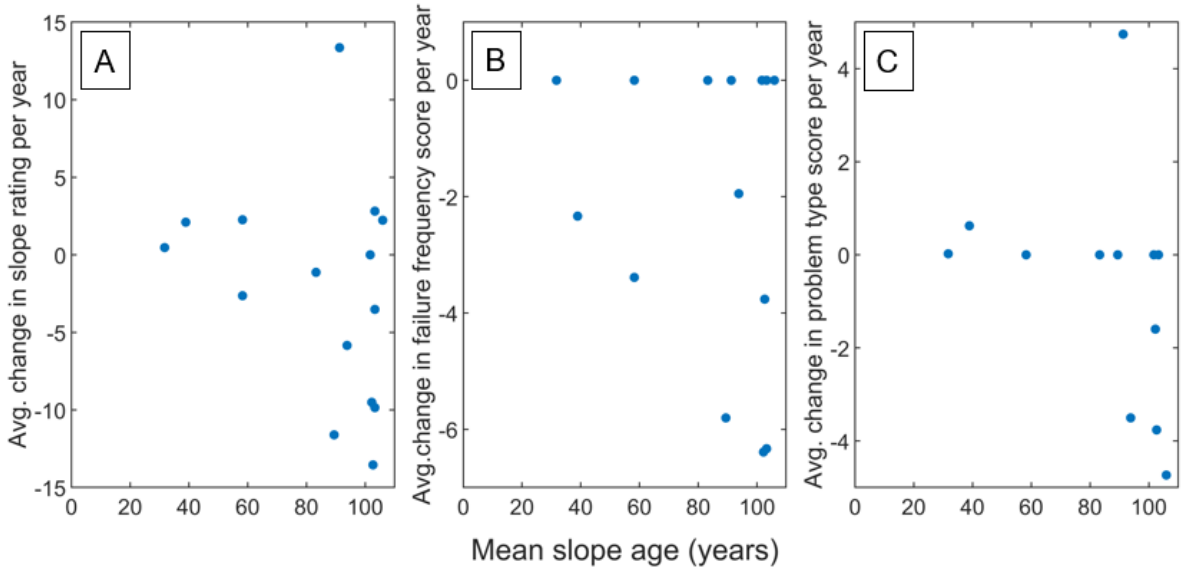

Figure 6.3. Average change in slope rating and rating hazard components per year vs. mean age of the slope for slopes that have been scaled.

Figure 6.4 shows a more direct comparison of the effects of scaling, where the difference is taken between the average of the ratings assigned before scaling and the average of the ratings assigned after scaling. Note that some inspections have occurred up to 12 years after scaling, and changes in rating may depend on how long after scaling the next inspection took place. Most slopes show an improvement in the overall rating, although some slopes maintain the same average rating or even an increased rating. Slopes either maintain the same average failure frequency and problem type score or improve in these categories. The changes in average slope rating and hazard components are variable in magnitude from 0-100.

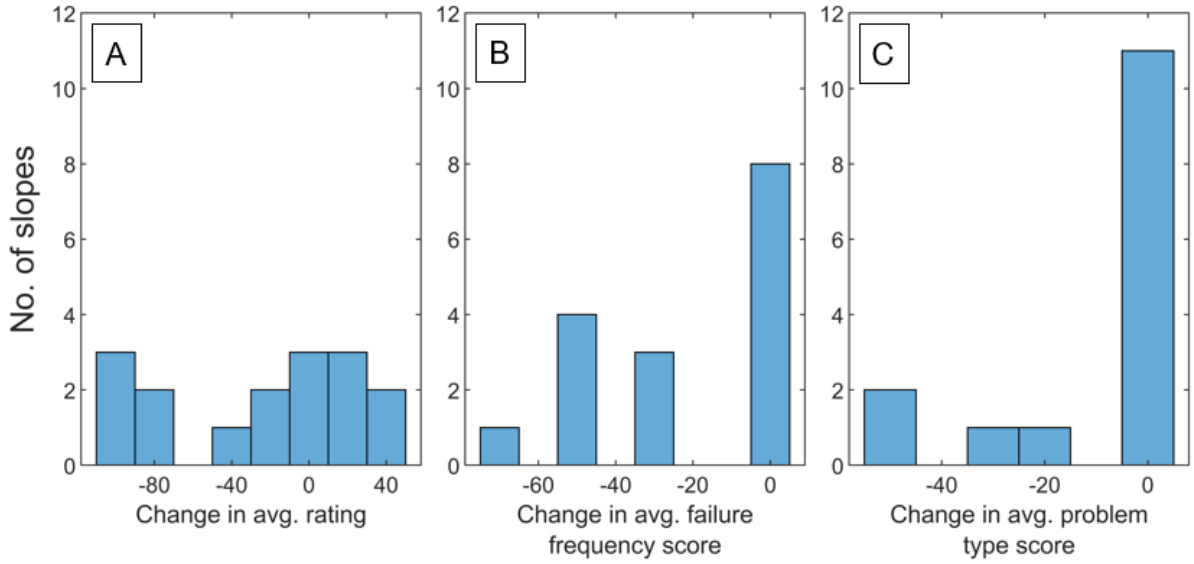

Figure 6.4. Change in average rating and rating hazard components after scaling.

Sixteen out of 72 slopes had rock bolts, dowels, and/or anchors installed. Several slopes have additional mitigation measures, such as scaling or even resloping. Figure 6.5 shows the average changes in slope rating, failure frequency, and problem type score per year vs. the mean age of the slope. Unlike the slopes that have been scaled, ratings and hazard component scores do not appear to increasingly improve with mean slope age. The overall slope rating may increase, indicating decline in slope performance, for younger slopes with a mean age less than 20 years. These slopes may include slopes that have been resloped, as the calculated age of the slope during an inspection before resloping would be negative due to the method of calculating ages. Most slopes improve in the failure frequency score regardless of mean slope age (Figure 6.5B), and the problem type score remains relatively constant over time regardless of mean slope age (Figure 6.5C). Thus, the catchment's ability to retain rockfall does not change, but failure frequency may decrease for slopes that have been bolted. Any changes in the slope rating, failure frequency, and problem type scores per year are relatively small: generally within a magnitude of 10 for slope rating and within a magnitude of five for the hazard components.

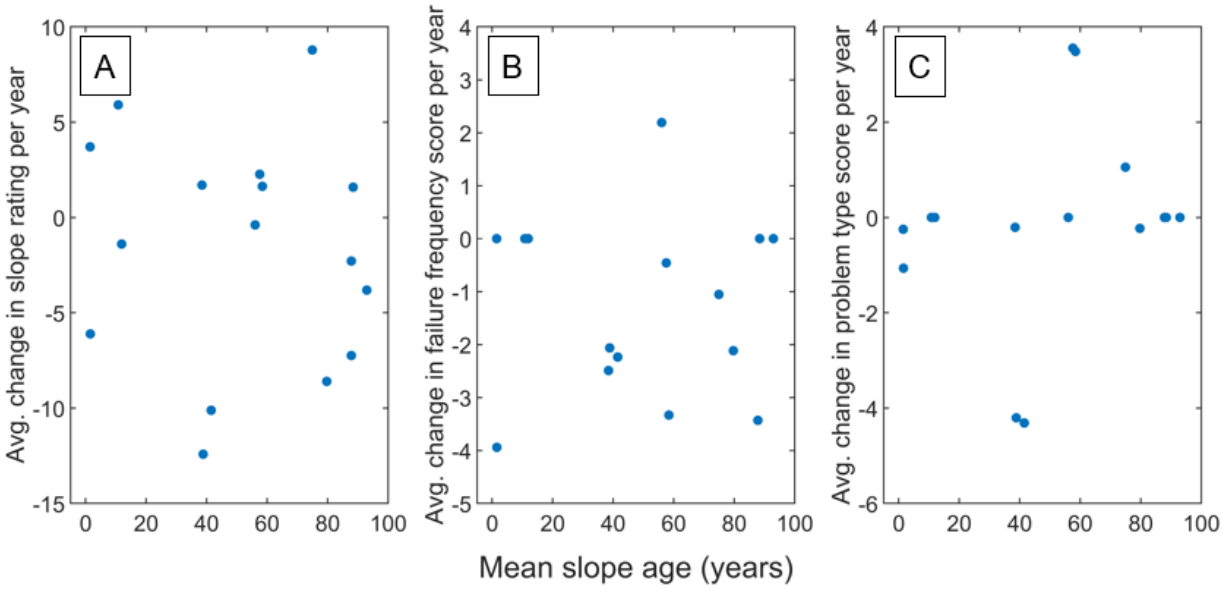

Figure 6.5. Average change in slope rating and rating hazard components per year vs. mean age of the slope for slopes that have been bolted.

Figure 6.6 depicts the depicts the differences between the averages of the ratings assigned before bolting and the average of the ratings assigned after bolting. Most slopes have a decreased or improved slope rating after bolting, although three slopes retain approximately the same rating, and four slopes have ratings that worsen on average (Figure 6.6A). The same general trends occur in the failure frequency scores (Figure 6.6B); however, most slopes retain approximately the same problem type score, and therefore the catchment's performance is considered to remain constant despite bolting.

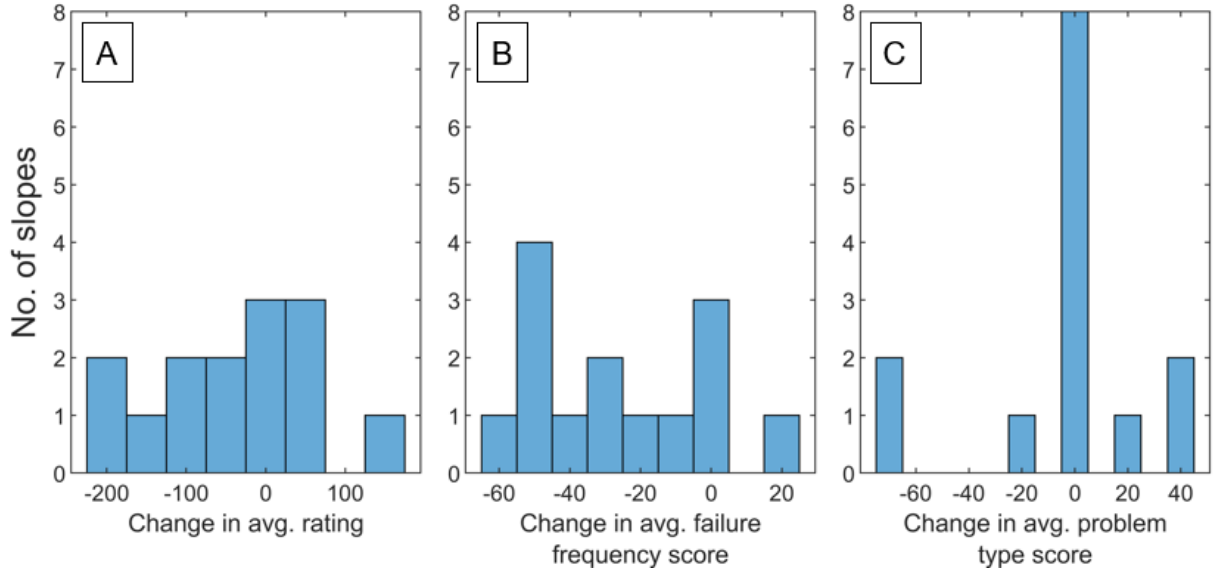

Figure 6.6. Change in average rating and rating hazard components after bolting.

Seven slopes out of 72 were resloped or cut back, and four of these slopes were also included in

the bolting subset. Figure 6.7 depicts the average changes in overall slope rating, failure frequency, and problem type scores per year vs. mean age of the slope. The mean ages of the slope are not directly comparable as they are in the scaled slopes and most of the bolted slopes. The calculated age of the slope would be negative if the inspection took place before resloping, and zero at the time of resloping. Therefore, Figure 6.7 is not necessarily helpful for discerning any trends of slope performance with age, but it is helpful in assessing the average change in ratings and hazard components per year on a slope-by-slope basis. Five out of the seven slopes experienced a decreased or improved slope rating on average (Figure 6.7A), and three experienced a decreased or improved failure frequency and problem type score (Figure 6.7B and C). The other four slopes did not see a change in failure frequency or problem type score per year on average. Again, the change in slope rating and the hazard components are small: generally within a magnitude of six for each.

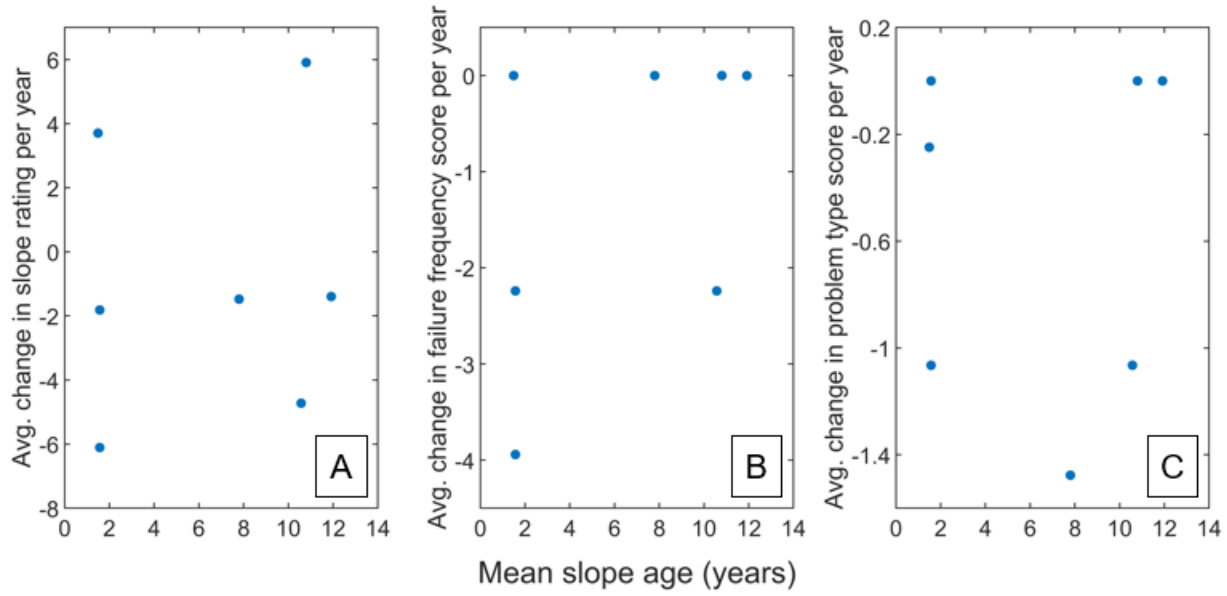

Figure 6.7. Average change in slope rating and rating hazard components per year vs. mean age of the slope for slopes that have been resloped.

Figure 6.8 indicates that most slopes improve in average slope rating, failure frequency, and problem type score after resloping, while others retain approximately the same average rating

after resloping.

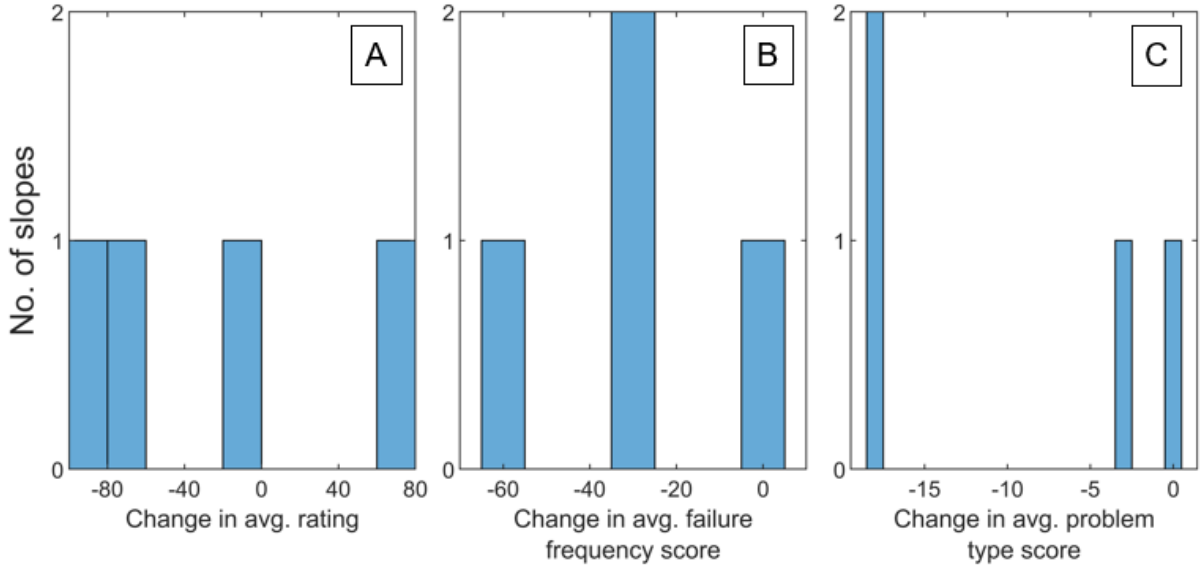

Figure 6.8. Change in average rating and rating hazard components after resloping.

6.4 Discussion

6.4.1 General Trends of Slope Performance through Time

There are no clear, consistent trends of slope performance, represented by the WSDOT slope rating, as a function of time or slope age. However, most slopes from WSDOT's USMS and most unmitigated slopes from the USMS either maintained or improved their slope rating through time (Figure 6.1A). Since the slope ratings involve factors relating to both consequence and hazard, these results do not strictly communicate how the hazard of the slope changes as a function of slope age. Therefore, the unmitigated slopes with available rating forms were also examined in Figure 6.2. Figure 6.2A-C indicates that the hazard components of the slope rating (i.e., rockfall failure frequency and the catchment performance) stayed the same or changed minimally each year (within six points for hazard components) regardless of slope age. That being said, the youngest slopes shown on Figure 6.2 have a mean age of approximately 20 years. Thus, slopes younger than 20 years may exhibit different behavior than what is shown. It is evident in Figures 6.1-6.2 that slope performance generally does not consistently worsen over time, even for unmitigated slopes, and that major rockfall frequency generally stays constant for slopes that were excavated over 20 years or more ago. Additionally, since rating components include qualitative scoring guidelines and different inspectors often rate the slopes throughout the years, change in slope performance may also have occurred due to variability in inspectors.

The results are not inconsistent with the time-since-excavation conceptual model. There is no strong evidence for mitigated or unmitigated slopes experiencing physical deterioration or performance deterioration through time, indicating that slopes may be fully weathered by 20 years after excavation.

6.4.2 Scaling

In general, scaled slopes improved in slope rating, failure frequency, and problem type score with mean age. However, scaling did produce variable responses in slopes, which can be observed when looking at ratings through time for individual slopes (Appendix D of Werley, 2024).

Responses to scaling include combinations of slope ratings staying the same, increasing (slope performance worsening), or decreasing (slope performance improving), while failure frequency and problem type scores stayed the same or decrease (improve). In all cases in which slope rating increased after scaling, corresponding to a worsening slope performance, factors related to consequence were the cause. The problem type score rarely increased, which corresponds to a decrease in rockfall staying within the catchment. In all cases, failure frequency either stayed the same or increased after scaling. Slopes that had an inspection within a year or even a month of scaling did not have an immediate decrease in failure frequency; thus, it is unlikely that the action of scaling biased inspectors to artificially lower failure frequency. The distribution of how much time has passed between scaling and the very next inspection is shown in Figure 6.9.

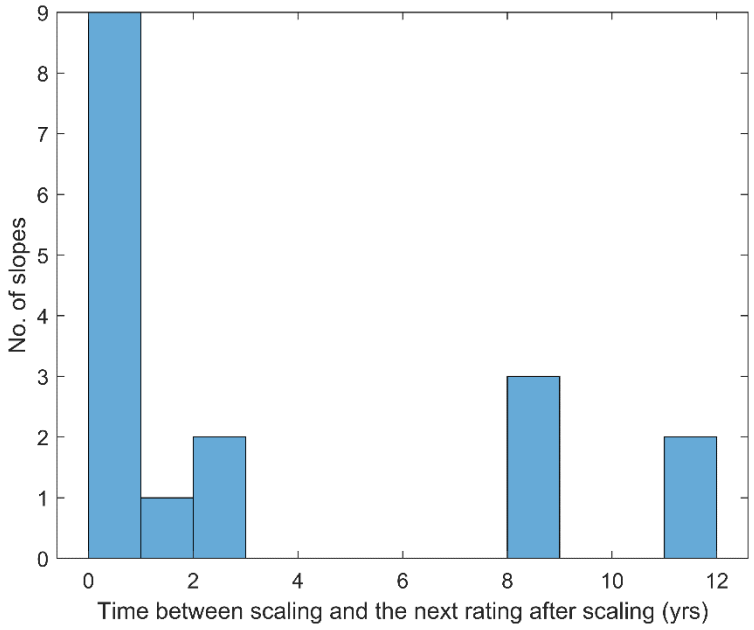

Figure 6.9. Distribution of time between scaling and the very next inspection, in which a new rating is assigned to the slope. Most slopes had an inspection within a year of scaling; however, likely not enough time had passed to assess the results of scaling, as the failure frequency score remained the same as before scaling.

The failure frequency score may have remained the same after scaling for several reasons. In the cases with inspections within 1-2 years after scaling, likely not enough time has passed to assess the effects of scaling, especially because the lowest point categories correspond to one failure or less in five years. In the cases that failure frequency stayed constant even up to 15 years after scaling, scaling may not have been effective, the effectiveness of scaling declined before the data was collected, or only small sections of the slope were scaled relative to the entire slope area.

Scaling small, unstable sections of the slope may have prevented major failures but did not keep the slope from producing rockfall in other areas, particularly following adverse weather (e.g., intense precipitation). This may have especially occurred in slopes that were large in surface area, such as Slope 183, or slopes that were scaled around areas of major rockfall and not the entire slope, such as Slope 2586. Additionally, weaker, more disintegrated rock masses with overlying colluvium, such as Slope 3197, may produce more raveling than intact, stronger rock masses, which would keep the failure frequency high despite scaling.

The problem type score is not considered to capture the effects of scaling as much as the failure frequency score since the performance of the catchment should be more dependent on the catchment geometry. Furthermore, most slopes did not have a change in average problem type score after scaling, indicating that problem type score is more independent of scaling. Therefore, a decrease or no change in the problem type score following scaling does not necessarily discount the effectiveness of scaling. However, in some specific cases such as Slope 520, large slabs that are noted in the slope documentation to reduce the ditch capacity were scaled, resulting in an increase in the problem type score while the failure frequency remained constant. Thus, the benefits of scaling can be included in an increased problem type score for this slope.

In the cases that slope rating and/or failure frequency improved, there was no evidence found that explains the improvement other than scaling. Thus, when slope performance and/or failure frequency improves, scaling is assumed to be the cause.

Since scaling is seen to improve or not affect rockfall frequency and therefore rates of physical deterioration, the results are not inconsistent with the conceptual model for scaling. The conceptual model indicates that rockfall frequency will return to its original state as the effects of scaling decline through time. No scaled slopes from the WSDOT dataset experience an increased failure frequency score after first declining; likely, not enough time has passed after scaling to capture this effect, or the failure frequency scoring categories are too broad to capture this effect. Alternatively, if scaling was not intensive and the next rating after scaling occurred 8-12 years later, the temporary decrease in failure frequency may not have been captured.

6.4.3 Bolting

The 16 out of 72 slopes that were bolted reflect different changes in slope rating and hazard components per year (Figure 6.5) than the scaled slopes. For each slope, the effect of bolting is not isolated. All 16 slopes had additional mitigation such as wire mesh, horizontal drains, shotcrete, rockfall fences, scaling, or even resloping.

The variable responses from bolting are also evident when examining the individual slope ratings through time and slope summaries. Based on the results in Figures 6.5 and 6.6, failure frequency is more controlled by bolting than the overall slope rating and problem type score. For instance, for some slopes, slope rating increased, corresponding to a worsening slope performance, while failure frequency decreases. Thus, consequence components of the rating that are independent of the effects of bolting were more likely contribute to a worsening slope performance.

In all cases, the failure frequency score either remained the same or decreased after bolting; it did not increase. Out of the slopes that had a new rating assigned within a year of bolting, none had a

decrease in failure frequency after that inspection. Thus, it is unlikely that the installation of bolts and other mitigation biased inspectors to artificially lower failure frequency. The distribution of how much time has passed between bolting and the very next inspection is shown in Figure 6.10.

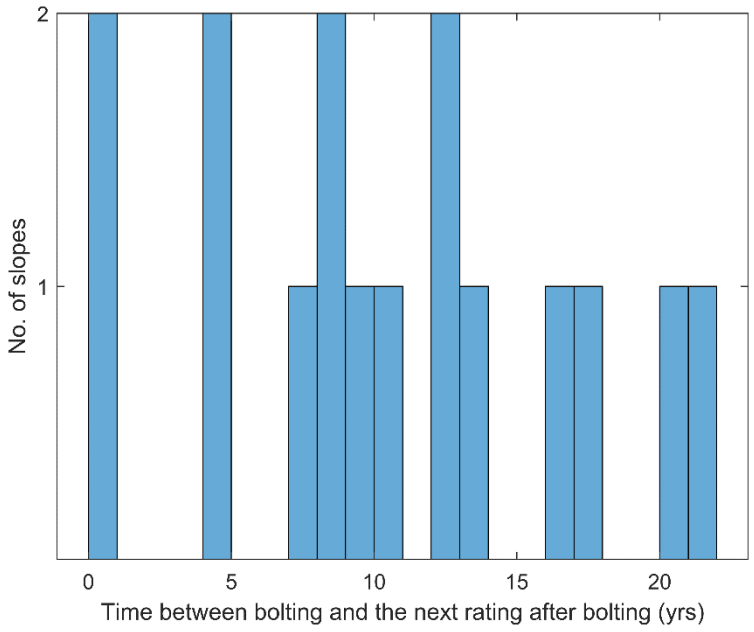

Figure 6.10. Distribution of time between bolting and the very next inspection, in which a new rating is assigned to the slope.

In some cases, the failure frequency score remained constant after bolting, even though there are ratings from 5-20 years after bolting. Some of these slopes, such as Slope 3045, may have bolting installed in small sections relative to the size of the entire slope area, and therefore the bolting may not have been effective enough to change the failure frequency. Alternatively, even with bolting in large sections relative to surface area, there may have been a reduction in failure frequency, but frequency was still high enough to remain within the 81-points category (more than one event per year). Other slopes had indications of frequent rockfall despite bolting and other mitigation measures, such as damage to rockfall fences, gabion barriers, and reports from maintenance. Failure frequency was often scored at 81 points in these cases. It is also possible that mitigation measures may not be appropriately placed on the slope to reduce frequency, even if designs follow best industry practices.

In other cases, failure frequency decreased after bolting. There is no evidence that disproves the effectiveness of bolting or the combined effect of other mitigation measures in these cases. For Slopes 1729, 1758, and 1759, the failure frequency remained constant after bolting until approximately 15-20 years later when it decreased. This is most likely due to variability in assessments due to different inspectors.

Since bolting either improves or does not affect rockfall frequency and therefore rates of physical deterioration, the results are broadly consistent with the bolting conceptual model. Bolts have not reached the end of their service life in the WSDOT slopes; thus, rockfall frequency has not increased after bolting.

6.4.4 Resloping

Four out of the seven resloped slopes had ratings before and after mitigation. Three slopes had a decrease in average failure frequency and problem type, while one slope had no change in failure frequency or problem type score (Figure 6.8). Out of the seven resloped slopes, Slope 223, 1311, 1864, and 1867 were also bolted.

Ratings through time for individual slopes also reveal that failure frequency does not increase after resloping. No ratings were assigned immediately after resloping (Figure 6.11); thus, enough time is considered to have passed to assess the effects of resloping. Any elevated amount of rockfall as a result of resloping and exposing fresh surfaces to the external environment may have occurred within five years of resloping; however, no inspections were conducted in this timeframe.

Slopes that were resloped or cut back can be considered analogous to slopes that are excavated for the first time. An increase in rockfall activity was expected immediately after resloping; however, ratings may have been taken too soon or late after resloping to experience this change in the failure frequency score. More likely, since the failure frequency score reflects major events that reach the roadway, the failure frequency score is unlikely to capture the changing rockfall activity as a result of resloping.

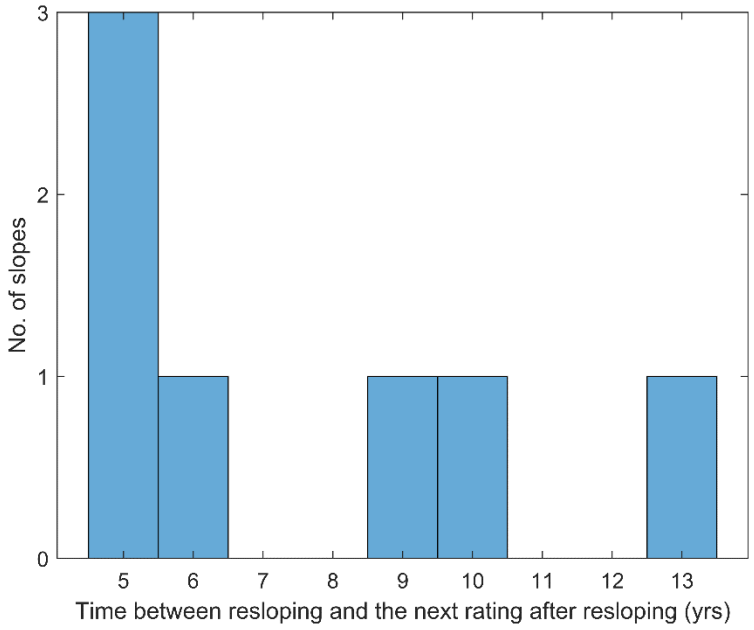

Figure 6.11. Distribution of time between resloping and the very next inspection, in which a new rating is assigned to the slope.

6.4.5 Data Limitations

Though the failure frequency score is used to represent rockfall frequency in this analysis, the true rockfall frequency is better represented with an MCF curve. Four scoring categories (3, 9, 27, and 81 points) with the highest failure frequency of more than one event per year is a

relatively coarse categorization. The interpretation of "failure" is also variable and depends on what maintenance reports to WSDOT's geotechnical office. A sizeable rockfall event may occur, but if it is contained in the ditch, it is less likely to be noted. Furthermore, the effects of scaling, bolting, and resloping on smaller rockfall events, such as volumes 1 m^3 or less, are unknown.

The nature of a semi-quantitative rating system may explain the lack of clear trends between slope rating and time since excavation or mitigation found in the different sub-analyses. Ratings are dependent on the inspector's interpretation of rating components, which may be variable between inspectors. The purpose of the USMS and the WSDOT rating system is to prioritize slopes for maintenance and identify slopes that would benefit from mitigation, not necessarily to analyze rockfall frequency and overall slope performance through time and time since mitigation. The analyses also consider older slopes rather than younger ones, with a mean age of 20 years or older. Slopes that have a mean age closer to zero are slopes with "negative" ages before resloping.

6.5 Conclusions

In this section, slope performance and rockfall frequency were evaluated over time since excavation of the cut slope, considering both unmitigated slopes and the effect of mitigation measures. The results of the analyses were ultimately compared to the conceptual models predicting rockfall frequency as a function of time since excavation, scaling, and bolting.

The analyses were conducted using data from WSDOT's USMS, which contained slope ratings through time and more extensive documentation for 72 slopes. Slope performance and rockfall frequency were found to be relatively constant over time, and failure frequency stayed the same or decreased after mitigation on average. Based on the findings, cut slopes generally do not experience physical deterioration or significant performance deterioration through time beyond a certain age, which is reflected in the conceptual model for rockfall frequency as a function of time since excavation. Slopes may reach an equilibrium level of hazard and not experience further physical deterioration after approximately 15-20 years. Mitigation measures were seen to improve physical deterioration rates, but commonly may not have reduced rockfall frequency to less than one event per year for magnitudes between 1-10 m^3. This provides some guidance for setting how much rockfall frequency should change in the conceptual models.

7.0 Relating Physical Slope Deterioration to Slope Performance Deterioration

The conceptual models developed in Section 3 predict changes in ditch effectiveness over time and rockfall frequency over time due to excavation of the cut slope, scaling, or rock bolting. Ditch effectiveness and rockfall frequency are typical inputs to slope risk assessments and slope performance deterioration modeling, which forecasts changes in risk throughout time.

To relate physical slope deterioration to slope performance deterioration, the proposed conceptual models are applied within the CDOT slope risk assessment framework developed by BGC Engineering. Furthermore, slope performance deterioration predicted by the conceptual models are compared to slope performance deterioration predicted by the current CDOT hazard deterioration models using six cut slopes monitored with remote sensing. Slope performance is represented with Annual Risk Exposure (ARE), which considers the hazard and consequences of rockfall failure. The hazard is represented with the likelihood that rockfall reaches the roadway, which is dependent on rockfall frequency, shadow angle (the angle between the slope crest and road shoulder), ditch effectiveness, and mitigation effectiveness (Sala and Vessely, 2022).

The current CDOT hazard deterioration models apply a continual decrease in ditch effectiveness and increase in rockfall frequency each year independent of the specific slope conditions. In contrast, the conceptual models predict changing ditch effectiveness and rockfall frequency that are dependent on the slope's geometry and age; thus, the predicted rate of slope performance deterioration may be more reliable (and lower) than the CDOT models.

7.1 CDOT Slope Risk Assessment Framework

In this analysis, the slope risk assessment framework developed for CDOT by BGC Engineering is used to compare ARE forecasted by the hazard deterioration models within the slope risk assessment framework and the proposed conceptual models. ARE is determined considering both hazards and consequences. Hazard considers rockfall frequency, the spatial probability of rockfall reaching the roadway, ditch effectiveness, and mitigation effectiveness (Sala and Vessely, 2022). Consequences consider the cost of a statistical life in Colorado, vehicle operating costs and lost wages, and the cost of maintaining the asset and clearing rockfall debris (Sala and Vessely, 2022).

Slopes are assessed through a desktop or an in-person inspection, which serve as inputs to the ARE calculation. Ditch effectiveness can be directly estimated by the inspector, or dimensions of the ditch are compared to the Rockfall Catchment Area Design Guide (Pierson et al., 2001) to estimate ditch effectiveness. Non-cumulative rockfall frequency is estimated for five rockfall volume classes (Table 5-1). The method of estimating rockfall frequency in the absence of a pre-existing magnitude-cumulative frequency (MCF) curve and an evaluation of this method's performance is detailed in Section 5. If the slope is scaled or has rock bolting, the inspector can choose to reduce the estimated rockfall frequency. In this analysis, however, remote-sensing-based MCF curves were used to estimate rockfall frequency for inputs in the slope risk assessment, and the estimation method is not used. If other mitigation is present, such as draped mesh, rockfall fences, or barriers, the algorithm directly applies a mitigation effectiveness factor to volume classes V_1 and V_2 (Sala and Vessely, 2022).

The slope risk assessment framework also includes deterioration modeling that was developed by BGC Engineering. ARE is forecasted for any point in time by applying two hazard deterioration models (rockfall frequency, which represents physical deterioration, and ditch effectiveness) and cost inflation. If the slope asset is a cut slope as opposed to a natural slope, rockfall frequency increases by 1.5% each year for each volume class. For natural slopes, the rockfall frequency remains constant. If the slope asset is a cut slope, ditch effectiveness deterioration is also applied. If rockfall frequency is 10 events per year or greater, the ditch effectiveness deteriorates by 3% each year. Otherwise, the ditch effectiveness deteriorates by 1.5% each year (M. Hille, personal communication, March 28, 2024).

7.2 Methods

To compare the changes in ARE forecasted by CDOT's current deterioration models and the conceptual models, these deterioration models were applied to six cut slopes in the Front Range region of Colorado that are monitored with remote sensing. Each slope has a rockfall inventory with at least two years of data, which has been used to develop a corresponding MCF curve (Figure 4.2). These slopes are named Vail Pass (VP), Idaho Springs (IS), Floyd Hill (FH), E, HI, and Manitou Springs (MS), with characteristics summarized in Section 4. Conceptual models were applied using the mathematical relationships defined in Section 3.

Slopes HI and Manitou Springs have concrete Jersey barriers between the ditch and road shoulder, and therefore the slope risk assessment framework applies mitigation effectiveness for volume classes V_1 and V_2 for these slopes. Slopes E and HI have rock bolts installed, but the effect of rock bolts was not considered when inputting rockfall frequency into the CDOT slope risk assessment. Likewise, though Slopes E, HI, and Floyd Hill have had scaling performed in the past, the effects of actual scaling efforts were not considered when inputting rockfall frequency. Each cut slope produces more than 10 events per year.

For each case, ARE was forecasted for 5, 10, 15, 20, 30, 40 and 50 years into the future with 0% cost inflations and 0% increase in average annual daily traffic. In other words, the "consequence" component of risk for each slope was held constant to isolate the influence of changing hazard per the considered deterioration models. The CDOT deterioration models were first applied to each cut slope. In terms of physical deterioration, the CDOT models apply a 1.5% increase in rockfall frequency and 3% decrease in ditch effectiveness each year. Ditch effectiveness is only applied to the V_1 and V_2 rockfall volume classes (i.e., ditch effectiveness is set to zero for larger volumes), and V_2 ditch effectiveness set to half of that for V_1. Next, the ditch effectiveness deterioration conceptual model was used in combination with the CDOT deterioration model for increasing rockfall frequency.

Two scenarios of the time-since-excavation conceptual model were applied while still using CDOT's ditch effectiveness deterioration: one that assumed each cut slope had just been excavated at the present time, and one that assumed each cut slope was 50 years in age and fully weathered (the latter being more reflective of the actual slope conditions, given the estimated ages of the slopes in question). In the first scenario, the remote sensing MCF parameters were used to represent rockfall frequency after the initial increase of rockfall activity at t_1. In the second scenario, the remote sensing MCF parameters represented rockfall frequency for the slope in its fully weathered state (i.e., constant rockfall frequency). In addition to being applied

without any other proposed conceptual model, the time-since-excavation conceptual model was also applied with the ditch effectiveness deterioration conceptual model for both scenarios. Lastly, the scaling conceptual model was applied with the second time-since-excavation scenario. In other words, the scaling conceptual model used the remote sensing MCF parameters for a_0 and b_0 and assumed that the slope was already fully weathered.

When calculating ditch-filling rates for application of the ditch effectiveness deterioration conceptual model, MCF parameters were assumed to be constant for simplicity, even though rockfall activity may be increasing according to the CDOT deterioration model or the time-since-excavation conceptual model. All slopes were also assigned an initial ditch effectiveness of 0.75.

Furthermore, unlike the CDOT deterioration model, the ditch effectiveness was applied to $V_{max,d}$ calculated from Equation 3.13, which represents the maximum volume the ditch can be expected to retain, and the maximum volume considered in ditch effectiveness deterioration. With that in mind, Vail Pass, HI, and Manitou Springs had ditch effectiveness applied in classes V_1-V_3, while the rest of the slopes had ditch effectiveness applied to classes V_1-V_2. The same value of ditch effectiveness was applied to each of these respective classes (i.e., below $V_{max,d}$, ditch effectiveness is treated as independent of rockfall volume).

Table 7-1 displays the parameters used in each of the conceptual models. Initial rockfall frequencies for each volume class were found by first normalizing the MCF "a" intercept parameter in terms of a 0.1-mile length, meaning the original a was divided by the slope length and multiplied by 0.1 mile. This was done to allow for a more direct comparison between slopes and because the slope risk assessment framework assigns risk values for 0.1-mile-long segments of slopes. The cumulative frequencies were then converted into non-cumulative frequencies, since this is the form required for the rockfall frequency input in the slope risk assessment framework provided for the analysis. Remote sensing MCF parameters for each slope and detailed inputs for the ditch effectiveness deterioration model regarding slope-specific geometries can be referenced in Appendix B. To note, the ditch effectiveness deterioration conceptual model required remote sensing MCF parameters that are normalized by slope surface area rather than 0.1-mile lengths.

Table 7-1. Parameters used in the conceptual models.

Model	Parameter	Value
Ditch effectiveness	DE_0	0.75
Ditch effectiveness	φ	35 degrees
Ditch effectiveness	$V_{min,d}$	0.001 m^3
Ditch effectiveness	f_w	1.85
Ditch effectiveness	f_B	1.3
Time-since-excavation	Δt	20 years
Time-since-excavation	t_1	0 years
Time-since-excavation	k_0	1.5
Time-since-excavation	k_f	1.5
Time-since-excavation	c	0.3
Scaling	V_{min}	1 m^3
Scaling	V_{max}	100 m^3
Scaling	Δt	15
Scaling	t_1	0 years
Scaling	k	0.75
Scaling	c	0.3

7.3 Results

The resulting ARE comparisons are shown in Figures 7.1-7.3, which indicate that the current CDOT hazard deterioration generally outputs the highest risk in terms of ARE. Rates of deterioration in all cases are dependent on the given slope. ARE values differ at time 0 in the cases that the ditch effectiveness deterioration conceptual model has been applied; this occurs because the ditch effectiveness conceptual model, unlike the CDOT ditch effectiveness deterioration, does not apply a factor of 0.5 to ditch effectiveness for rockfall volume classes that are not V_1. Furthermore, for Vail Pass, HI, and Manitou Springs, ditch effectiveness is applied to the V_3 class in addition to V_1 and V_2. The CDOT ditch effectiveness deterioration model applies a ditch effectiveness of zero to classes V_3-V_5 for all slopes.

Likewise, the scaling and time-since-excavation conceptual models have different ARE values at time 0 in Figure 7.3. Scaling is set to occur at time 0 in Figure 7.3, causing an immediate decrease in rockfall frequency at time 0, while rockfall frequency is constant in the time-since-excavation conceptual model for the fully weathered slope case.

Figure 7.1 compares the ARE between different combinations of deterioration models with the assumption that slopes were recently excavated at time 0. The time-since-excavation conceptual model outputs a higher ARE than the CDOT hazard deterioration models until the slope reaches equilibrium and is fully weathered. Similarly, the ditch effectiveness deterioration conceptual model outputs a lower ARE than the time-since-excavation conceptual model and the combined ditch effectiveness deterioration and time-since-excavation conceptual model until the slope is fully weathered.

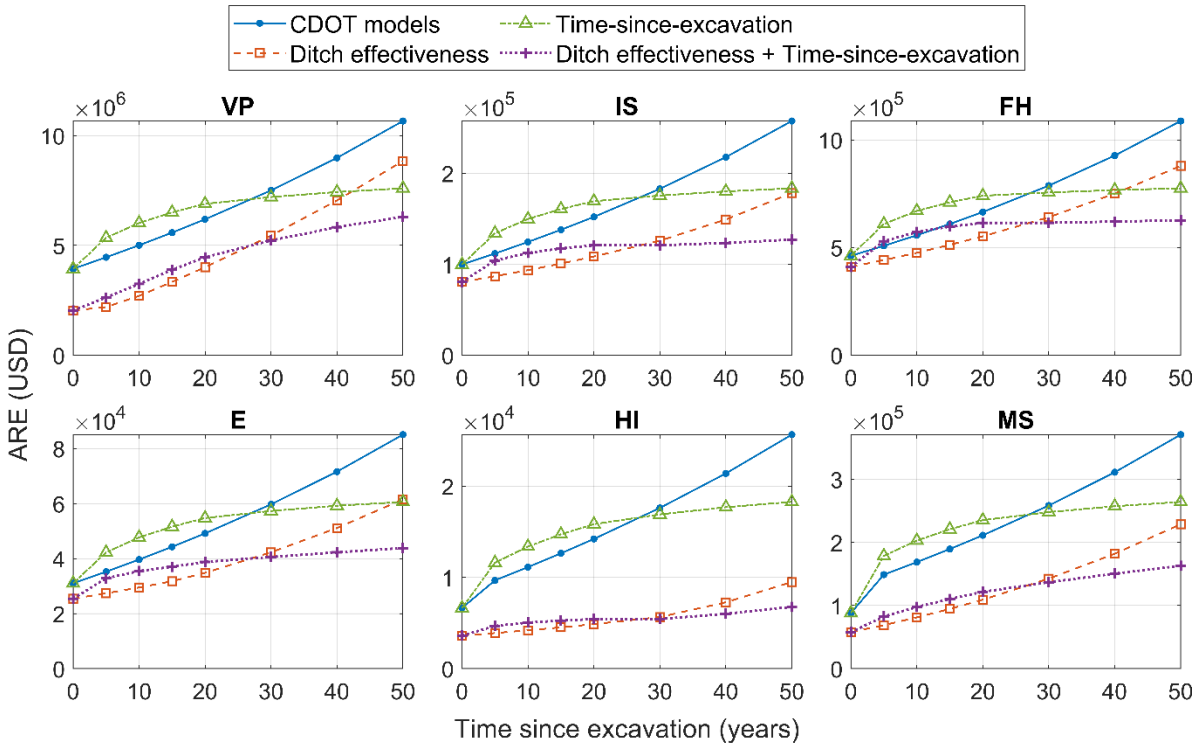

Figure 7.1. ARE comparison between different combinations of deterioration models. The "time-since-excavation" conceptual model assumes that slopes were recently excavated at time 0. The "ditch effectiveness" deterioration conceptual model is applied with the CDOT model for rockfall frequency increase, and the "time-since-excavation" conceptual model is applied with the CDOT ditch effectiveness deterioration model.

The time-since-excavation conceptual model applied in Figure 7.2 assumes that the slopes are already fully weathered; this scenario outputs a lower ARE than the CDOT hazard deterioration models at all points in time after time 0 since rockfall is no longer increasing. The combined ditch effectiveness deterioration and time-since-excavation conceptual models consistently output the lowest ARE in Figure 7.2.

Figure 7.3 provides an illustrative example of how scaling might temporarily improve the ARE by decreasing rockfall frequency. Scaling is assumed to be effective for 15 years in this example; after 15 years, ARE returns to the same value as predicted by the time-since-excavation conceptual model, assuming that slopes are fully weathered and have constant rockfall frequency.

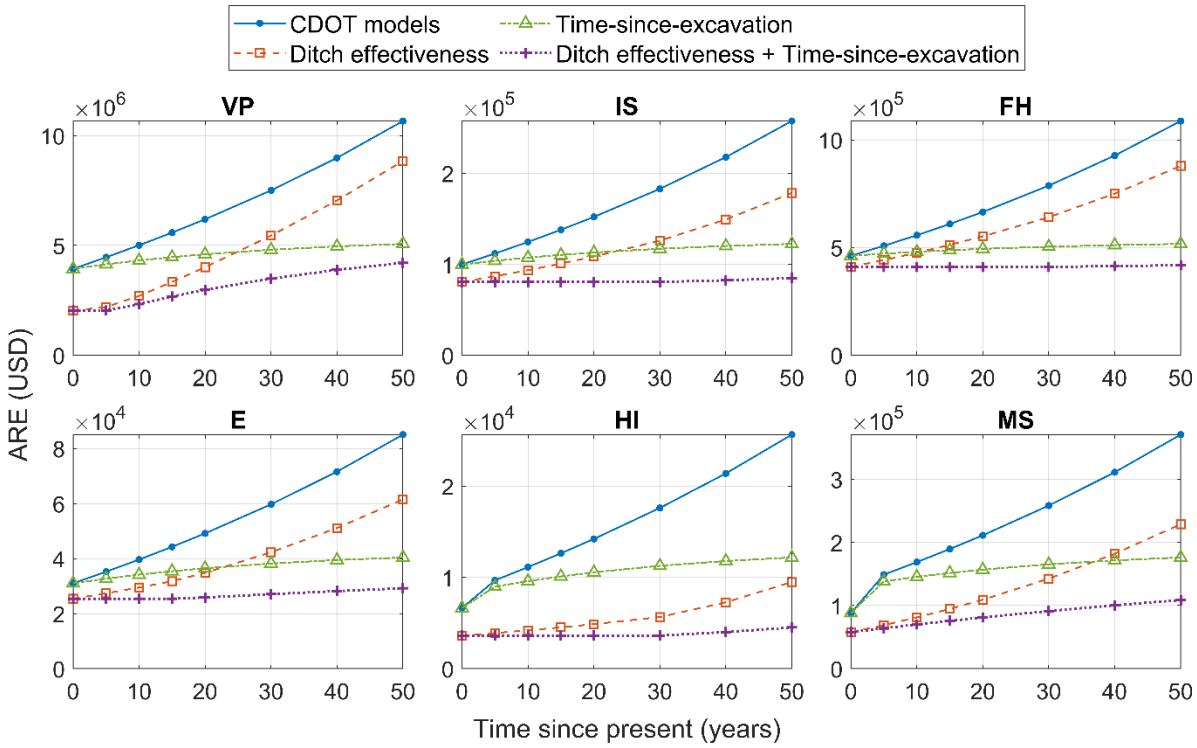

Figure 7.2. ARE comparison between different combinations of deterioration models. The time-since-excavation conceptual model assumes that slopes are fully weathered. The "ditch effectiveness" deterioration conceptual model is applied with the CDOT model for rockfall frequency increase, and the "time-since-excavation" conceptual model is applied with the CDOT ditch effectiveness deterioration model.

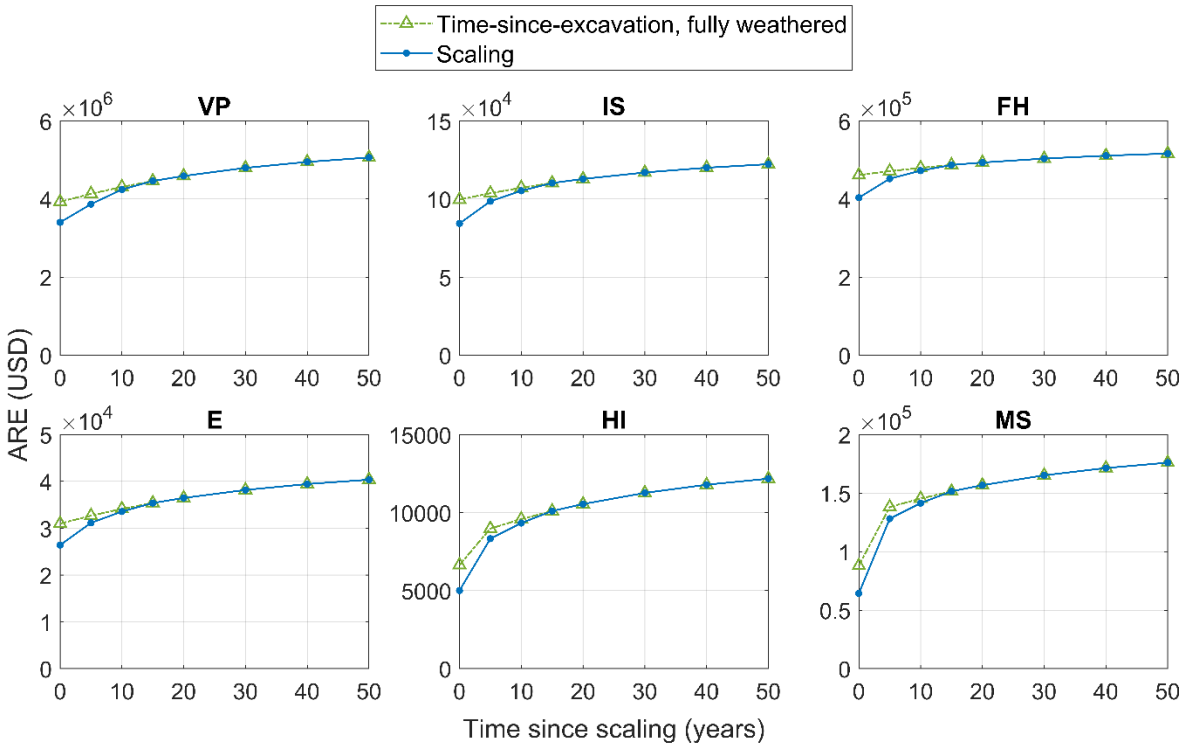

Figure 7.3. ARE comparison between scaling conceptual model and time-since-excavation conceptual model, assuming fully weathered slopes. The "time-since-excavation" and "scaling" conceptual models are applied with the CDOT ditch effectiveness deterioration model.

7.4 Discussion

Figures 7.1-7.3 indicate that the conceptual models generally produce lower ARE values than the current CDOT hazard deterioration models across all slopes. Thus, the CDOT hazard deterioration models are more conservative by applying both a 1.5% increase in rockfall frequency and a 3% decrease in ditch effectiveness each year.

The CDOT hazard deterioration models may be conservative relative to the ditch effectiveness deterioration conceptual model because the conceptual model considers more inputs that are slope-specific, such as the MCF curve and ditch geometry. The ditch effectiveness deterioration conceptual model predicts that ditch effectiveness will remain constant until a talus pile forms to the point where the ditch is filled to the horizontal. If the slope has a lower rockfall frequency, such as Idaho Springs or Floyd Hill, or a wide ditch, it will take longer for the ditch effectiveness to begin decreasing, thereby maintaining a slower rate of increasing ARE through time. In the cases of Idaho Springs and Floyd Hill, for example, it takes approximately 30 years before the ditch effectiveness begins decreasing. Furthermore, though the conceptual model predicts that ditch effectiveness deteriorates at an increasing rate, this rate is dependent on the rockfall frequency of the slope, as represented by the MCF curve parameters. This rate may be less than the 3% decrease in ditch effectiveness each year predicted by the CDOT model, as is the case for all slopes except Vail Pass.

Furthermore, in the CDOT model, a ditch effectiveness of zero is applied for rockfall volume classes V_3-V_5, and the ditch effectiveness is half as effective for class V_2. In the conceptual model, the ditch effectiveness is applied to a volume class depending on the largest rockfall volume that the ditch may retain, which is dependent on ditch geometry.

The CDOT hazard deterioration models are conservative relative to the time-since-excavation conceptual model if the slope is fully weathered, or if the total amount of rockfall frequency increase due to excavation is small relative to CDOT's annual 1.5% increase in rockfall frequency. The time-since-excavation conceptual model predicts that rockfall frequency will remain constant once the slope fully weathers, thereby resulting in a decreasing rate of performance deterioration. Contrastingly, the rockfall frequency increases at an increasing rate in the CDOT model.

When the ditch effectiveness deterioration conceptual model is coupled with the time-since-excavation conceptual model, ARE values decrease further, particularly if the slope is fully weathered. Rates of performance deterioration are higher for Vail Pass and Manitou Springs than the rest of the cut slopes since the ditch effectiveness deteriorates at a faster rate for these slopes.

The scaling conceptual model illustrates how scaling may further reduce ARE values (Figure 7.7). When scaling is no longer effective after $t_1 + \Delta t$, scaling may be applied again at a slope if resources allow.

7.5 Conclusions

In this section, forecasted ARE at different points of time was compared between the current CDOT hazard deterioration models and the proposed conceptual models. The CDOT hazard deterioration models consist of a 3% decrease in ditch effectiveness each year, and a 1.5% increase in rockfall frequency each year. The conceptual models applied in the analysis include the ditch effectiveness deterioration, time-since-excavation, and scaling conceptual models.

The results of the ARE comparison between different deterioration models using the baseline cases indicate that the current CDOT hazard deterioration models are generally conservative relative to the conceptual models. Each conceptual model and combination of conceptual models predict lower ARE values throughout time than the CDOT models, except in the case that the slopes are not yet fully weathered. However, once the slopes are fully weathered, the predicted ARE is lower than the CDOT models.

Using conceptual models that are evidence-based with parameters specific to a cut slope, the rate of predicted slope performance deterioration may be lower than what is predicted by a "one-size-fits-all" approach. This typically results in lower predicted ARE, thereby allowing for more distinct prioritization of slope management activities.

8.0 Conclusions and Recommendations

8.1 Research Summary

Deterioration modeling used to forecast changes in risk in cut slopes and other geotechnical assets is in its early stages of implementation. Therefore, existing deterioration models such as Markov models or a constant physical deterioration rate may not be the best approach for forecasting changes in cut slope risk. This research proposes a new deterioration framework using conceptual models that provide evidence-based predictions of how ditch effectiveness and rockfall frequency change through time. The conceptual models for rockfall frequency additionally include the effect of mitigation measures, specifically scaling and rock bolting. The ditch effectiveness deterioration conceptual model was provided with step-by-step recommendations on how to apply the model and estimate model parameters. The ditch effectiveness deterioration conceptual model was also evaluated using numerical modeling of 2D rockfall trajectories and simulation of a growing talus pile in the ditch.

Rockfall activity was quantified using MCF curves for seven cut slopes in Colorado using remote sensing-based rockfall inventories. These MCF curves can be used for hazard assessments as well as critical inputs for initial rockfall frequency in the conceptual models. The conceptual models ultimately predict physical deterioration, or changing rockfall activity through time. In the absence of a remote sensing, the MCF curve may be estimated. An estimation method developed by BGC Engineering was tested and compared against the remote sensing-based MCF curves.

Slope performance over time and the time-since-excavation conceptual model were evaluated using a dataset of slope ratings over time from the WSDOT USMS. This evaluation led to preliminary guidance for estimating parameters in the conceptual model. Lastly, physical deterioration was linked to performance deterioration using the CDOT slope risk assessment framework and forecasting risk values at different points in time for six Colorado cut slopes.

8.2 Conclusions

From the work described above, the following main conclusions were reached:

- The ditch effectiveness deterioration conceptual model is based on the principle that ditch effectiveness remains constant until the ditch is filled with rockfall debris so that its angle is horizontal. Then the ditch effectiveness decreases linearly as a function of the cross-sectional area of the talus pile forming in the ditch from rockfall debris. Once the talus pile in the ditch reaches its angle of repose, the ditch effectiveness can be considered zero. The ditch effectiveness deterioration rate decreases over time. Numerical modeling (Appendix A) supports the trends shown in the conceptual model, although the conceptual model may be conservative for shallower cut slopes with an overall slope angle less than 45 degrees. The conceptual model may be modified to account for this.

- The time-since-excavation conceptual model predicts that rockfall frequency will increase at the time of excavation. Then rockfall frequency increases at a decreasing rate as the slope reaches a new hazard equilibrium, meaning a consistent weathering front

exists within the slope. After the slope fully weathers, the underlying rockfall hazard remains approximately constant.

- The scaling conceptual model predicts that rockfall frequency will decrease at the time of scaling, ignoring any short-term increases in rockfall frequency immediately after scaling. As scaling loses its effectiveness, rockfall frequency will increase until it reaches its former frequency before scaling. The rock bolting conceptual model predicts the same trends, although rock bolts are expected to be effective for much longer than scaling. Both scaling and rock bolting are effective for a certain rockfall volume range.

- The conceptual models do not consider the effects of climate change and seasonal fluctuations of the MCF curve. Climate change may alter physical deterioration rates, but consideration of such an influence is outside the scope of this research.

- Historical levels of rockfall activity for seven Colorado cut slopes are quantified with MCF curves. Differences in MCF distributions are mainly a result of lithology and geological structure.

- The BGC Engineering MCF curve estimation method exhibits up to one order of magnitude of error and some potential improvements are suggested in Section 5.

- Based on analysis of the WSDOT data, physical deterioration may cease by 15-25 years after excavation of the cut, although the exact amount of time likely depends on lithology. Slope performance deterioration also appears be negligible after approximately 20 years (i.e., risk remains constant when cost inflation and average annual daily traffic increases are not considered).

- The proposed conceptual models may be used to link physical deterioration to performance deterioration within the CDOT slope risk assessment framework. Overall, the proposed conceptual models tend to predict less slope performance deterioration than the current CDOT hazard deterioration models, especially for existing slopes.

- The amount that rockfall frequency changes as a result of excavation or scaling (k_0/k_f and k, respectively) will have a large influence on the forecasted risk values. These parameters also have the largest uncertainty in terms of what their recommended values should be.

8.3 Recommendations for Implementation

The conceptual models predicting ditch effectiveness deterioration and changes in rockfall frequency through time are evidence-based and forecasted less performance deterioration than predicted by an example of current hazard deterioration models. Therefore, the conceptual models are recommended to be incorporated into the current deterioration modeling and slope risk assessment framework developed by BGC Engineering for CDOT. The models should be incorporated in such a way that the user only needs to input the parameters described in Section 3. If CDOT is considering climate change in deterioration modeling, a separate model for hazard evolution due to climate change should be used in conjunction with the conceptual models.

The user may choose to apply the rockfall frequency conceptual models separately or couple the rockfall frequency models. For instance, scaling and rock bolting can be applied to reflect a greater reduction in rockfall frequency but assuming the slope is fully weathered. Alternatively, the scaling and bolting models can be applied with the time-since-excavation model that assumes the slope is still weathering.

Stronger parameter guidance for the time-since-excavation, scaling, and bolting conceptual models is needed and may be a topic for future research. A range of plausible k_0/k_f and k values for the time-since-excavation, scaling, and bolting conceptual models has the most uncertainty. Ideal datasets to determine ranges of k_0/k_f and k would use remote sensing to repeatedly monitor rockfall frequency 5-10 years after a cut slope was excavated, scaled, or bolted. Using such data, the change in the MCF curve could be evaluated on an annual basis. These parameters should also be fine-tuned for different rock mass and lithology types, which would require datasets showing changes in the MCF curve over time for multiple slopes with differing characteristics.

The analyses in Section 6 provide preliminary guidance for how long after excavation the slope may weather until a point of rockfall hazard equilibrium is reached (i.e., up to ~15-25 years). Additionally, literature provides values for how long scaling may be effective and for the service life of rock bolts. However, the parameter Δt may also be better constrained for specific rock mass and geology types in each of the rockfall frequency conceptual models.

8.4 Adaptation of Findings to Other Geohazards

The physical deterioration modeling framework may be adapted to suit other geohazards, such as debris flows. In the case of debris flows, a similar approach is recommended, which involves the identification of variables used to calculate hazard that may change over time. For instance, magnitude-frequency or MCF relationships of debris flows are also used for hazard assessment (Liu et al., 2007; Hungr et al., 2008; Jakob and Nolde, 2024), which may change over time. Furthermore, inverse power laws may be used to approximate the MCF distribution for debris flows or landslides in general (Hungr et al., 2008). Magnitude is often represented by the volume of material in the debris flow, peak discharge, or runout (Jakob, 2005; Liu et al., 2007), while frequency may be calculated from a return period (Jakob and Nolde, 2024).

The magnitude of debris flows may depend on the following (Jakob, 2005):

- Volume of initiating failure
- Volume entrained along the transport channel
- Volumes deposited along the transport channel

If a valley has experienced multiple prior debris flows, the volume of the initiating failure may decrease over time as the basin transitions from transport-limited to weathering-limited, thereby changing the slope or valley's MCF distribution. For instance, Bovis and Jakob (1999) found that a multiple regression model used to predict debris flow frequency improved when categorizing basins into weathering- and transport-limited, and frequency prediction for weathering-limited basins was more prone to error. This indicates that there is a difference in MCF distributions between these two basin types.

The time-since-excavation conceptual model may be modified to represent debris flow frequency as a function of time since the first known initiated debris flow, or the cumulative volume removed in past events, and the magnitude of the event.

Mitigation for debris flows that reduce the frequency of debris flows may include diversion structures or berms, which would have analogous impacts as rockfall mitigation measures on rockfall MCF curves, such as scaling and bolting.

References

Allen, S. and Huggel, C. (2013). Extremely warm temperatures as a potential cause of recent high mountain rockfall. *Global and Planetary Change*, 107, 59-69. https://doi.org/10.1016/j.gloplacha.2013.04.007

Anderson, S. A. and Rivers, B. S. (2013). Capturing The Impacts of Geotechnical Features on Transportation System Performance. *Geo-Congress 2013,* 1640-1649. https://doi.org/10.1061/9780784412787.164

Anderson, S.A., Dodson, M.D., and Ortiz, T. (2017a). Risky Business: Identifying an Acceptable Rockfall Standard. *GEOSTRATA,* 21(5). https://doi.org/10.1061/geosek.0000288

Anderson, S. A., Dodson, M. D., and Greer, M. (2017b). Application of a Risk-Based Rock Slope Standard. *Proceedings of the 3rd North American Symposium on Landslides.*

Anderson, S. A., Vessely, M., Dowling, C., and Carter, R. (2022). *Geotechnical Asset Management for Slopes* (Publication No. 0092-21-06). Wisconsin DOT. https://wisconsindot.gov/documents2/research/0092-21-06-final-report.pdf

Andrew, R. D., and L. A. Pierson. (2012). Stabilization of Rockfall. In Rockfall: Characterization and Control, (A. K. Turner and R. L. Schuster, Eds.). Transportation Research Board, 468–493.

Applied Engineering Management Corporation (AEM), (2020). *Risk and Resilience Analysis Procedure: A Manual for Calculating Risk to CDOT Assets from Flooding, Rockfall, and Fire Debris Flow.* https://www.codot.gov/programs/planning/assets/cdot-rnr-analysis-procedure-8-4-2020-v6.pdf

Apted, M. J., Kemeny, J. M., Martin, C. D., and James, R. J. (2006). Independent Analysis of Seismicity and Rockfall Scenarios for the Yucca Mountain Repository. *Proceedings from the 2006 WM Symposia.*

Arndt, B., Arpin, B., Higgins, J. D., and Thompson, P. (2016). *Guidelines for Certification and Management of Flexible Rockfall Protection Systems* (Publication No. 823). National Cooperative Highway Research Program. https://doi.org/10.17226/23519

Arosio, D., Longoni, L., Mazza, F., Papini, M., and Zanzi, L. (2013). Freeze-Thaw Cycle and Rockfall Monitoring. *Landslide and Science and Practice,* 2. https://doi.org/10.1007/978-3-642-31445-2_50

Bajni, G., Camera, C.A.S., and Apuani, T. (2021). Deciphering meteorological influencing factors for Alpine rockfalls: a case study in Aosta Valley. *Landslides,* 18, 3279-3298. https://doi.org/10.1007/s10346-021-01697-3

Beckstrand, D., Mines, A., Thompson, P.D., and Benko, B. (2015). Development of Mitigation Cost Estimates for Unstable Soil and Rock Slopes Based on Slope Condition.

Proceedings from the 95th Transportation Research Board Annual Meeting. https://trid.trb.org/View/1393607

Beckstrand, D., Black, B., Mines, A., George, B., Thompson, P., and Stanley, D. (2017). *Rockfall Hazard Process Assessment (*Publication No. FHWA/MT-17-008/8239-001). Montana Department of Transportation. https://ntrl.ntis.gov/NTRL/dashboard/searchResults/titleDetail/PB2018100920.xhtml

Beckstrand, D., and Mines, A. (2017). Jump-starting a geotechnical asset management program with existing data*. Transportation Research Record*, 2656(1), 23–30. https://doi.org/10.3141/2656-03

Beckstrand, D, Stanley, D., Thompson, P., Bilderback, E., Wittie, M., Kanewala, U., Cuelho, E., and Anderson, D.A. (2019). *Unstable Slope Management Program for Federal Land Management Agencies* (Publication No. FHWA-FLH-19-002). FHWA. https://highways.dot.gov/sites/fhwa.dot.gov/files/docs/federal-lands/tech-resources/31011/usmp-field-manual.pdf

Beckstrand, D. L., Mines, A.E., George, B.A., Black, B.A. (2020). *Estimating and Contracting Rock Slope Scaling Adjacent to Highways: A Synthesis of Highway Practice* (Publication No. 555). National Cooperative Highway Research Program. https://doi.org/10.17226/25824

Besl, P. J., and McKay, N. D. (1992). A method for registration of 3-D shapes. *IEEE Transactions on Pattern Analysis and Machine Intelligence*, *14*(2), 239–256. https://doi.org/10.1109/34.121791

Blades, D., Constable, D., Lubkin, S., Matias, E., Beatty, W., Buck, J., Rozycki, R., Christenson, A., and Chang, C. (2018). *FHWA Computation Procedure for the Bridge Condition Measures* (Publication No. FHWA-HIF-18-023)*.* FHWA. https://rosap.ntl.bts.gov/view/dot/43548

Boadi, R. A., Thompson, P. D., Serigos, P., Bektas, B., and Xu, G. (2022). *Bridge Element Deterioration for Midwest States* (Publication No. TPF-5(432)). Wisconsin Department of Transportation. https://pooledfund.org/Details/Study/655

Bonneau, D., DiFrancesco, P.-M., and Hutchinson, D. J. (2019). Surface Reconstruction for Three-Dimensional Rockfall Volumetric Analysis. *ISPRS International Journal of Geo-Information*, *8*(12), 548. https://doi.org/10.3390/ijgi8120548

Bovis, M.J., and Jakob, M. (1999). The role of debris supply conditions in predicting debris flow activity. *Earth Surface Processes and Landforms,* 24(11), 1039-1054. https://doi.org/10.1002/(SICI)1096-9837(199910)24:11%3C1039::AID-ESP29%3E3.0.CO;2-U

Brawner, C. O. (1994). *Rockfall Hazard Mitigation Methods. Participant Workbook, NHI Course No. 13219* (Publication No. FHWA SA-93-085). U.S. Department of Transportation, FHWA.

Briggs, K. M., Dijkstra, T. A., and Glendinning, S. (2019). Evaluating the deterioration of geotechnical infrastructure assets using performance curves. *International Conference on Smart Infrastructure and Construction 2019: Driving data-informed decision-making*, 429–435. https://doi.org/10.1680/icsic.64669.429

Briggs, K. M., Dijkstra, T. A., and Glendinning, S. (2022). Assessing the Deterioration of Ageing Infrastructure Earthworks. *GEOSTRATA,* 26(4), 26-33. https://www.readgeo.com/geostrata/august_september_2022/MobilePagedArticle.action?articleId=1809521#articleId1809521

CDOT (2022). *Transportation Asset Management*. Colorado Department of Transportation. https://www.codot.gov/programs/tam

Chang, L., Dollevoet, R. P. B. J., and Hanssen, R. F. (2018). Monitoring Line-Infrastructure with Multisensor SAR Interferometry: Products and Performance Assessment Metrics. *IEEE Journal of Selected Topics in Applied Earth Observations and Remote Sensing*, 11(5), 1593–1605. https://doi.org/10.1109/JSTARS.2018.2803074

Chen, X., Du, W., Chen, L., Ma, B., Gong, S., Jiang, H., and Wang, W. (2022). Mechanical Strength Decay Evaluation of Excavation Unloaded Rock Mass under Freeze-Thaw Conditions. *Appl. Sci.,* 12, https://doi.org/10.3390/app122312205

Cheung, R. W., and Tang, W. H. (2005). Reliability of Deteriorating Slopes. *Journal of Geotechnical and Geoenvironmental Engineering,* 131(5), 589-297. https://doi.org/10.1061/(ASCE)1090-0241(2005)131:5(589)

Clauset, A., Shalizi, C. R., and Newman, M. E. J. (2009). Power-Law Distributions in Empirical Data. *SIAM Review*, *51*(4), 661–703. https://doi.org/10.1137/070710111

De Graff, J.V. and Gallegos, A.J. (2012). The Challenge of Improving Identification of Rockfall Hazard after Wildfires. *Environmental and Engineering Geoscience*, 18(4), 389-397. https://doi.org/10.2113/gseegeosci.18.4.389

Delonca, A., Gunzburger, Y., and Verdel. T. (2014). Statistical correlation between meteorological and rockfall databases. *Nat. Hazards Earth Syst. Sci.,* 14, 1953-1964. https://doi.org/10.5194/nhess-14-1953-2014

DiFrancesco, P.M., Bonneau, D.A., and Hutchinson, D.J. (2020). The Implications of M3C2 Projection Diameter on 3D Semi-Automated Rockfall Extraction from Sequential Terrestrial Laser Scanning Point Clouds. *Remote Sensing,* 12(11). https://doi.org/10.3390/rs12111885.

DiFrancesco, P.M., Bonneau, D.A., and Hutchinson, D.J. (2021). Computational Geometry-Based Surface Reconstruction for Volume Estimation: A Case Study on Magnitude-Frequency Relations for a LiDAR-Derived Rockfall Inventory. *International Journal of Geo-Information,* 10 (157). https://doi.org/10.3390/ijgi10030157

Dornan, D.L. (2002). Asset management: remedy for addressing the fiscal challenges facing highway infrastructure. *International Journal of Transport Management,* 1(1), 41-54. https://doi.org/10.1016/S1471-4051(01)00005-2

Douglas, G.R. (1980). Magnitude Frequency Study of Rockfall in Co. Antrim, N. Ireland. *Earth Surface Processes,* 5(2), 123-129. https://doi.org/10.1002/esp.3760050203

Ehrlich, M. Pereira de Costa, D., and Silva R.C. (2021). Long-term monitoring of the behavior of a talus-colluvium deposit. *Landslides,* 18, 2225-2245. https://doi.org/10.1007/s10346-021-01649-x

Ersöz, T., Topal, T. (2018a). Weathering and Excavation Effects on the Stability of Various Cut Slopes in Flysch-Like Deposits. *Geotech Geol Eng,* 36, 3707–3729 https://link.springer.com/article/10.1007/s10706-018-0566-z#citeas

Ersöz, T., Topal, T. (2018b). Assessment of rock slope stability with the effects of weathering and excavation by comparing deterministic methods and slope stability probability classification (SSPC). *Environmental Earth Sciences, 77*. https://doi.org/10.1007/s12665-018-7728-4

Ester, M., Kriegel, H.-P., Sander, J., and Xu, X. (1996). A Density-Based Algorithm for Discovering Clusters in Large Spatial Databases with Noise. *Proceedings of 2nd International Conference on Knowledge Discovery and Data Mining (KDD-96)*.

FHWA. (2007). *Geotechnical Technical Guidance Manual*. FHWA. https://highways.dot.gov/federal-lands/pddm/geotechnical-technical-guidance-manual

FHWA. (2021). *Asset Management: Transportation Asset Management Plans*. U.S. Department of Transportation Federal Highway Administration. https://www.fhwa.dot.gov/asset/plans.cfm

FHWA. (2022). *Applying Transportation Asset Management to Intelligent Systems Assets: A Primer. Chapter 6. Maximizing Performance—Lifecycle Planning.* U.S. Department of Transportation Federal Highway Administration. https://ops.fhwa.dot.gov/publications/fhwahop20047/chap6.htm

Fishman, K. L., and Withiam, J. L. (2011). *LRFD Metal Loss and Service-Life Strength Reduction Factors for Metal-Reinforced Systems* (Publication No. 675). National Cooperative Highway Research Program. https://doi.org/10.17226/14497

Gautreau, G.P., Lee, A., and Ferguson, N. (2023). *Geotechnical Asset Management for Louisiana* (Publication No. FHWA/LA.22/664). Louisiana Department of Transportation and Development. https://www.ltrc.lsu.edu/pdf/2023/FR_664.pdf

Girardeau-Montaut, D. (2024). *CloudCompare* (2.13.1) [Computer software]. https://www.cloudcompare.org/

González, Y.T., Briggs, K.M., Svalova, A., and Glendinning, S. (2023). Evaluating the likelihood of slope failure in ageing earthworks using Bayesian updating. *Infrastructure Asset Management,* 10(4), 207-222. https://doi.org/10.1680/jinam.23.00005

Graber, P. and Santi, P. (2022). Power law models for rockfall-frequency magnitude distributions: review and identification of factors that influence the scaling component. *Geomorphology*, 418. https://doi.org/10.1016/j.geomorph.2022.108463

Guerin, A., Stock, G.M., Radue, M.J., Jaboyedoff, M., Collins, B.D., Matasci, B., Avdievitch, N., and Derron, M.H. (2020). Quantifying 40 years of rockfall activity in Yosemite Valley with historical Structure-from-Motion photogrammetry and terrestrial laser scanning. *Geomorphology*, 356, https://doi.org/10.1016/j.geomorph.2020.107069

Hack, R. and Price, D. (1997). Quantification of Weathering. Engineering Geology and the Environment; *Proceedings of an International Symposium of the IAEG*, 145-150.

Hantz, D., Dussauge-Peisser, C., Jeannin, M., and Vengeon, J-M. (2003). Rock Fall Hazard Assessment: From Qualitative to Quantitative Failure Probability. *Proceedings of the International Conference on Fast Slope Movements,* 263-267.

Hantz, D., Colas, B., Dewez, T., Lévy, C., Rossetti, J.P., Guerin, A., and Jaboyedoff, M. (2020). Quantitative characterization of rock hazards of diffuse origin. *Rev. Gr. Geotech.,* 163. https://doi.org/10.1051/geotech/2020011

Ho, C.L. and Norton, S. (1991). *Development of an Unstable Slope Management System* (Publication No. GC-8720). Washington Department of Transportation. https://www.wsdot.wa.gov/research/reports/fullreports/270.1.pdf

Hollander, J. (2024). *Development of a High Temporal Resolution Rockfall Database using Structure-From-Motion Photogrammetry and Analysis of Seasonal- and Weather-Rockfall Relationships* [Unpublished master's thesis]. Colorado School of Mines.

Huisman, M., Hack, R., and Nieuwenhuis, J.D. (2006). Predicting Rock Mass Decay in Engineering Lifetimes: The Influence of Slope Aspect and Climate. *Environmental and Engineering Geoscience*, 12(1), 39-51. https://doi.org/10.2113/12.1.39

Huisman, M., Nieuwenhuis, J.D., and Hack, R. (2011). Numerical modelling of combined erosion and weathering of slopes in weak rock. *Earth Surface Processes and Landforms*, 36, 1705-1714. https://doi.org/10.1002/esp.2179

Hungr, O., Evans, S.G., and Hazzard, J. (1999). Magnitude and frequency of rockfalls and rock slides along the main transportation corridors of southwestern British Columbia. *Canadian Geotechnical Journal*, 36(2), 224-238. https://doi.org/10.1139/t98-106

Hungr, O., McDougall, S., Wise, M., and Cullen, M. (2008). Magnitude–frequency relationships of debris flows and debris avalanches in relation to slope relief. *Geomorphology,* 96, 355-365. https://doi.org/10.1016/j.geomorph.2007.03.020

Imaizumi, F., Trappmann, D., Matsuoka, N., Cánovas, J.A.B., Yasue, K., and Stoffel, M. (2020). Interpreting rockfall activity on an outcrop–talus slope system in the southern Japanese Alps using an integrated survey approach. *Geomorphology,* 371, https://doi.org/10.1016/j.geomorph.2020.107456

IPWEA. (2015). *International Infrastructure Management Manual*. International Edition 2015.

ISO. (2014). *ISO 55000: Asset management – Overview, principles, and terminology*. https://img1.wsimg.com/blobby/go/b653c9ee-535c-4528-a9c5-bb00166ad0dc/downloads/1bsmknus2_894046.pdf

Jakob, M. (2005). Debris-flow hazard analysis. In M. Jakob and O. Hungr (Eds.) *Debris-flow Hazards and Related Phenomena (*pp. 411-443) Springer. https://doi.org/10.1007/3-540-27129-5_17

Jakob, M., and Nolde, N. (2024). Statistical Techniques for Debris-Flow Frequency–Magnitude Analyses. In M. Jakob, S. McDougall, and P. Santi (Eds.), *Advances in Debris-flow Science and Practice (*pp. 249-271). Springer. https://doi.org/10.1007/978-3-031-48691-3

Janeras, M., Lantada, N., Núñez-Andrés, M., Hantz, D., Pedraza, O., Cornejo, R., Guinau, M., García-Sellés, D., Blanco, L., Gili, J.A., and Palau, J. (2023). Rockfall Magnitude-Frequency Relationship Based on Multi-Source Data from Monitoring and Inventory. *Remote Sensing*, 15(8), https://doi.org/10.3390/rs15081981.

Jiang, S., Li., D., Zhang, L., and Zhou, C. (2014). Time-dependent system reliability of anchored rock slopes considering rock bolt corrosion effect. *Engineering Geology,* 175, 1-8.

Keller, J.W., Siddoway, C., Morgan, M.L., Route, E.E., Grizzell, M.T., Sacerdoti, R., and Stevenson, A. (2003). "Geologic Map of the Manitou Springs Quadrangle, El Paso and Teller Counties, Colorado." https://ngmdb.usgs.gov/Prodesc/proddesc_78127.htm

Kellerer-pirklbauer, A., Lieb, G.K., Avian, M., and Carrivick, J. (2016). Climate change and rock fall events in high mountain areas: numerous and extensive rock falls in 2007 at Mittlerer Burgstall, central Austria. *Geografiska Annaler: Series A, Physical Geography*, 94, 59-78. https://doi.org/10.1111/j.1468-0459.2011.00449.x

Kellogg, K. S., Shroba, R. R., Premo, W. R., and Bryant, B. (2011). "Geologic Map of the Eastern Half of the Vail 30' × 60' Quadrangle, Eagle, Summit, and Grand Counties, Colorado." https://pubs.usgs.gov/sim/3170/

Kendorski, F.S. (2003). Rock Reinforcement Longevity. *Geo-strata*, Fall 2003, 9-12. https://www.agapito.com/wp-content/uploads/2016/09/Rock-Reinforcement-Longevity.pdf

Kirkham, R.M., Streufert, R.K., Cappa, J.A., Shaw, C.A., Allen, J.L., and Schroeder, T.J. (2009). "Geologic Map of the Glenwood Springs Quadrangle, Garfield County, Colorado." https://ngmdb.usgs.gov/Prodesc/proddesc_94610.htm

Lague, D., Brodu, N., and Leroux, J. (2013). Accurate 3D comparison of complex topography with terrestrial laser scanner: Application to the Rangitikei canyon (N-Z). *ISPRS Journal of Photogrammetry and Remote Sensing*, *82*, 10–26. https://doi.org/10.1016/j.isprsjprs.2013.04.009

Lane, R., and Fishman, K.L. (2005). Condition Assessment and Service Life Estimation for Rock Reinforcement: Case Study. *Proceedings of the 85th Annual TRB Meeting.*

Lane, R. (2006). Assessing the Condition and Estimating the Longevity of Rock Reinforcement Systems. *TR News 244, May-June 2006*, 36-37. https://onlinepubs.trb.org/onlinepubs/trnews/trnews244rpo.pdf

Lato, M. Gauthier, D. Quinn, P., Hutchinson, D.J., Kromer, R., Edwards, T., and Riopel, J. (2015). 3D Data Collection for Rapid Rock Fall Response Situations. *Proceedings of GeoQuébec 2015,* 513.

Lato, M., Quinn, P., McDougall, Strouth, A. Pritchard, M., and Sirois, D. (2016). Probabilistic Rock Fall Assessment: Accounting for the Effects of Engineered Mitigation. *Proceedings of GeoVancourver 2016.*

Lin, P., Yuan, X. X., and Tovilla, E. (2019). Integrative modeling of performance deterioration and maintenance effectiveness for infrastructure assets with missing condition data. *Computer-Aided Civil and Infrastructure Engineering*, 34(8), 677–695. https://doi.org/10.1111/mice.12452

Liu, J.J., Li, Y., Su, P.C., and Cheng, Z.L. (2007). Magnitude-frequency relations in debris flow. *Environ Geol.* 55, 1345-1354. https://doi.org/ 10.1007/s00254-007-1083-1

Luciani, A., Todaro, C., and Peila, D. Maintenance and risk management of rockfall protection net fences through numerical study of damage influence. *Frattura ed Integrità Strutturale*, 43, 241-250. https://doi.org/10.3221/IGF-ESIS.43.19

Luckman, B.H. (1976). Rockfalls and rockfall inventory data: Some observations from surprise valley, Jasper National Park, Canada. *Earth Surface Processes,* 1(3), 287-298. https://doi.org/10.1002/esp.3290010309

Macciotta, R., Hendry, M., Cruden, D.M., Blais-Stevens, A., and Edwards, T. (2017). Quantifying rock fall probabilities and their temporal distribution associated with weather seasonality. *Landslides,* 14, 2025-2039. http://dx.doi.org/10.1007/s10346-017-0834-7

Macedo, J., Burns, S.E., Torres, J., Jung, Y.S., Liu, C., and Tsai Y. (2023). *Towards the Implementation of a Geotechnical Asset Management Program in the State of Georgia* (Publication No. FHWA-GA-23-2011). Georgia Department of Transportation. https://rosap.ntl.bts.gov/view/dot/67653

Mainieri, R., Eckert, N., Corona, C., Lopez-Saez, Stoffel, M., and Bourrier, F. (2022). Limited impacts of global warming on rockfall activity at low elevations: Insights from two

calcareous cliffs from the French Prealps. *Progress in Physical Geography: Earth and Environment,* 47(1), https://doi.org/10.1177/03091333221107624.

Malsam, A.C., Walton, G., Schovanec, H.E., Bonneau, D.A., DiFrancesco, P., and Hutchinson, D.J. (2021). An Analysis of Seasonal Rockfall Trends at Floyd Hill: A Slope Along I-70, East of Idaho Springs, CO. *Proceedings of the 55th U.S. Rock Mechanics/Geomechanics Symposium*.

Malsam, A. (2022). *Characterization of rockfall activity and identification of weather-rockfall relationships using high temporal resolution remote sensing methods* (Publication No. 29206245) [Master's thesis, Colorado School of Mines]. ProQuest Dissertations Publishing.

Martinović, K., Gavin, K., and Reale, C. (2016). Assessing the Vulnerability of Irish Rail Network Earthworks. *Transportation Research Procedia*, 14, 1904–1913. https://doi.org/10.1016/j.trpro.2016.05.157

McKibbins, L., Spink, T. and Power, C. (2019) *Deterioration modelling of civil engineering infrastructure assets* (Publication No. C874). CIRIA. https://www.ciria.org/CIRIA/Books/Free_publications/C784F.aspx#:~:text=Deterioration%20modelling%20of%20civil%20engineering%20infrastructure%20assets%20(C784),deterioration%20and%2For%20its%20outcomes.

Mines, A.E., Beckstrand, D., Thompson, P. D., Boundy, B., Helm, S., and Jackson, J. (2018). Estimating Event Likelihood for Rock Slope Assets on Transportation Networks. *Transportation Research Record*, 2672(52), 316–324. https://doi.org/10.1177/0361198118777622

Mines, A.E., Beckstrand, D.L., and Bunn, M.D. (2023). *Development of a Geotechnical Asset Management Collection and Rating Program for Missouri Department of Transportation* (Publication No. cmr 23-004). Missouri Department of Transportation Construction and Materials Division. https://rosap.ntl.bts.gov/view/dot/66994

Mirzaei, Z., Adey, B., Klatter, L., and Thompson, P.D. (2014). *Overview of Existing Bridge Management Systems*. International Association of Bridge Maintenance and Safety, Bridge Management Committee. https://www.researchgate.net/publication/322754699_Overview_of_existing_Bridge_Management_Systems_-_Report_by_the_IABMAS_Bridge_Management_Committee

Morcous, G., Hanna, A., Rivard, H. (2002). Modeling Bridge Deterioration Using Case-based Reasoning. *Journal of Infrastructure Systems*, 8(3). https://doi.org/10.1061/(ASCE)1076-0342(2002)8:3(86)

Nicholson, D.T. (2000). *Deterioration of Excavated Rockslopes: Mechanisms, Morphology and Assessment* (Publication No. uk.bl.ethos.416598). [Doctoral dissertation, University of Leeds]. White Rose eTheses Online.

Nicholson, D. T., Lumsden, A. C., Hencher, S. R., Bromhead, E., Dixon, N., and Ibsen, M. L. (2000). Excavation-Induced Deterioration of Rockslopes. *Landslides: Landslides in research, theory, and practice, Proceedings of the 8th International Symposium, Cardiff, Wales,* 1105-1110. https://www.hencherassociates.com/app/download/5810051294/2000+Nicholson+Lumsden+Hencher.pdf

Oester, N., Group, R., and Ortiz, Ty. (2019). Implementation and Application of Geotechnical Asset Management in Colorado. *Proceedings of the 70th Highway Geology Symposium.* https://www.highwaygeologysymposium.org/wp-content/uploads/70th_HGS-OPT.pdf

Omar, T. (2018). *Condition Assessment of Concrete Bridge Decks Using Ground Condition Assessment of Concrete Bridge Decks Using Ground and Airborne Infrared Thermography and Airborne Infrared Thermography* (Publication No. 5252) [Doctoral dissertation, University of Western Ontario]. Electronic Thesis and Dissertation Repository.

Omar, T., and Nehdi, M. L. (2018). Condition assessment of reinforced concrete bridges: Current practice and research challenges. *Infrastructures*, 3(3). https://doi.org/10.3390/infrastructures3030036

Patnaik, A., Musa, A., Marchetty, S., and Liang, R. (2019). Full-Scale Testing and Performance Evaluation of Rockfall Concrete Barriers. *Journal of the Transportation Research Board*, 2522(1). https:///doi.org/10.3141/2522-03

Phillips, C. (2024). *Quantifying Causes and Variability of Rockfall Activity: Comparison of Multiple Colorado Rock Slopes Monitored Using Terrestrial Remote Sensing* [Unpublished master's thesis]. Colorado School of Mines.

Pierson, L.A. (1991). *The Rockfall Hazard Rating System*. Oregon Department of Transportation. https://rosap.ntl.bts.gov/view/dot/22762

Pierson, L.A., Gullixson, C.F., and Chassie, R.G. (2001). *Rockfall Catchment Area Design Guide* (Publication No. SPR-3(032)). Oregon Department of Transportation. https://www.oregon.gov/odot/Programs/ResearchDocuments/RokfallCatchAreaDesMetric.pdf

Pierson, L. A., and Vierling, M.P. (2012). Mitigation Selection. In A. K. Turner and R. L. Schuster (Eds.). *Rockfall Characterization and Control* (pp. 445-467). Transportation Research Board.

Postill, H., Helm, P. R., Dixon, N., Glendinning, S., Smethurst, J. A., Rouainia, M., Briggs, K. M., El-Hamalawi, A., and Blake, A. P. (2021). Forecasting the long-term deterioration of a cut slope in high-plasticity clay using a numerical model. *Engineering Geology*, 280. https://doi.org/10.1016/j.enggeo.2020.105912

Power, C., Mian, J., Spink, T., Abbott, S., and Edwards, M. (2016). Development of an Evidence-based Geotechnical Asset Management Policy for Network Rail, Great Britain. *Procedia Engineering,* 143, 726–733. https://doi.org/10.1016/j.proeng.2016.06.112

Pratt, C., Macciotta, R., and Hendry, M. (2018). Quantitative relationship between weather seasonality and rock fall occurrences north of Hope, BC, Canada. *Bulletin of Engineering Geology and the Environment*, 78, 3239-3251. https://doi.org/10.1007/s10064-018-1358-7

Pritchard, O., Ní Bhreasail, Á., Campbell, G., Carluccio, S., Willis, M., and Codd, J. (2018). Practical remote survey applications for improved geotechnical asset management on England's strategic road network. *Proceedings of the 7th Transport Research Arena.* https://www.researchgate.net/publication/324861711_Practical_remote_survey_applications_for_improved_geotechnical_asset_management_on_England's_strategic_road_network

Randall, Jack. (2022). *National Highways Geotechnical Asset Performance: Deterioration Modelling for Decision Support* (Publication No. 37395). Mott MacDonald. https://nationalhighways.co.uk/media/o30l3f4r/national-highways-geotechnical-asset-performance_rev2e_20220818_approved_for-issue.pdf

Ravanel, L. and Deline, P. (2014). Rockfall Hazard in the Mont Blanc Massif Increased by the Current Atmospheric Warming. *Engineering Geology for Society and Territory*, 1, 425-428. https://doi.org/10.1007/978-3-319-09300-0_81

Rocscience. (2023). RocFall2 software, Version 8.022. https://www.rocscience.com/software/rocfall

Romana, M. (1985). New adjustment rating for application of the Bieniawski classification to slopes. *Proceedings of international symposium on rock mechanics, mining civil works,* pp.59–63.

Romana, M.R. (1993). A Geomechanical Classification for Slopes: Slope Mass Rating. In Hudson, J.A (Ed.). *Rock Testing and Site Characterization: Principles, Practice and Projects* (pp. 575-600). Elsevier. https://doi.org/10.1016/B978-0-08-042066-0.50029-X

Sala, Z. and Vessely, M. (2022). *Rockfall Risk Assessment Framework – Working Draft*. Project Memorandum, BGC Engineering.

Salunke, R. Nobahar, M., and Khan, M.S. (2023). A Cross-Platform Approach Using Remote Sensing and Geophysical Monitoring to Streamline Geotechnical Asset Management. *Geo-Congress 2023,* 471-481. https://doi.org/10.1061/9780784484692.048

Sanford-Bernhardt, K. L., Loehr, J Erik, and Huaco, D. (2003). Asset Management Framework for Geotechnical Infrastructure. *Journal of Infrastructure Systems,* 9(3). https://doi.org/10.1061/ASCE1076-034220039:3107

Sarro, R., Pérez-Rey, I., Tomás, R., Alejano, L.R., Hernández-Gutiérrez, L.E., and Mateos R.M. (2021). Effects of Wildfire on Rockfall Occurrence: A Review through Actual Cases in Spain. *Appl. Sci.*, 11(6). https://doi.org/10.3390/app11062545

Sasiharan, N., Muhunthan, B., Badger, T.C., Shu, S., and Carradine, D.M. (2006). Numerical analysis of the performance of wire mesh and cable net rockfall protection systems. *Engineering Geology,* 88(1-2), 121-132. https://doi.org/10.1016/j.enggeo.2006.09.005

Sass, O. (2005). Temporal Variability of Rockfall in the Bavarian Alps, Germany. *Arctic, Antarctic, and Alpine Research,* 37 (4), 564-573. https://doi.org/10.1657/1523-0430(2005)037[0564:TVORIT]2.0.CO;2

Scavia, C., Barbero, M., Castelli, M., Marchelli, M., Peila, D., Torsello, G., and Vallero, G. (2020). Evaluating Rockfall Risk: Some Cirtical Aspects. *Geosciences* 10, 89. https://doi.org/10.3390/geosciences10030098

Scott, G.R. (1972). "Geologic Map of the Morrison Quadrangle, Jefferson County, Colorado." https://ngmdb.usgs.gov/Prodesc/proddesc_9620.htm

Sheridan, D.M. and Marsh, S.P. (1976). "Geologic Map of the Squaw Pass quadrangle, Clear Creek, Jefferson, and Gilpin Counties, Colorado." https://doi.org/10.3133/gq1337

Sims P.K., 1964. "Geology of the Central City Quadrangle, Colorado." https://ngmdb.usgs.gov/Prodesc/proddesc_722.htm

Spink, T. (2019). Strategic geotechnical asset management. *Quarterly Journal of Engineering Geology and Hydrogeology*, 53(2), 304-320. https://doi.org/10.1144/qjegh2019-014

Stanley, D. A., and Pierson, L. A. (2013). Geotechnical Asset Management of Slopes: Condition Indices and Performance Measures. *Geo-Congress 2013*, 1658-1667. https://doi.org/10.1061/9780784412787.166

Stoffel, M., Schneuwly, D., Bollschweiler, M., Lièvre, I., Delaloye, R., Myint, M., and Monbaron, M. (2005). Analyzing rockfall activity (1600–2002) in a protection forest—a case study using dendrogeomorphology. *Geomorphology* 68(3-4), 224–241.

Tating, F., Hack. R., and Jetten, V. (2013). Engineering aspects and time effects of rapid deterioration of sandstone in the tropical environment of Sabah, Malaysia. *Engineering Geology,* 159, 20-30. https://doi.org/10.1016/j.enggeo.2013.03.009

Thomas, O., and Sobanjo, J. (2013). Comparison of Markov Chain and Semi-Markov Models for Crack Deterioration on Flexible Pavements. *Journal of Infrastructure System*s, 19(2), 186–195. https://doi.org/10.1061/(asce)is.1943-555x.0000112

Thompson, P. D. (2017). *Geotechnical Asset Management Plan: Technical Report* (Publication No. STP000S(802)(B)). Alaska Department of Transportation. https://dot.alaska.gov/stwddes/desmaterials/mat_geotech_services/assets/gam_plan_tech_report.pdf

Thurlby, R. (2013). Managing the asset time bomb: A system dynamics approach. *Proceedings of the Institution of Civil Engineers: Forensic Engineering,* 166(3), 134–142. https://doi.org/10.1680/feng.12.00026

Transportation Research Record Board (TRB) (2018). Managing Highway Rock Slope Scaling. *Presentations from the 97th Annual Meeting of the Transportation Research Board.* https://onlinepubs.trb.org/onlinepubs/circulars/ec260.pdf

Turner, A.K. (1996). Colluvium and Talus. In A.K. Turner and R.L. Schuster (Eds.). *Landslides: Investigation and Mitigation* (pp.525-554). Transportation Research Board.

van Veen, M., Hutchinson, D.J., Kromer, R., Lato, M., and Edwards, T. (2017). Effects of sampling interval on the frequency - magnitude relationship of rockfalls detected from terrestrial laser scanning using semi-automated methods. *Landslides*, 14, 1579-1592. https://doi.org/10.1007/s10346-017-0801-3

Vessely, M., Robert, W., Richrath, S., Loehr, E., and Boeckmann, A. (2019). *Geotechnical Asset Management for Transportation Agencies, Volume 2: Implementation Manual* (Publication No. 903). National Cooperative Highway Research Program. https://doi.org/10.17226/25364

Walton, G. and Diederichs, M.S. (2015). A New Model for the Dilation of Brittle Rocks Based on Laboratory Compression Test Data with Separate Treatment of Dilatancy Mobilization and Decay. *Geotechnical and Geological Engineering*, 33, 661-679.

Walton, G. and Weidner, L. (2022). Accuracy of Rockfall Volume Reconstruction from Point Cloud Data—Evaluating the Influences of Data Quality of Data Quality and Filtering. *Remote Sensing*, 15(1). https://doi.org/10.3390/rs15010165

Walton, G., Christiansen, C., Kromer, R., and Silaev, A. (2023). Evaluation of rockfall trends at a sedimentary rock cut near Manitou Springs, Colorado, using daily photogrammetric monitoring. *Landslides,* 20(12), 2657-2674. https://doi.org/10.1007/s10346-023-02121-8

Waseem, A., Tappenden, K., St Michel, G., and Skirrow, R. (2022). Alberta Transportation Geotechnical Asset Management (GAM) Framework Development, GAM Planner Application Pilot Study. *Proceedings of the 2022 Transportation Association of Canada Conference & Exhibition*. https://www.tac-atc.ca/sites/default/files/conf_papers/am4_waseema.pdf

Weidner, L. and Walton, G. (2021). Monitoring the Effects of Slope Hazard Mitigation and Weather on Rockfall along a Colorado Highway Using Terrestrial Lidar Scanning. *Remote Sensing,* 13, 4584. https://doi.org/10.3390/rs13224584

Wellman, E.C., Akbulut, N.A., and Kemeny, J. (2023). Ground Support Asset Management. *Proceedings of the 57th U.S. Rock Mechanics/Geomechanics Symposium.* https://doi.org/10.56952/ARMA-2023-0527

Williams, J.G., Rosser, N.J., Hardy, R.J., and Brain, M.J. (2019). The Importance of Monitoring Interval for Rockfall Magnitude-Frequency Estimation. Journal of Geophysical Research: Earth Surface, 124(12), 2841-2853. https://doi.org/10.1029/2019JF005225

Werley, K. (2024). *Towards an Evidence-Based Approach for Forecasting Cut Slope Deterioration*. Colorado School of Mines.

Wolf, R.E., Bouali, E.H., Oommen, T., Dobson, R., Vitton, S., Brooks, C., and Lautala, P. (2015). *Final Report: Sustainable Geotechnical Asset Management along the Transportation Infrastructure Environment Using Remote Sensing* (Publication No. RITARS-14-H-MTU). Michigan Technological University, U.S. Department of Transportation. https://rosap.ntl.bts.gov/view/dot/38809

Wollenberg-Barron, T., Macciotta, R., Gräpel, C., Tappenden, and Skirrow, R. (2023). S042 Rock Slope: Use of remote sensing with rock slope rating systems for Geotechnical Asset Management. *Proceedings of the 76th Canadian Geotechnical Conference.* https://www.researchgate.net/publication/374740352_S042_Rock_Slope_Use_of_remote_sensing_with_rock_slope_rating_systems_for_Geotechnical_Asset_Management

Wyllie, D.C. and Mah, C.W. (2004). Rock Slope Engineering: Civil and Mining, 4th ed. Spon Press, New York.

Appendix A: Numerical Evaluation of the Ditch Effectiveness Deterioration Conceptual Model

A.1 Introduction

To evaluate the validity of the proposed ditch effectiveness deterioration conceptual model, numerical modeling was performed with various combinations of cut slope and ditch geometries according to the procedure outlined in Figure A.1 and detailed in the following sections.

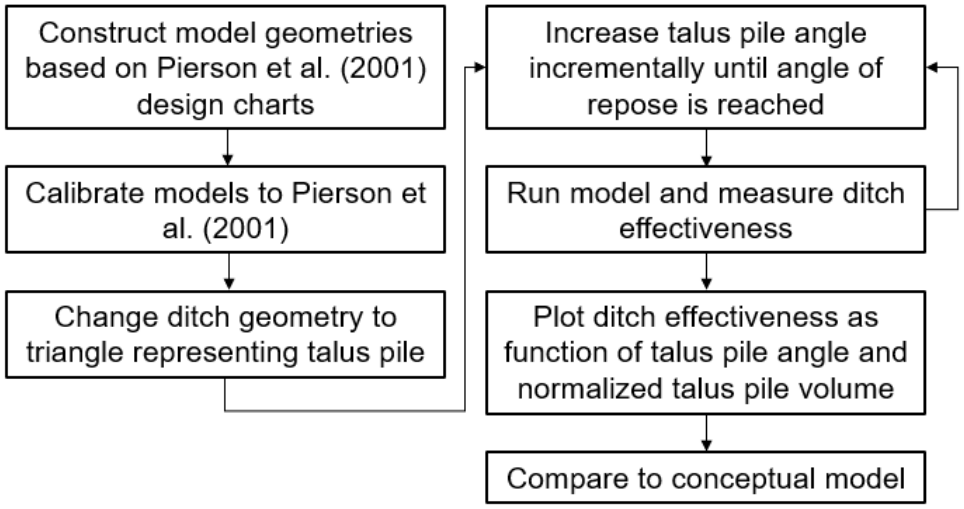

Figure A.1. Workflow for evaluation of conceptual model using numerical simulations.

A.2 Methods

Numerical modeling was performed in RocFall2 (Rocscience, 2023) using a lumped mass analysis. All model geometries were constructed to be consistent with Pierson et al. (2001). First, 24 models were used for calibration to Pierson et al.'s (2001) design guidelines. Ditch-filling and talus pile formation was then simulated with each cut slope angle and height and by approximating the talus pile as a triangle. The talus pile angle was increased incrementally until the angle of repose was reached, and the simulated ditch effectiveness was recorded for each increment.

The 24 models used for calibration had geometries according to Table A-1 and were constructed using Pierson et al.'s (2001) design guidelines. Ditch effectiveness was measured as the proportion of rockfall that did not reach the road. Cut slopes were defined using coordinates with 0.1 m vertical spacing. A 0.45 m horizontal offset was included in the center of cut slopes if the corresponding cut slope in Pierson et al.'s (2001) field testing included that offset for presplit blasting.

Calibrated parameters are shown in Table A-2. The standard deviation applied to the model coordinates was calibrated to represent macroscopic slope roughness and varies depending on cut slope angle and height. Note that the standard deviation was only applied to the rock slope

coordinates; in all models, the ditch geometry (including talus pile geometries discussed later) was treated as fully deterministic.

Table A-1. Calibration geometries.

Cut slope angle	Cut slope height (m)	Ditch slope	Ditch width (m)	Target proportion rockfall retained	Case no.
4V:1H	12.2	1V:4H	2.7	0.90	4.1
4V:1H	12.2	1V:4H	4.8	0.99	4.2
4V:1H	12.2	1V:6H	2.9	0.90	4.3
4V:1H	12.2	1V:6H	4.9	0.99	4.4
4V:1H	24.4	1V:4H	6.8	0.90	4.5
4V:1H	24.4	1V:4H	12.3	0.99	4.6
4V:1H	24.4	1V:6H	9.4	0.90	4.7
4V:1H	24.4	1V:6H	14.8	0.99	4.8
2V:1H	12.2	1V:4H	3.5	0.90	2.1
2V:1H	12.2	1V:4H	4.9	0.99	2.2
2V:1H	12.2	1V:6H	5.2	0.90	2.3
2V:1H	12.2	1V:6H	7.3	0.99	2.4
2V:1H	24.4	1V:4H	5.7	0.90	2.5
2V:1H	24.4	1V:4H	8.1	0.99	2.6
2V:1H	24.4	1V:6H	6.9	0.90	2.7
2V:1H	24.4	1V:6H	10.5	0.99	2.8
1V:1H	12.2	1V:4H	3.7	0.90	1.1
1V:1H	12.2	1V:4H	4.9	0.99	1.2
1V:1H	12.2	1V:6H	6.7	0.90	1.3
1V:1H	12.2	1V:6H	9.8	0.99	1.4
1V:1H	24.4	1V:4H	7.1	0.90	1.5
1V:1H	24.4	1V:4H	11	0.99	1.6
1V:1H	24.4	1V:6H	10.5	0.90	1.7
1V:1H	24.4	1V:6H	15	0.99	1.8

Intact weathered bedrock, gravel road, and asphalt properties from the default material library in RocFall were initially used to represent the cut slope, ditch, and road shoulder, respectively. The coefficients of normal and tangential restitution were altered for the ditch material to fine tune ditch effectiveness results following adjustments to the slope coordinate standard deviation values. The bedrock friction angle and coefficients of normal and tangential restitution were not substantially modified, while asphalt parameters were kept fully unchanged. Since less uncertainty is involved in the material parameters rather than the standard deviation of slope coordinates (e.g., literature values exist for different materials), the same material parameters were used in each model. However, there is non-uniqueness in the calibration parameters since the scenario is underdetermined; thus, multiple sets of calibration parameters may exist.

Three rockfall groups were used in a lumped mass analysis, with masses calculated based on a density of 2650 kg/m3 and the measured diameters from Pierson et al.'s (2001) field testing.

Consistent with the field testing, 40%, 30%, and 30% of rockfalls had diameters of 0.3, 0.6, and 0.9 m, respectively. Five thousand spherical rockfalls were simulated with no initial velocity. All models but Case 2.1 (Table A-1) were calibrated within ±0.05 of the target ditch effectiveness.

Table A-2. Calibrated model parameters.

Property	Model	Value (m)
X and Y slope coordinate std. dev.	4V:1H, 12.2 m cut slopes	0.0015
X and Y slope coordinate std. dev.	4V:1H, 24.4 m cut slopes	0.0030
X and Y slope coordinate std. dev.	2V:1H, 12.2 m and 24.4 m cut slopes	0.0021
X and Y slope coordinate std. dev.	1V:1H, 12.2 m cut slope, 1V:4H ditch slope	0.0065
X and Y slope coordinate std. dev.	1V:1H, 12.2 m cut slope, 1V:6H ditch slope	0.0075
X and Y slope coordinate std. dev.	1V:1H, 24.4 m cut slopes	0.0075
Material	Parameter	Value
Ditch	Normal restitution	0.43
Ditch	Normal restitution, std. dev.	0.10
Ditch	Tangential restitution	0.93
Ditch	Tangential restitution, std. dev.	0.01
Ditch	Friction angle (deg)	10.0
Bedrock	Normal restitution	0.36
Bedrock	Normal restitution, std. dev.	0.04
Bedrock	Tangential restitution	0.86
Bedrock	Tangential restitution, std. dev.	0.04
Bedrock	Friction angle (deg)	25.0

The initial geometries used for simulating ditch-filling and talus pile formation include the following, each with the 1V:4H ditch slope, 0.99 ditch effectiveness case:

- 4V:1H, 12.2 m cut slope
- 4V:1H, 24.4 m cut slope
- 2V:1H, 12.2 m cut slope
- 2V:1H, 24.4 m cut slope
- 1V:1H, 12.2 m cut slope
- 1V:1H, 24.4 m cut slope

To simulate talus pile formation, a talus pile was approximated as a triangle and extended from the point the ditch met the road to the cut slope. For simplicity, the simulation of talus pile growth assumes that rockfall debris is deposited across the entire ditch width, with more material accumulating closer to the slope than far away.

The talus pile angle was increased incrementally according to Table A-3 until the angle of repose was reached. In this case, the angle of repose was set to 35 degrees, or 7V:10H (Turner, 1996; Ehrlich et al., 2021). Negative angles represent a talus pile that has not yet filled the ditch to the horizontal. A negative talus pile angle equivalent to the ditch slope corresponds to an empty ditch.

Table A-3. Talus pile angles.

Talus pile angle	Talus pile angle (deg)
-1V:4H	-14.0
-1V:8H	-7.13
Flat	0.00
1V:8H	7.13
1V:4H	14.0
1V:2H	26.6
7V:10H	35.0

The initial ditch slope geometry uses the original calibration parameters for the ditch material for the 0.99 ditch effectiveness cases. However, after the initial geometry, the material parameters for the ditch were changed to a bare talus pile from RocFall's material library with a friction angle of 35 degrees (Table A-4). This means that in all cases other than the initial geometry, rocks are impacting talus rather than gravel of an empty ditch; thus, a change in parameters was required to better represent rockfall kinematics. All other parameters are consistent with the rockfall inputs from the calibration models and calibration parameters for the corresponding geometry (Table A-2).

After running a model for each cut slope geometry and talus pile angle, the proportion of rockfall that did not reach the road was recorded as ditch effectiveness.

Table A-4. Talus pile parameters.

Coefficient of normal restitution	Coefficient of tangential restitution	Std dev for coefficients	Friction angle (deg)
0.32	0.82	0.04	35

A.3 Results

Numerical modeling results (Figure A.2) reflect a deterioration in ditch effectiveness with increasing talus pile angle, which corresponds to an increase in cross-sectional area of the talus pile. To match the conceptual model, ditch effectiveness as a function of cross-sectional area of the talus pile should be linear once the area is greater than 0 m. Recall that negative areas

represent the empty space between the top of the talus pile and horizontal. Talus pile cross-sectional area was additionally normalized by ditch width to allow for more direct comparison of models with varying ditch widths.

The 4V:1H model results can be reasonably approximated as a linear trend, which agrees with the conceptual model in Figure 3.1. Recall that a slightly convex ditch effectiveness deterioration as a function of talus pile angle corresponds with a linear ditch effectiveness deterioration as a function of talus pile area.

Numerical model results deviate from the conceptual model for the shallower cut slopes: 2V:1H and 1V:1H. Both models show a slower rate of ditch effectiveness deterioration than expected. In the 2V:1H model, the slow rate of deterioration is followed by a relatively abrupt decrease of ditch effectiveness to zero for the 12.2 m cut slope height and to 0.24 for the 24.4 m height.

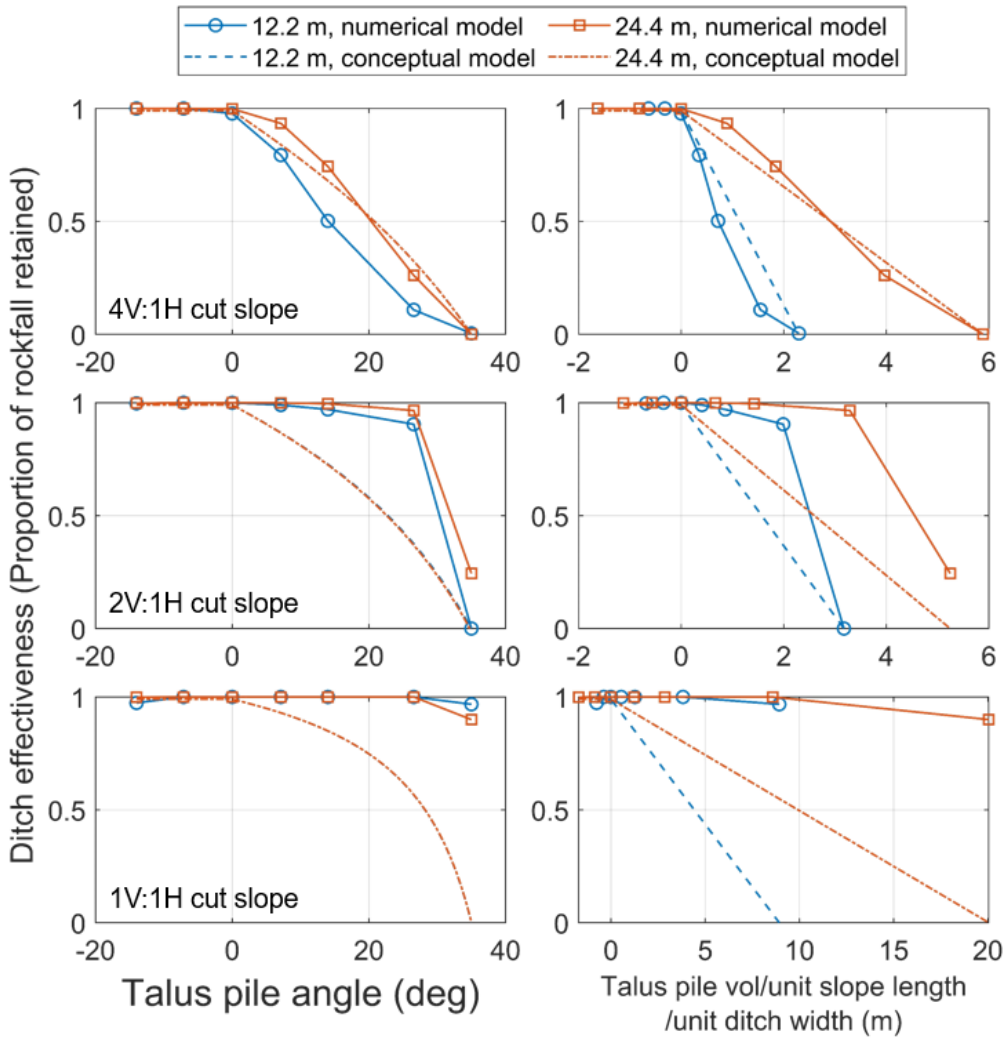

Figure A.2. Ditch effectiveness deterioration as a function of talus pile angle (left) and talus pile volume normalized by slope length and ditch width (right) for numerical modeling results and conceptual model.

A.4 Discussion

A.4.1 Influence of Cut Slope Angle on Numerical Modeling Results and Numerical Limitations

The steeper, 4V:1H cut slope numerical model was found to reasonably agree with the conceptual model for forecasting ditch effectiveness deterioration. Similar to the conceptual model, Figure A.2 shows that initial ditch effectiveness is retained for the 4V:1H cut slope until the talus pile angle is positive, meaning above the horizontal; this is attributed to the small increases in angle over this range being offset by a lower coefficient of restitution due to the loose debris, particularly since a slope dipping toward the road has not yet formed.

Numerical models exhibit similar ditch effectiveness trends across different cut slope heights, but ditch effectiveness deterioration differs substantially depending on cut slope angle. As cut slope angles become shallower, ditch effectiveness deterioration deviates from the conceptual model, and the conceptual model is conservative relative to the numerical modeling results for shallower cut slope angles.

The results of the shallower cut slopes are considered unreasonable due to limitations in the numerical modeling (Figure A.3). For example, RocFall2 cannot simulate the specific talus pile mechanics and lacks consideration of clast-to-clast interactions. The talus pile is represented as a continuous material, but in reality, a pile contains interlocking blocks of varying sizes and exhibits the potential for dislodging of previously deposited rockfall debris from the talus pile. As a talus pile approaches its angle of repose, rockfall blocks are expected to have a “one-in-one-out” interaction with the talus pile on average. Since the talus pile is represented as a single block of continuous material, this interaction doesn’t occur in the numerical models, leading to an overestimation of ditch effectiveness.

Furthermore, in Figure A.2, it is observed that the normalized talus pile area increases at a faster rate with talus pile angle for the 1V:1H cut slope, and to a lesser extent, the 2V:1H cut slope, due to shallower cut slope angle. Thus, relative to steeper cut slopes, shallower cut slopes produce taller talus piles when the talus pile width is assumed to span the entire ditch width. In the numerical models, rockfall motion transitions from bouncing-dominated to rolling-dominated as the cut slope angle decreases. As talus piles come higher on the shallower slopes, the talus pile essentially behaves as a ramp for rockfall to roll down, and rockfall runout is primarily influenced by talus pile friction in this case (Figure A.3C). With larger talus piles and more rolling due to shallow cut slope angles, rockfall is less likely to bounce out of the ditch and more likely to remain on the talus pile. In reality, considering clast-to-clast interactions, an incoming rolling block would likely dislodge clasts in the talus pile such that some debris would end up beyond the original ditch extent, even if it did not include the rockfall in question (Figure A.3D). In the steeper cut slopes, rockfall motion is bouncing-dominated, which decreases the influence of rolling friction and increases runout distance, all else being equal.

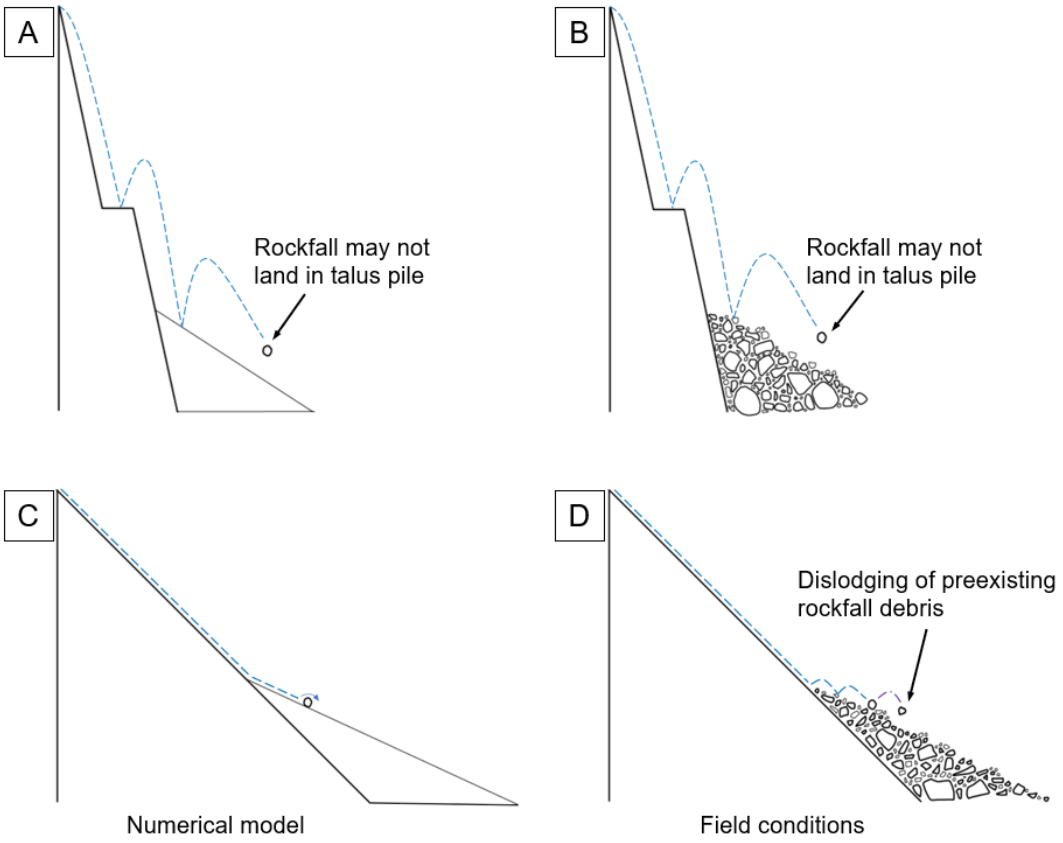

Figure A.3. Comparison of rockfall motion in the numerical models (A and C) vs. field conditions (B and D). Bouncing and falling rockfall motions are more present in steeper cut slopes (A and B), while rolling motions are more present in shallower cut slopes (C and D). However, because the talus pile is represented as a continuous, solid material, clast-to-clast interactions which may affect ditch effectiveness are not considered. For instance, rockfall may dislodge previous rockfall debris from the talus pile.

A.4.2 Possible Deviations from the Conceptual Model in Field Conditions

In field conditions, deviations may occur from the conceptual model for shallower cut slopes due to possible different talus pile formation processes dependent on the cut slope angle. For instance, in the case of steeper slopes, more bouncing will cause variable positions where rockfall debris is deposited, causing the talus pile angle to build over time (Figure A.4). However, in shallower cut slopes, rolling motion may result in a talus pile concentrated at the base of the slope which expands in width and height over time while maintaining the angle of repose (Figure A.4B). When simulating talus pile formation in the numerical models, the talus pile was defined to span across the entire ditch width at all times and incrementally increased in angle.

With a different talus pile formation process for shallow cut slopes (and what was simulated in the numerical modeling), the underlying assumption of the conceptual model as described in Section 3.3.1 would not be expected to hold, meaning the initial ditch effectiveness may be retained even after the talus pile angle reaches zero. If the talus pile angle is at its angle of repose

but does not span across the entire ditch width, the ditch effectiveness may be retained until the talus pile width is approximately equivalent to the ditch width. Recommendations on how the conceptual model may be modified to reflect this scenario are discussed previously in Section 3.3.

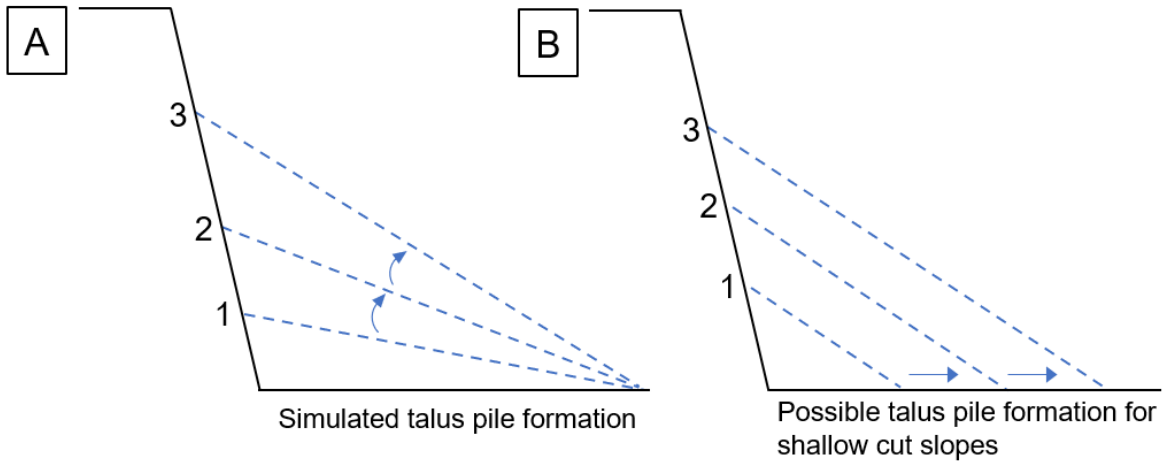

Figure A.4. Different talus pile formation processes. The talus pile formation process simulated in the numerical modeling (A) may apply more to steeper cut slopes, while the alternative talus pile formation process (B) may apply to shallower cut slopes which have rolling-dominated rockfall motion.

A.5 Conclusions

To evaluate the ditch effectiveness deterioration conceptual model, 2D rockfall trajectories and runout were simulated in RocFall2 with cut slope and ditch geometries calibrated to Pierson et al. (2001). The talus pile geometry was represented as a continuous triangle, and the talus pile angle was increased incrementally until the angle of repose was reached, which was predicted to result in a ditch effectiveness of zero. The numerical rockfall modeling results for the 4V:1H cut slope can be considered to reasonably approximate the conceptual ditch effectiveness deterioration model, as ditch effectiveness as a function of the cross-sectional area of the talus pile is approximately linear in the modeling results.

The numerical modeling results for the shallower cut slope angles did not reflect ditch effectiveness deterioration as the conceptual model proposes. This is attributed to limitations in the numerical modeling, as well as the assumed talus pile formation process. Specifically, in the case of shallow cut slopes where rockfall motion is dominated by rolling, talus piles may initially form at their angle of repose and increase in width over time. Thus, ditch effectiveness would not begin to decrease until the talus pile had grown to nearly fill the full ditch width. Possible modifications to the conceptual model are suggested in Section 3 to account for this type of behavior.

Appendix B: Supplemental Material for Comparison of Slope Performance Deterioration Using the CDOT Hazard Models and the Proposed Conceptual Models

Table B-1. Remote sensing MCF parameters for each slope used in the sensitivity analysis. Intercept parameter, a, normalized by slope area is used for ditch effectiveness deterioration, while a normalized by 0.1 mile is used in the time since excavation and scaling models.

Slope	a (events/yr/m^2)	a (events/yr/0.1 mile)	b
Vail Pass	9.00×10^{-4}	7.600	0.855
Idaho Springs	1.27×10^{-4}	0.158	0.971
Floyd Hill	4.42×10^{-5}	0.341	0.734
E	1.22×10^{-4}	0.808	0.749
HI	2.02×10^{-4}	0.994	0.922
Manitou Springs	9.00×10^{-4}	3.713	0.683

Table B-2. Ditch effectiveness deterioration model inputs.

Slope	w (m)	δ (deg)	α (deg)	l_b (m)
Vail Pass	5.00	15	70	60.66
Idaho Springs	2.50	15	80	18.12
Floyd Hill	2.00	10	72	44.77
E	2.75	10	80	46.09
HI	4.00	15	80	30.14
Manitou Springs	6.00	0	75	27.68